

INSTRUMENTATION FOR MEASUREMENT OF AXIAL LOAD  
IN DRILLED SHAFTS

by

Walter R. Barker  
Lymon C. Reese

Research Report 89-6

Soil Properties as Related to Load-Transfer  
Characteristics of Drilled Shafts

Research Project 3-5-65-89

conducted for

The Texas Highway Department

in cooperation with the  
U. S. Department of Transportation  
Federal Highway Administration

by the

CENTER FOR HIGHWAY RESEARCH  
THE UNIVERSITY OF TEXAS AT AUSTIN

November 1969

The opinions, findings, and conclusions expressed in this publication are those of the authors and not necessarily those of the Federal Highway Administration.

## PREFACE

This report is the sixth in a series of reports from Research Project 3-5-65-89 of the Cooperative Highway Research Program. It describes the development, installation and results of various instrumentation systems used in drilled shafts tests. Recommendations for the instrumentation of drilled shafts for future tests are presented.

This report is the product of the combined efforts of many people. Technical contributions were made by Michael W. O'Neill, Harold H. Dalrymple, Frederick E. Koch and James N. Anagnos. Preparation and editing of the manuscript were done by Art Frakes, Beth Davis and Eddie B. Hudepohl.

Dr. Ervin S. Perry served as a technical reader and his helpful comments and suggestions are appreciated.

The Texas Highway Department Project Contact Representatives, Messrs. Horace Hoy and H. D. Butler along with the personnel from District Number 12 and the Houston Urban Office have been helpful and cooperative in the development of the work. Thanks are due them as well as the U. S. Bureau of Public Roads who jointly sponsored the work.

Walter R. Barker

Lymon C. Reese

November 1969

This page replaces an intentionally blank page in the original.

-- CTR Library Digitization Team

## LIST OF REPORTS

Report No. 89-1, "Field Testing of Drilled Shafts to Develop Design Methods," by Lymon C. Reese and W. Ronald Hudson, describes the overall approach to the design of drilled shafts based on a series of field and laboratory investigations.

Report No. 89-2, "Measurements of Lateral Earth Pressure in Drilled Shafts," by Lymon C. Reese, J. Crozier Brown, and H. H. Dalrymple, describes the development and evaluation of pressure gages to measure lateral-earth pressures on the drilled shaft.

Report No. 89-3, "Studies of Shearing Resistance Between Cement Mortar and Soil," by John W. Chuang and Lymon C. Reese, describes the overall approach to the design of drilled shafts based on field and laboratory investigations.

Report No. 89-4, "The Nuclear Method of Soil-Moisture Determination at Depth," by Clarence J. Ehlers, Lymon C. Reese, and James N. Anagnos, describes the use of nuclear equipment for measuring the variations of moisture content at the drilled shaft test sites.

Report No. 89-5, "Load Distribution for a Drilled Shaft in Clay Shale," by Vasant N. Vijayvergiya, W. Ronald Hudson, and Lymon C. Reese, describes the development of instrumentation capable of measuring axial load distribution along a drilled shaft, the development, with the aid of full-scale load testing, of a technique of analysis of observed data, and the correlation of observed data with the Texas Highway Department cone penetration test.

Report No. 89-6, "Instrumentation for Measurement of Axial Load in Drilled Shafts," by Walter R. Barker and Lymon C. Reese, describes the development and performance of various instrumentation systems used to measure the axial load distribution in field tests of full-scale drilled shafts.

This page replaces an intentionally blank page in the original.

-- CTR Library Digitization Team

## ABSTRACT

A major problem in the full-scale load test of drilled shafts is defining the load distribution along the length of the shaft. Defining the load distribution requires the measurement of load in the shaft at various points along the shaft's length.

One phase of the drilled shaft test being conducted by The University of Texas involves developing a suitable instrumentation system for measurement of load in drilled shafts. To date a total of four shafts have been instrumented with a combination of five different instrumentation systems. Three of the five systems were designed and constructed at The University of Texas at Austin.

As the result of the instrumentation and subsequent testing of these four drilled shafts, an electrical instrumentation system developed at The University of Texas has been adopted as the instrumentation system to be used in the instrumentation of future shafts of the project.

This page replaces an intentionally blank page in the original.

-- CTR Library Digitization Team

## SUMMARY

Research Report No. 89-6, the sixth in a series of reports issued under Research Project 3-5-65-89 of the Cooperative Highway Research Program, describes the development and performance of various instrumentation systems which were used to measure the distribution of axial load in the field testing of four drilled shafts. Primary emphasis was placed on a strain-measuring transducer, the Mustran cell (Figs 2.9 and 2.10), which was designed and constructed at The University of Texas at Austin. The other devices used were telltales (Fig 2.1), embedment strain gages (Fig 2.2), Gloetzl cells (Fig 2.3), and a bottomhole cell (Fig 2.7).

The results of the instrumentation and testing of the four shafts demonstrated the Mustran instrumentation system to be the more desirable system for the purposes of the project. The system was found to be reliable, sensitive, and stable. The accuracy of the system was found to depend mainly on uniformity in the cross-sectional dimensions of the shaft. On the basis of the results obtained from the testing of these four shafts, the Mustran instrumentation system was adapted for the instrumentation of other shafts in the project remaining to be tested axially.

This page replaces an intentionally blank page in the original.

-- CTR Library Digitization Team

## IMPLEMENTATION STATEMENT

During the course of Research Project 3-5-65-89 of the Cooperative Highway Research Program, the Mustran instrumentation system has proven to be an excellent system for the measurement of axial loads in drilled shafts. The system is, therefore, recommended for the instrumentation of drilled shafts which are to be tested axially.

Construction details, installation procedures, and operation instructions for the Mustran instrumentation system are contained in the report. From the information presented in the report, persons conducting a drilled shaft test should be able to construct and employ the Mustran instrumentation system.

This page replaces an intentionally blank page in the original.

-- CTR Library Digitization Team

TABLE OF CONTENTS

PREFACE . . . . .	iii
LIST OF REPORTS . . . . .	v
ABSTRACT . . . . .	vii
SUMMARY . . . . .	ix
IMPLEMENTATION STATEMENT . . . . .	xi
NOMENCLATURE . . . . .	xv
CHAPTER I. INTRODUCTION . . . . .	1
Project Description . . . . .	1
Theory . . . . .	2
Shaft Instrumentation for Axial Load . . . . .	6
Historical Background of Shaft Instrumentation . . . . .	9
CHAPTER II. AXIAL LOAD MEASURING DEVICES . . . . .	11
Telltales . . . . .	12
Embedment Gage . . . . .	14
Gloetzl Cell . . . . .	14
Bottomhole Cell . . . . .	17
Mustran Cells Type 1 and Type 2 . . . . .	22
CHAPTER III. MONTOPOLIS AND SAN ANTONIO TEST SITES . . . . .	35
Montopolis Test Site . . . . .	35
Load Application . . . . .	37
Test . . . . .	37
Results . . . . .	37
San Antonio Test Site . . . . .	39
Test Results . . . . .	41
CHAPTER IV. HOUSTON SH 225 TEST SITE . . . . .	43
Shaft 1 . . . . .	43
Load Application . . . . .	51
Readout System for Embedment Gages, Bottomhole Cell, and Mustran Cells . . . . .	55

Load Tests . . . . .	58
Results . . . . .	58
Data Reduction . . . . .	65
Shaft Bending . . . . .	69
Discussion of Test Results . . . . .	72
Shaft 2 . . . . .	76
Load Application . . . . .	85
Results . . . . .	85
Shaft Bending . . . . .	88
Discussion of Test Results . . . . .	88
CHAPTER V. CONCLUSIONS AND RECOMMENDATIONS . . . . .	97
Conclusions . . . . .	97
Recommendations . . . . .	99
REFERENCES . . . . .	103

## NOMENCLATURE

<u>Symbol</u>	<u>Typical Units</u>	<u>Definition</u>
$A$	sq ft	Cross-sectional area of shaft
$A_B$	sq in	Area of a Mustran cell bar
$A_c$	sq ft	Effective cross-sectional area of shaft
$A_{cc}$	sq in	Area of a column of concrete
$A_E$	sq in	Area of a Mustran cell end cap
$A_R$	sq in	Area of the reduced section of bar for a Mustran cell
$A_1 , A_2 , A_3 , \dots$		Constants for regression line
$c$	lbs/sq ft	Apparent cohesion of soil
$d$	inches	Diameter of a shaft
$E_c$	lbs/sq ft	Young's modulus of elasticity of concrete
$E_o$	microvolts	Gage reading
$E_s$	psi	Modulus of elasticity of steel
$dF$	lbs	Shearing force developed on an elemental surface area of shaft
$K$		Gage factor
$L_B$	inches	Length of a Mustran cell bar not including the length of the reduced section
$L_E$	inches	Length of a Mustran cell end cap

$L_R$	inches	Length of the reduced section of bar for a Mustran cell
$q$	lbs	Average load in shaft between two points
$Q_T$	lbs	Total load on top of shaft
$Q_z$	lbs	Total load in shaft at a point located a distance $z$ from the top of shaft
$R$	lbs	Total peripheral load on shaft
$V$	volts	Voltage applied to gage
$w_T$	ft	Total vertical movement of top of shaft
$X$		Independent variable for regression line
$z$	ft	Vertical coordinate from top of shaft to a point in the shaft
$\Delta_c$	inches	Deformation between the ends of a column of concrete
$\Delta_m$	inches	Deformation between the end caps of a Mustran cell
$\epsilon$	inches/inch	Strain
$\epsilon_c$	inches/inch	Concrete strain
$\epsilon_s$	inches/inch	Steel strain
$\epsilon_z$	inches/inch	Strain at point $z$
$\theta$	degrees	Angular distance around a shaft

CHAPTER I  
INTRODUCTION

A drilled shaft is a deep foundation constructed by drilling a hole and filling it with concrete. The bottom of the hole may be enlarged, either to increase the bottom bearing area or to resist uplift. For axial loads, the shaft thus becomes a concrete column supported by both bottom bearing and side friction.

Drilled shafts are used frequently in modern day construction. In areas of relatively stiff clays and dense sand where holes may be drilled without the use of casing, drilled shafts are being found to be more economical than driven piles. An even greater saving can be realized if the full capacity of these shafts can be predicted and utilized in design.

The predicting of the full capacity of the shafts involves the determination of the shaft and soil interaction. One approach to the determination of the shaft and soil interaction is to conduct axial load tests on full-scale drilled shafts and to measure the basic parameters of the interaction. If the relationship between the basic parameters can be determined, then this relationship may be used in developing a technique for the design of future drilled shafts.

Project Description

The University of Texas is currently involved in axial load tests of full-scale drilled shafts for the purpose of determining the load-carrying characteristics for such shafts. To date, four shafts, located at three

widely separated sites, have been instrumented and tested. These sites, all located in the south central and southeastern part of Texas, are designated as the Montopolis site, the San Antonio site, and the Houston SH 225 site. The Montopolis site and the San Antonio site were each the location of a single shaft, with the Houston SH 225 site being the location of two shafts. Work is proceeding in instrumenting an additional two shafts to be located at the Houston SH 225 site. Thus, at the completion of the project, a total of six shafts will have been instrumented and tested.

### Theory

A typical drilled shaft is shown in Fig. 1.1a. The applied load is transferred to the soil, partly by the friction along the side of the shaft and partly by the bearing support at the bottom of the shaft. Thus, the load carried by the shaft may be defined by the equation

$$Q_T = \int_0^l \int_0^{360^\circ} (dF)(d\theta)(dz) + Q_B \dots \dots \dots (1.1)$$

where

$Q_T$  = the total load at the top of the shaft,

$dF$  = the shearing force developed on an elemental surface area of the shaft,

$Q_B$  = the bearing support at the tip of the shaft,

$l$  = the length of the shaft,

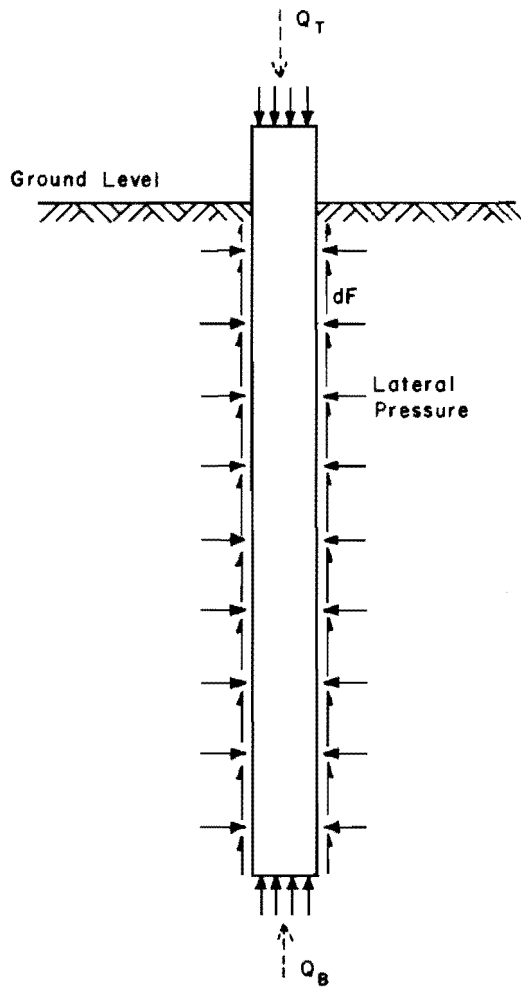


Fig. 1.1a. Forces Acting on a Drilled Shaft (After Vijayvergiya, Ref. 14)

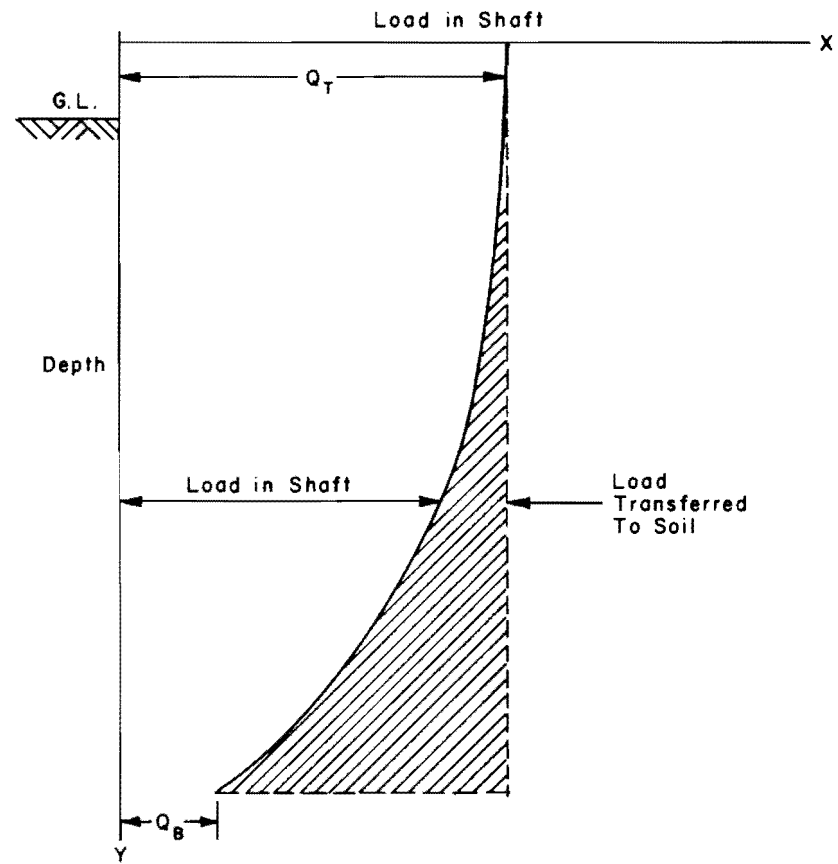


Fig. 1.1b. Typical Curve for Load Distribution in a Shaft (After Vijayvergiya, Ref. 14)

$d\theta$  = an incremental distance around the circumference of the shaft, and

$dz$  = an incremental distance along the depth of the shaft.

The term  $\int_0^l \int_0^{360^\circ} (dF)(d\theta)(dz)$  represents the total load supported by the side friction. If the shearing stress is considered to be constant around the circumference of the shaft, and a single valued function of the depth, then the total side friction may be expressed by

$$R = \int_0^l (dF)(\pi d)(dz) \dots \dots \dots (1.2)$$

where

$R$  = the total side friction, and

$d$  = the diameter of the shaft.

A plot of the load carried by the shaft as a function of the depth is called the load-distribution curve and may be defined by the equation

$$Q_z = Q_t - \int_0^z (dF)(\pi d)(dz) \dots \dots \dots (1.3)$$

or

$$Q_z = Q_t - R_z \dots \dots \dots (1.4)$$

where

$Q_z$  = the total load in the shaft at a depth  $z$ , and

$R_z$  = the total load transferred to the soil by side friction  
from the ground surface to a depth  $z$ .

The load-distribution curve becomes the basis for the parameters of shaft movement and load transfer, which relate the shaft behavior to the soil properties. A typical load distribution along a drilled shaft is shown in Fig. 1.1b. The load transferred per unit length of the shaft at any point is represented by the slope of the load-distribution curve at the point. Calculating the movement at a point along the length of the shaft involves the movement of the top of the pile and the deformation of the pile between the top and the point. The top movement is measured directly for each applied load by the use of dial gages.

The strain of the shaft at any point is represented by the load at the point divided by the effective shaft area and concrete modulus of elasticity which would be expressed in equation form as

$$\epsilon_z = Q_z / A_c E_c \dots \dots \dots (1.5)$$

The deformation of the shaft between the top and any point may then be calculated by integrating the strain function from the top of the shaft to the point or

$$\Delta = \int_0^z \epsilon_z dz = \frac{1}{A_c E_c} \int_0^z Q_z dz \dots \dots \dots (1.6)$$

The net movement of the shaft at the point is then computed by subtracting the computed shaft deformation from the movement measured at the top of the shaft. In equation form this would be expressed as

$$w_z = w_T - \frac{1}{A_c E_c} \int_0^z Q_z dz \dots \dots \dots (1.7)$$

where

$w_z$  = the movement of a point at a depth  $z$  ,

$w_T$  = the downward movement of the top of the shaft,

$A_c$  = the effective area of the concrete, and

$E_c$  = the modulus of elasticity of the concrete.

Thus, if the load-distribution curve can be defined, the load transfer and shaft movement at any point along the shaft may be found by analytical techniques. If a method can be found to relate this load transfer and shaft movement to the soil properties, then a rational method is available for predicting the total side friction developed in drilled shafts and thus effecting a more economical design (Ref. 1).

A method by which the load-distribution curve is defined involves conducting full-scale field tests on drilled shafts and measuring at various levels the load carried by the shafts.

#### Shaft Instrumentation for Axial Load

The development of instrumentation capable of measuring the axial load along the length of a drilled shaft is a major problem. The problems

involved are inherent in the properties of concrete. Gages embedded in concrete are exposed to moisture and chemical action. The concrete undergoes physical changes during curing and during loading which may affect gage readings. The properties of the concrete may vary from location to location in the shaft. During placing, gages are exposed to possible damage from the handling equipment and from the wet concrete. After embedment very little if anything can be done to repair a damaged gage.

An ideal system of instrumentation should have:

- (1) a degree of accuracy which is compatible with the objectives of the test,
- (2) a sensitivity such that the desired resolution is obtained,
- (3) a durability to remain operational during the testing period,
- (4) a stability to give reliable results,
- (5) a cost which will not be prohibitively high,
- (6) a method of readout which will be compatible with the testing procedure, and
- (7) a relatively easy method of installation.

The instrumentation utilized in a drilled shaft test may be classified as direct-mechanical, direct-electrical, indirect-mechanical, and indirect-electrical. A direct system is a system by which the load carried by the shaft is measured directly and is independent of the properties of the concrete. In nearly all load tests the load applied to the top of the shaft is measured through some direct means. An indirect system measures the strain in the shaft. The load in the shaft is then determined by the equation

$$Q_z = E_c \cdot A_c \cdot \epsilon_c \dots \dots \dots (1.8)$$

where

$Q_z$  ,  $E_c$  , and  $A_c$  are as previously defined, and

$\epsilon_z$  = the measured strain at a depth  $z$  .

Thus the indirect system is dependent on the modulus of elasticity of the concrete and on the area of the shaft. This dependence on the modulus of elasticity and area of the concrete severely limits the accuracy of the indirect systems.

The type of signal generated by gages determines if the system is classified as an electrical or a mechanical system. By this use of this classification, the SR-4 electrical resistance gage, linear variable transformers, and inductances are examples which would be classified as electrical instrumentation systems. A few examples of mechanical systems are fluid pressure measured by Bourdon tube gages, dial indicators, and vibrating-wire gages. Mechanical systems tend to be more stable and reliable over long periods of time. Offsetting the stability and reliability of mechanical systems is the fact that they do not lend themselves to automatic readout nor do the signals lend themselves to amplification such that a high degree of resolution is obtained. The electrical instrumentation systems do lend themselves to automatic readout and to amplification but under certain conditions may not be stable or reliable. Also, the electrical systems are proven to be more subject to damage in handling. Thus, both the mechanical and electrical systems have advantages and disadvantages.

### Historical Background of Shaft Instrumentation

In most of the early load tests on drilled shafts only the applied load was measured. A number of these tests were analyzed by Skempton (Ref. 2). The analysis was based on an estimation of the load carried at the base of the shaft. The load carried by the base was estimated by the formula

$$Q_B = 9 \cdot c \cdot A \dots\dots\dots(1.9)$$

where

$c$  = the apparent cohesion of the soil, and

$A$  = the area of the base.

The total load transferred by side friction was assumed to be equal to the difference between the applied load and the estimated bottom load. No attempt was made to define the load distribution along the length of the shafts.

A direct-electrical cell for measuring the load at the bottom of a shaft was developed by Whitaker, Cooke, and Clarke (Ref. 3). The cell consisted of two steel plates separated by eight steel pillars, instrumented with foil-type electrical resistance strain gages. The cell was used in a shaft test conducted by Whitaker and Cooke (Ref. 4) and proved to be very successful.

DuBose (Ref. 5) attempted to measure the load distribution in a drilled shaft by the use of a single electrical resistance strain gage attached to the vertical reinforcing. The U. S. Corps of Engineers, in shaft tests at San Antonio (Ref. 6), expanded the method used by DuBose by using a full

bridge circuit attached to the reinforcing. A different approach was used in tests conducted by Mohan and Kumar (Ref. 7). In these tests, electrical strain gages were placed inside a 2-inch-diameter pipe which was embedded in the shaft.

An indirect-mechanical system developed by Raymond International, Inc. (Ref. 8) consists of a system of unstrained rods called telltales. These will be described later in this report.

A cell similar in construction to the cell developed by Whitaker, Cooke, and Clarke is currently being used in tests conducted by Osgerby and Taylor (Ref. 9). This cell uses a vibrating-wire gage instead of an electrical resistance strain gage, as used previously by Whitaker, Cooke, and Clarke. Use of the vibrating-wire gage appears to produce a cell which is very stable over a long period of time.

## CHAPTER II

### AXIAL LOAD MEASURING DEVICES

Although other types of instrumentation were used in the tests being conducted by The University of Texas at Austin, this study is concerned with the instrumentation being used to measure axial loads in the shaft. Primary emphasis will be placed on the strain measuring cell developed by The University of Texas, which has been adopted for use in future tests. The systems used for axial load measurements in the four drilled shafts tested to date consisted of one indirect-mechanical (telltales), one direct-mechanical (Gloetzl), one direct-electrical (bottomhole cell), and two indirect-electrical (embedment gages, and Mustran cells).

Other instrumentation used in connection with the tests included lateral pressure cells to measure the lateral earth pressure against the shaft, thermocouples for measuring the in-shaft temperature, an in situ device for measuring shear strength of soil, and a nuclear method of soil-moisture determination. The lateral pressure cell used was developed at The University of Texas and is reported by Brown (Ref. 10). The device used for in situ strength determination was also developed at The University of Texas and is reported by Campbell (Ref. 11). Soil-moisture determinations were made at each site with a Troxler Model 200B portable scaler and Model 104 depth moisture probe. A study of this equipment was made by Ehlers (Ref. 12).

Following is a brief description of each of the five types of axial load-measuring devices utilized in load tests thus far conducted.

### Telltales

Telltales are mechanical devices for measuring the deformation between two points along the shaft. If the concrete properties and the deformation between two points are known, the average load,  $q$ , in the shaft between the two points may be calculated by

$$q = \epsilon A_c E_c \dots \dots \dots (2.1)$$

where

$\epsilon$  = the average value of strain in the concrete between the two points given by the total deformation divided by the distance between the two points.

The basic system of telltales used in these tests was adopted from the system developed by Raymond International, Incorporated (Ref. 8). The system as shown in Fig. 2.1 consists of steel rods with one end anchored within the shaft and enclosed in a tube to prevent bond along the length of the rod. As the load is applied the differential movement between the top of the shaft and the top of the unstrained rod is measured by the use of an Ames dial gage. This differential movement is then taken as the deformation of the shaft between the top of the shaft and the point of anchorage of the rod.

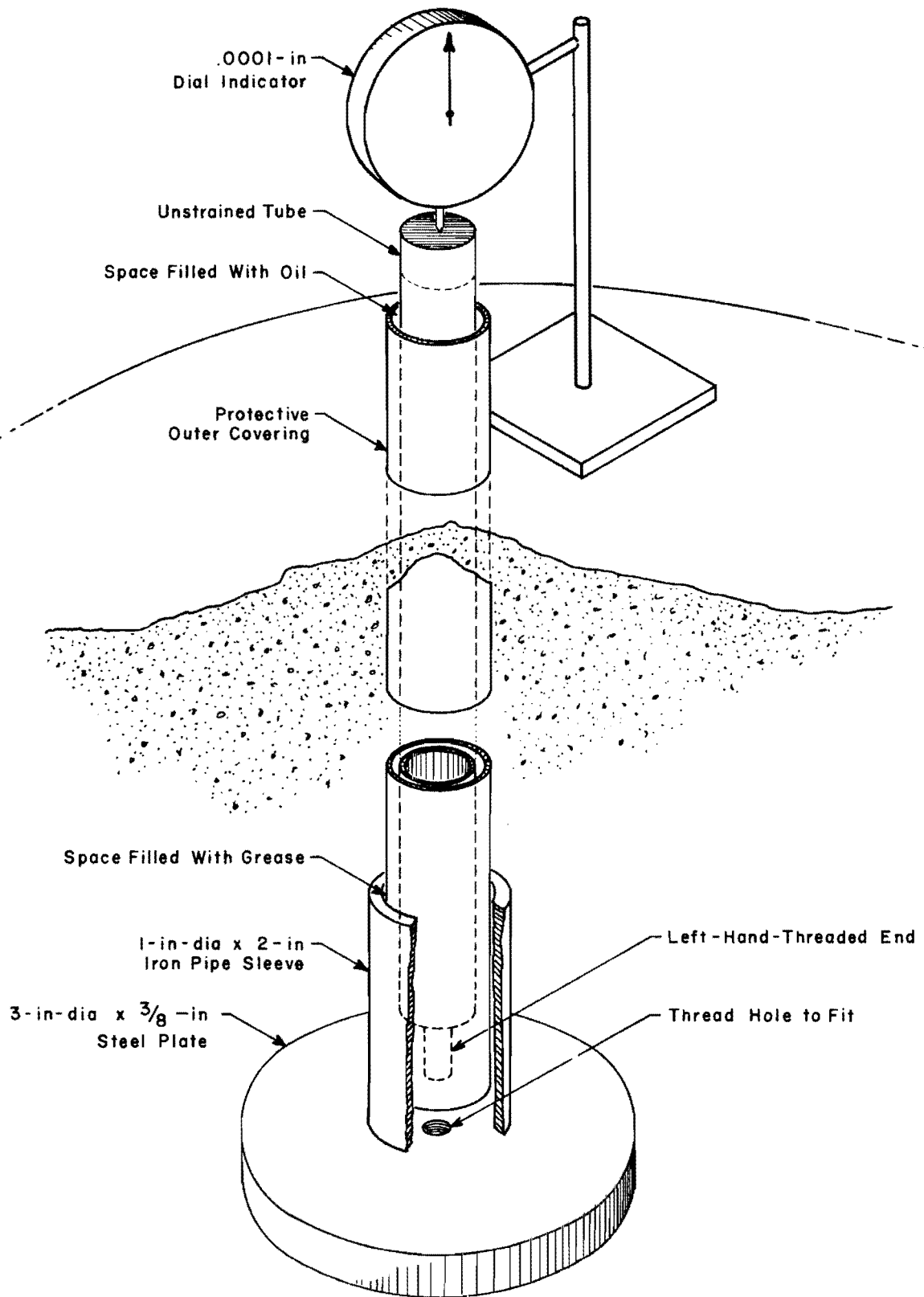


Fig. 2.1. Details of the Assembly of the Telltale System  
(After Reese and Hudson, Ref. 13)

### Embedment Gage

The embedment gage used in these tests is a resistance wire strain gage designed specifically for use in concrete. The gage, manufactured by Tokyo Sokki Kenkyujo Company of Japan, consists of a wire gage sandwiched between two pieces of resin plate whose outer faces are coated with rough material for good bond. The gage shown in Fig. 2.2 comes attached with a 2-meter-long, vinyl, lead wire. The specifications of the gage are as follows:

Gage type	PML-60
Nominal gage length	60 mm
Nominal gage width	1 mm
Nominal resistance	120 ohms
Gage factor	2.11
Base dimensions	125 x 13 x 5 mm

Laboratory studies conducted by Vijayvergiya (Ref. 14) indicate that accurate strain measurements were obtained when the gage was cast in small concrete cylinders.

### Gloetzl Cell

The Gloetzl cell is a direct-mechanical system for measuring concrete stress. The complete Gloetzl system consists of the Gloetzl cell, a hand-operated hydraulic pump, two Bourdon-tube pressure gages, and pressure lines. The construction of the cell is shown in Fig. 2.3. In principle, the valve is designed to open and to bypass hydraulic fluid when the pressure of the hydraulic fluid is equal to the fluid pressure inside the cell.

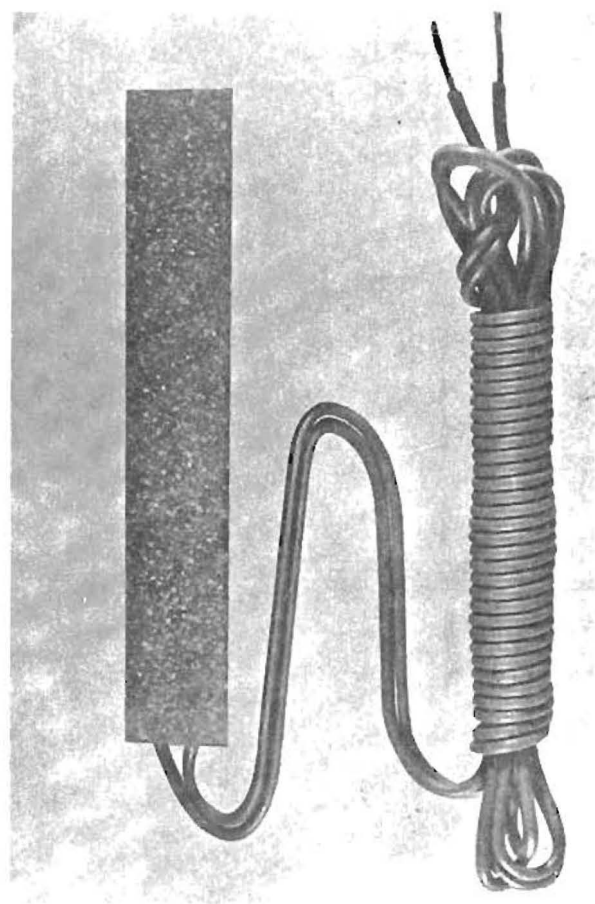


Fig. 2.2. PML-60 Type Embedment Strain Gage

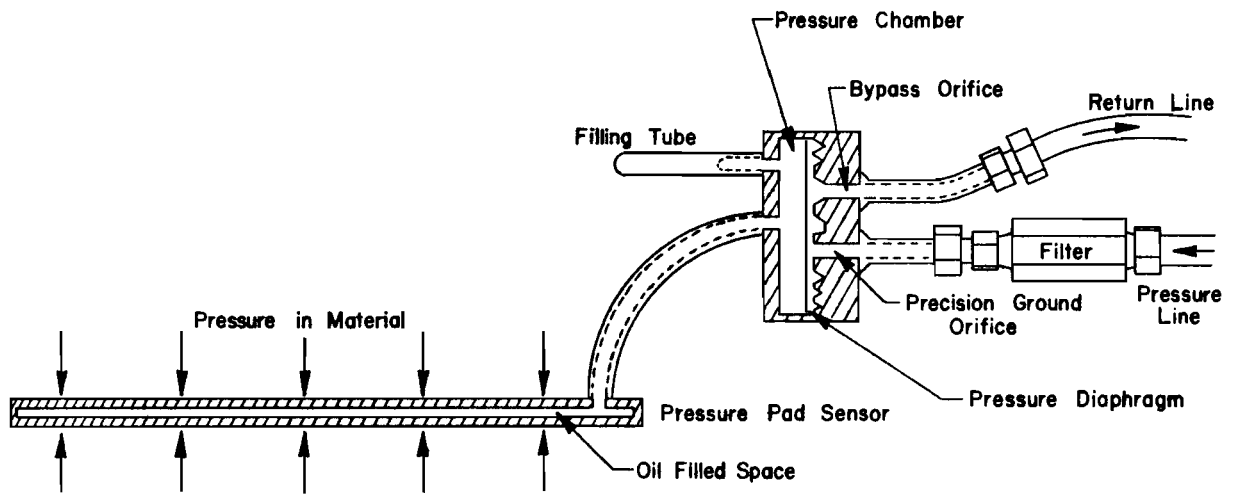


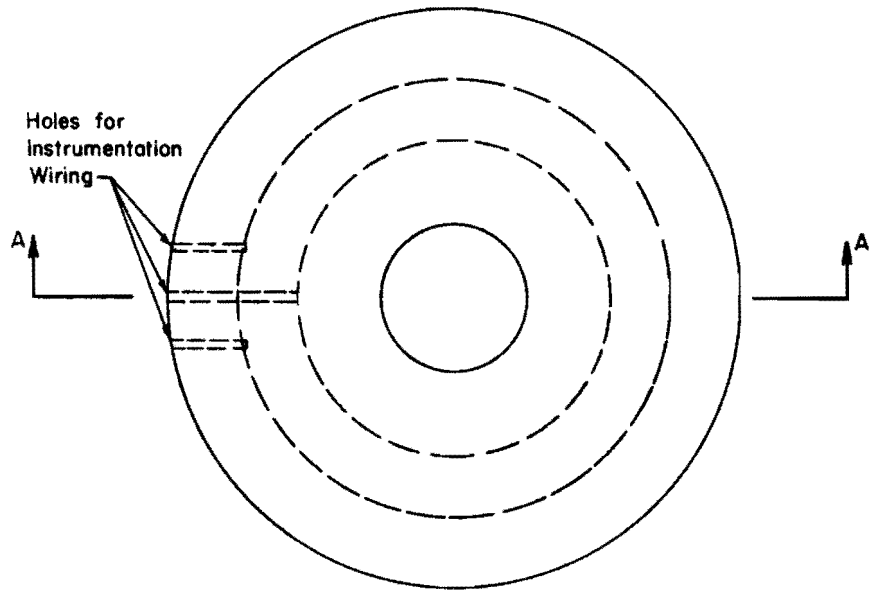
Fig. 2.3. Schematic of Gloetzl Cell

Thus, by using the pump to increase the hydraulic fluid pressure to the point of bypass, a measure of the internal cell pressure is obtained. By assuming that the internal fluid pressure is equal to stress in the concrete, the load in the shaft may be determined.

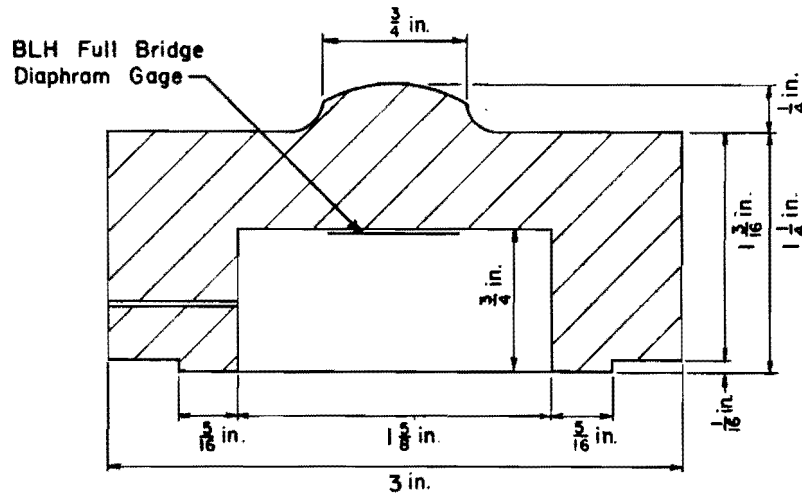
#### Bottomhole Cell

The bottomhole cell was designed and constructed at The University of Texas for the purpose of measuring the load carried by the base of the shaft. The design is similar to that used by Whitaker, Cooke, and Clarke (Ref. 4). The cell is a direct-electrical device consisting of three diaphragm-type load cells (Fig. 2.4) separating two 1-1/2-inch-thick steel plates. The diameter of the cell is slightly less than that of the shaft so that when the cell is placed at the bottom of the shaft the entire load is transferred through the cell. Calibration tests were conducted on both the individual load cells and the complete assembly. The calibrated curve for the completed cell (Fig 2.5) indicated a linear relationship between output and applied load. The load cells were wired as shown in Fig. 2.6 to give a single output which is the sum of the output from the three load cells.

Waterproofing of the cell was provided by encasing the periphery of the cell in a neoprene rubber sheet cut from a truck innertube. The edges of the steel plates were coated with rubber-to-metal cement and the neoprene sheet was banded to each steel plate by two steel bands. All wiring was brought to the surface through a 3/8-inch copper tube. Another 3/8-inch copper tube was installed to provide means for circulating nitrogen through the system. The completed cell is shown in Fig. 2.7.



NOTE: Machined from a High Carbon Cold Rolled Steel And Case Hardened



SECTION A-A

Fig. 2.4. Diaphragm Load Cell for Bottomhole Cell

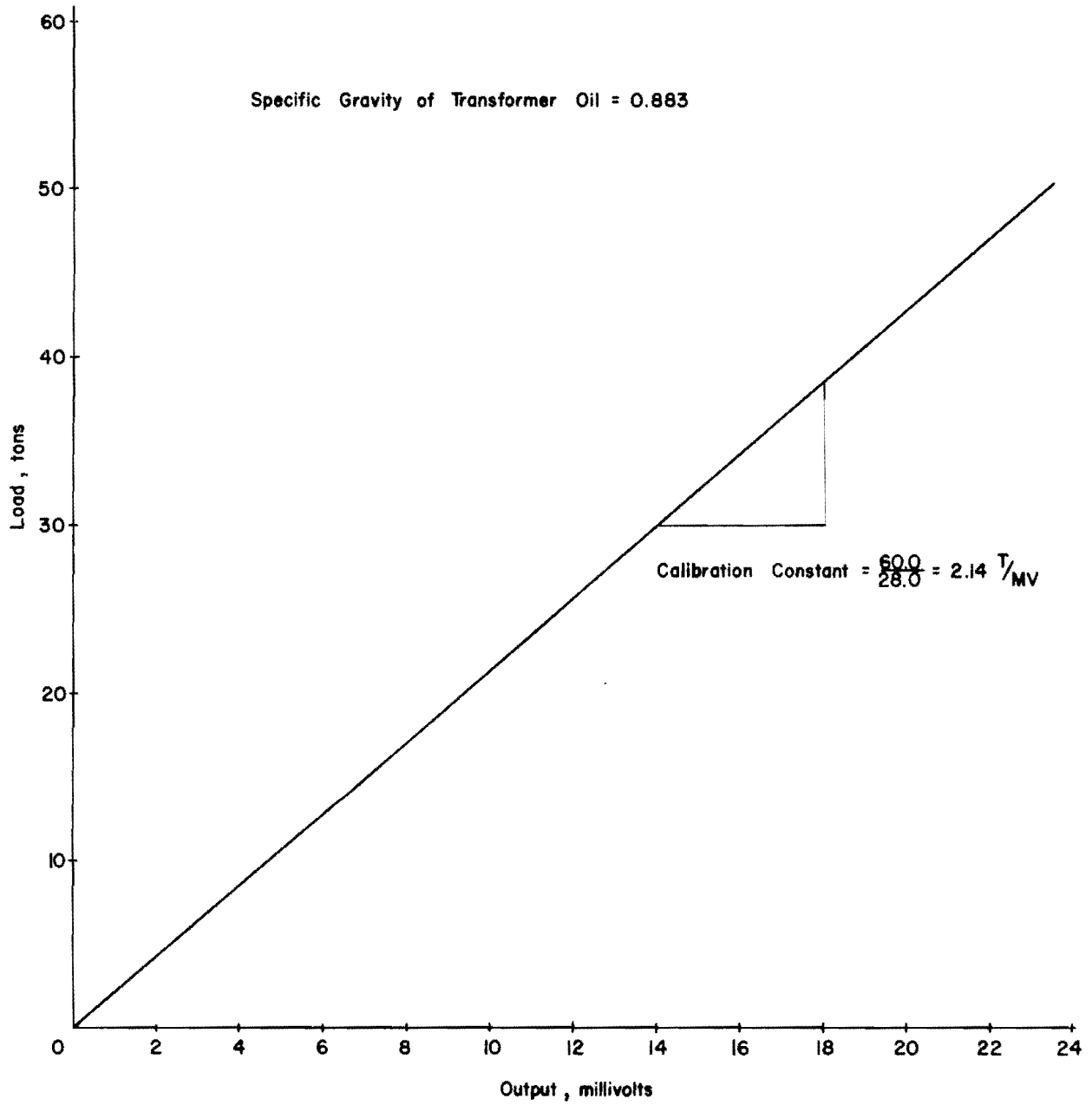


Fig. 2.5. Calibration Curve for Bottomhole Cell

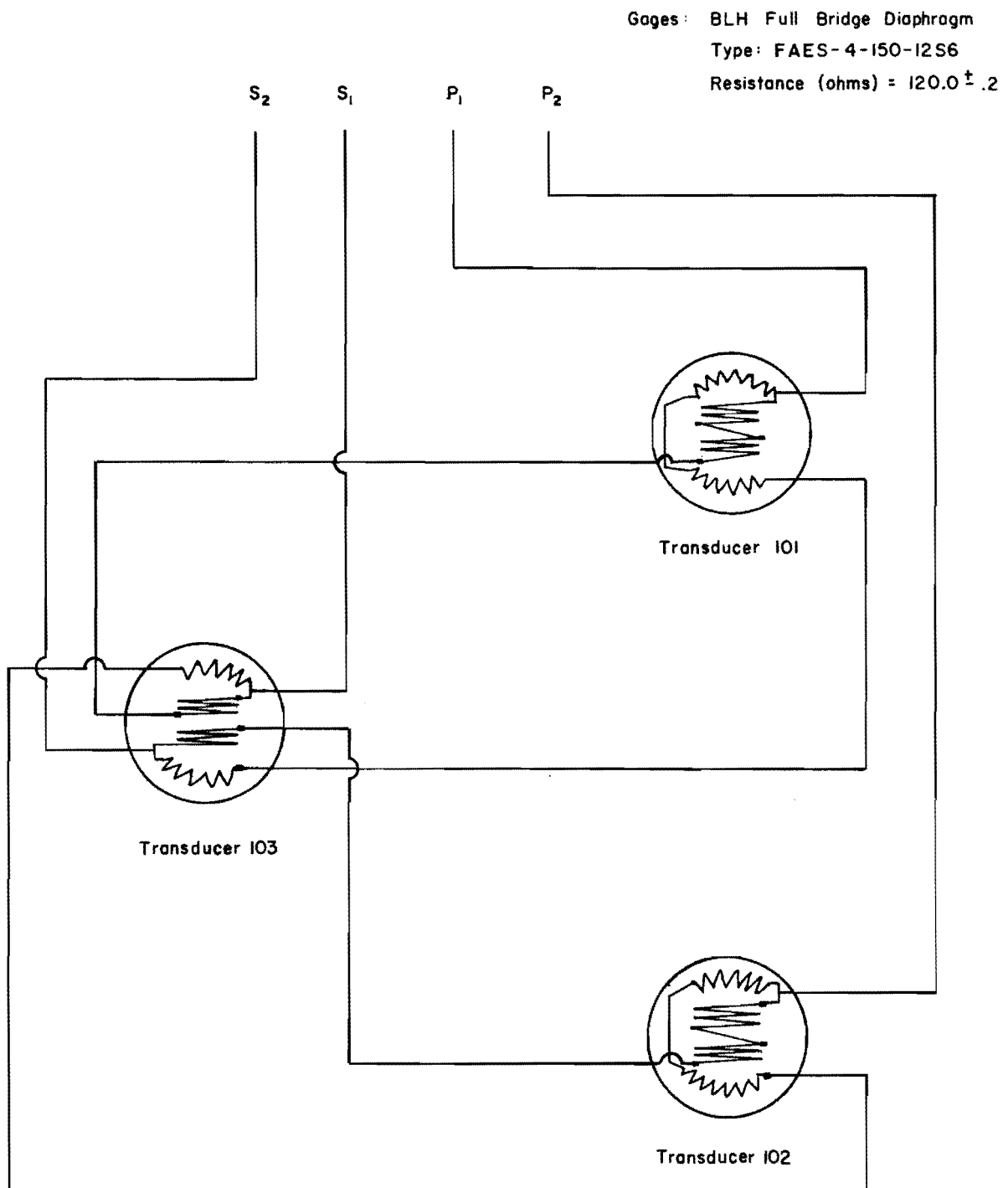


Fig. 2.6. Wiring Diagram for Bottomhole Cell

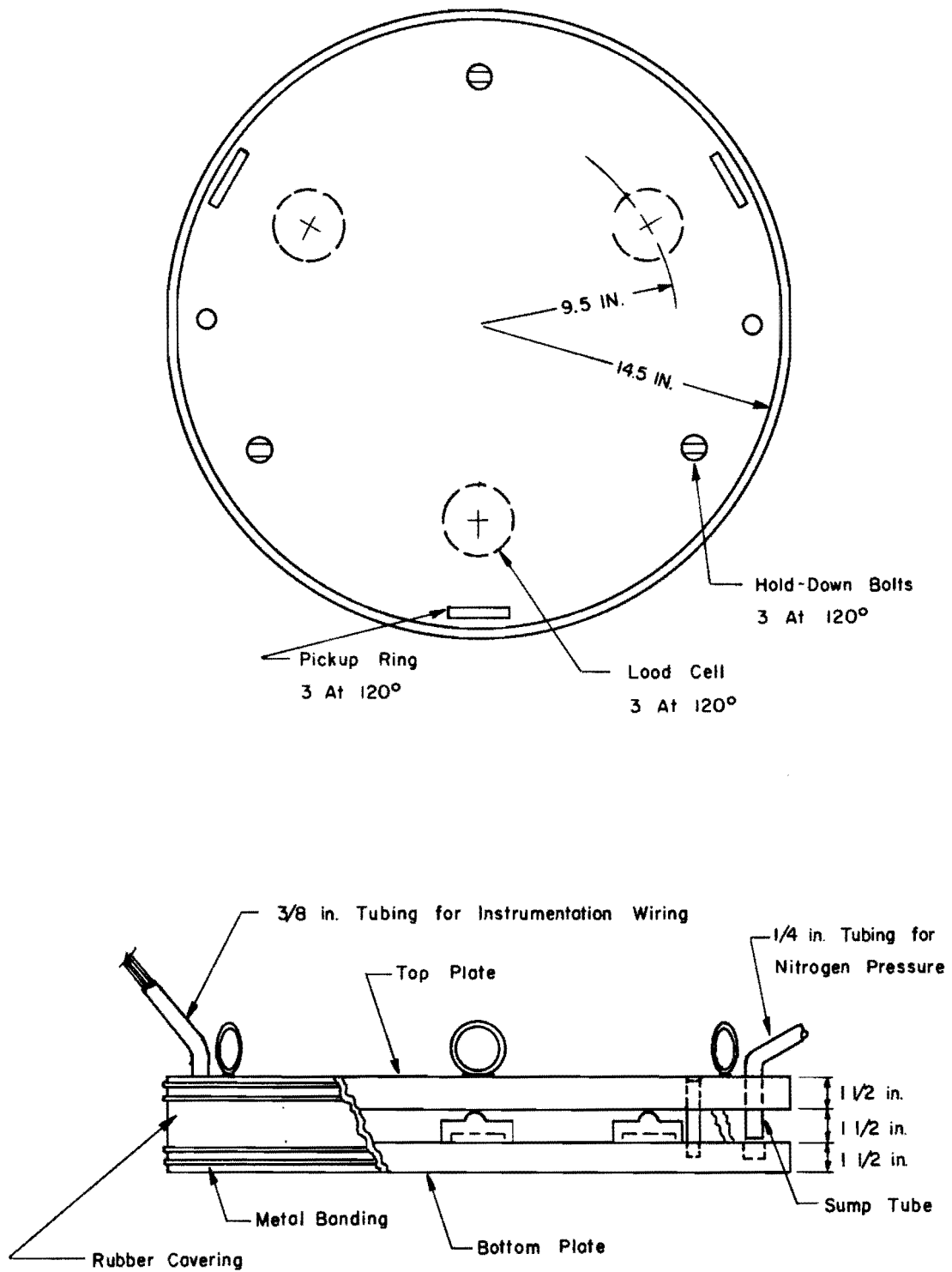


Fig. 2.7. Bottomhole Cell

### Mustran Cells Type 1 and Type 2

The Mustran cell has been developed at The University of Texas to meet specific needs of the drilled shaft project.

The principle of the Type 1 and Type 2 cells is the same in that deformation between two points in the shaft is measured by the use of strained bars which are instrumented with electrical resistance gages. The bar is a length of one-half-inch by one-half-inch mild cold-rolled steel bar. The bar is instrumented by the use of two 90° (tee) foil rosettes to form a full four-arm bridge circuit. An instrumented bar of cell Type 1 is shown in Fig. 2.8. The foil gages used were BLH-Type-FAET-25C-1256 having the specifications

Gage factor	2.02 ± 1%
Resistance	120 ohms ± .2

The ends of the bar are machined to form a one-fourth-inch diameter by one-half-inch-long threaded stud. The bar of the Type 1 cell is four inches long, shoulder to shoulder, with a reduced section in the center. The Type 2 cell has a bar 5-1/2-inches long, shoulder to shoulder, with a constant cross section. The end caps, identical for both types, were machined from 2-1/2-inch diameter cold-rolled mild steel. Construction details of cell Types 1 and 2 may be seen in Figs. 2.9 and 2.10, respectively.

In designing the cell an attempt was made to match the relative cell stiffness with the stiffness of the displaced concrete. The cell stiffness was adjusted by adjusting the length of the instrumented bar.

The design formulas for the Type 1 cell were derived by considering the deformation,  $\Delta_m$ , of the cell caused by an applied load,  $P$ .

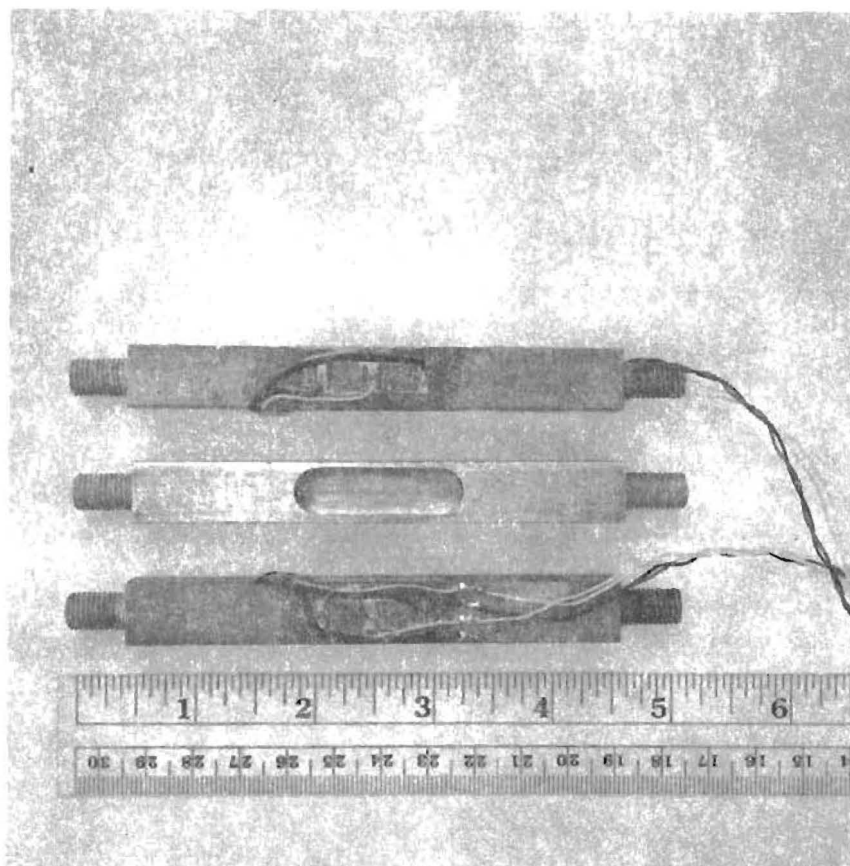


Fig. 2.8. Instrumented Bars of Mustran Cell, Type 1

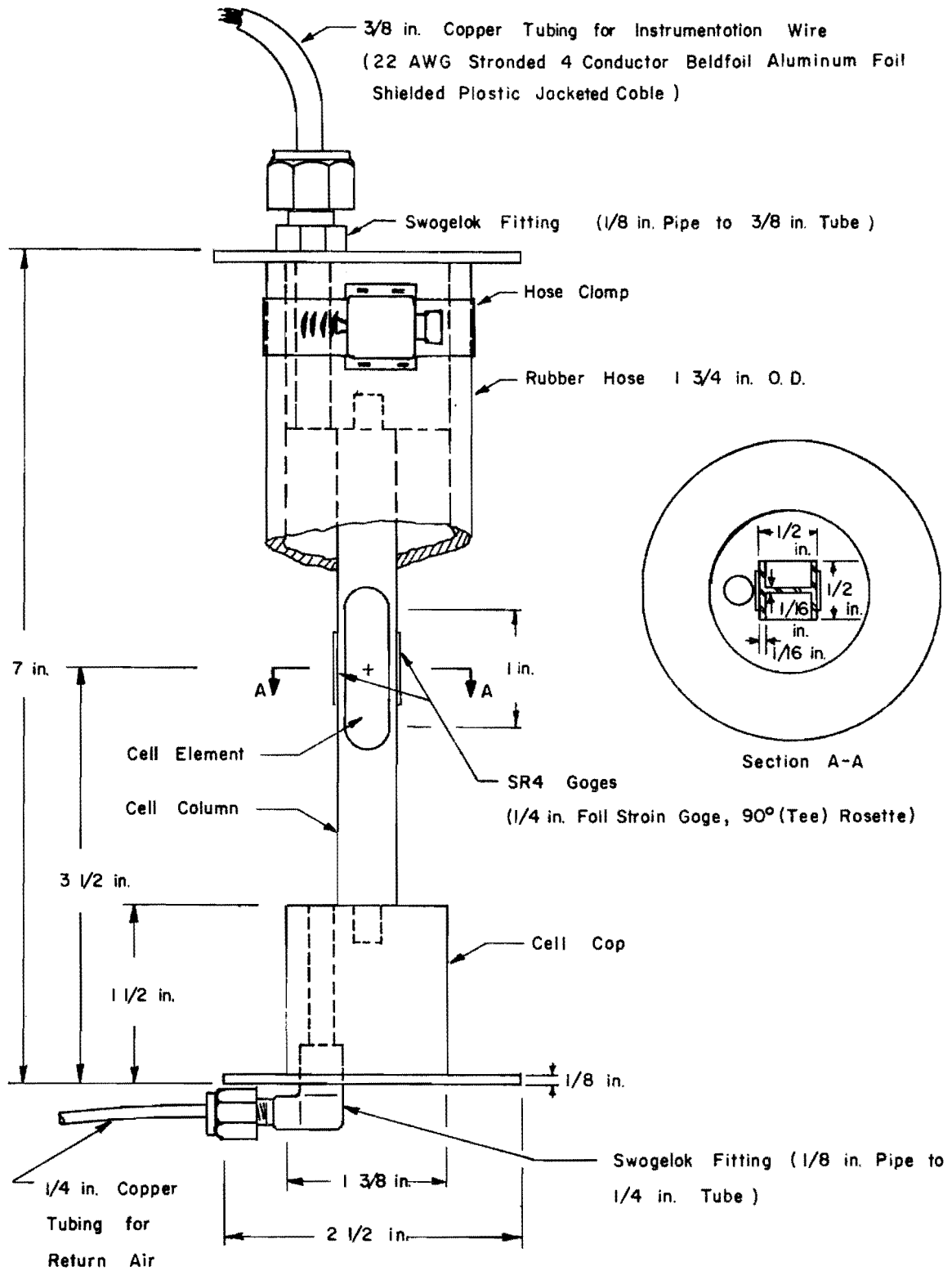


Fig. 2.9. Mustran Cell, Type 1

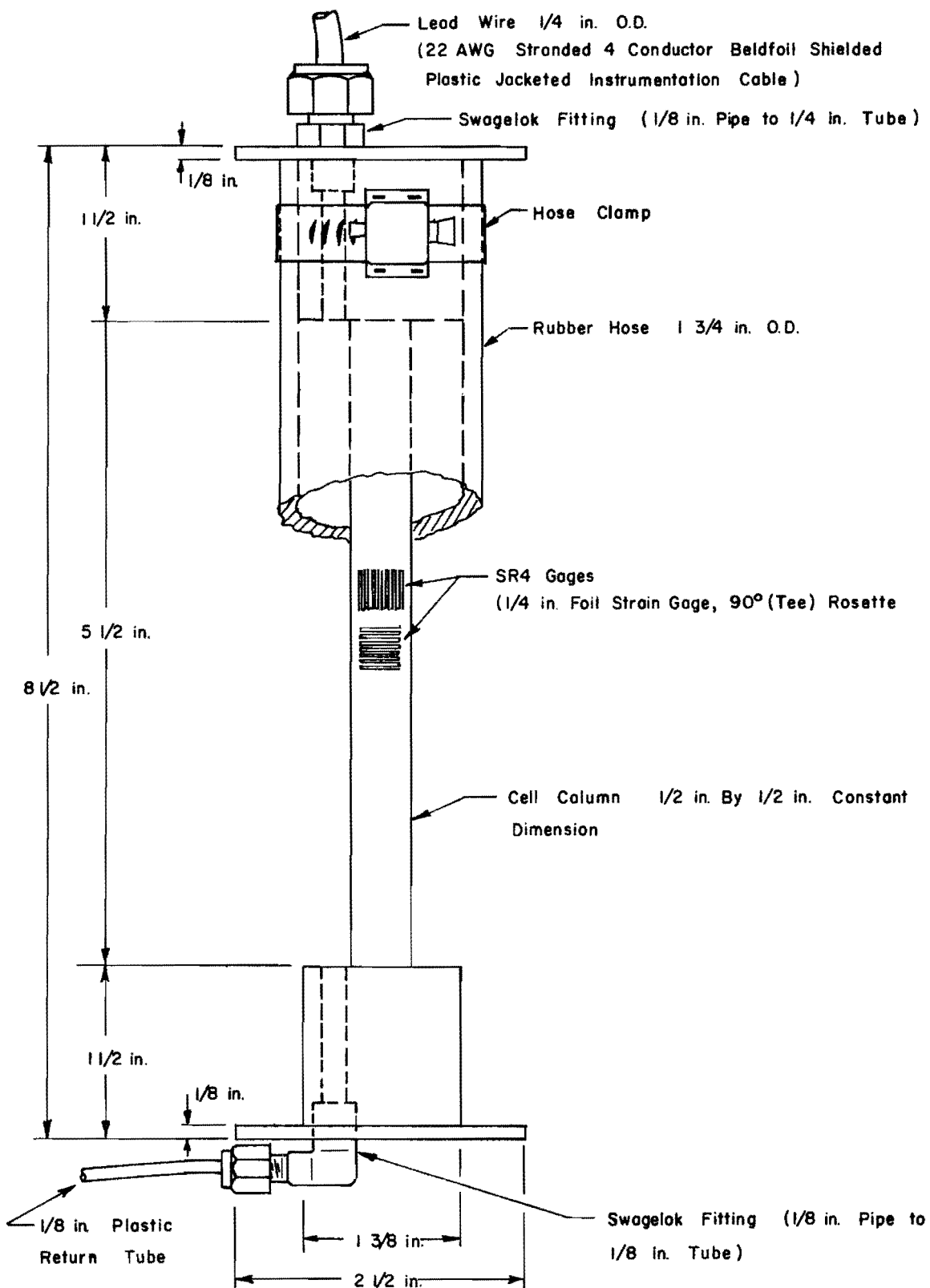


Fig. 2.10. Mustran Cell, Type 2

$$\Delta_m = \frac{2 \cdot L_E \cdot P}{A_E \cdot E_S} + \frac{L_B \cdot P}{A_B \cdot E_S} + \frac{L_R \cdot P}{A_R \cdot E_S} \dots \dots \dots (2.2)$$

where

- $E_S$  = the modulus of elasticity of the steel,
- $A_R$  = the area of the reduced section of the bar,
- $L_R$  = the length of the reduced section,
- $A_E$  = the area of one end cap,
- $L_E$  = the length of an end cap,
- $A_B$  = the area of the bar, and
- $L_B$  = the length of the bar not including the length of the reduced section.

If this same load,  $P$ , is applied to a column of concrete displaced by the cell, the deformation,  $\Delta_c$ , of the column is given by the equation

$$\Delta_c = \frac{P}{A_{cc} \cdot E_c} \cdot L_c \dots \dots \dots (2.3)$$

where

- $L_c$  = the length of the column of concrete,
- $A_{cc}$  = the area of the column, and
- $E_c$  = the modulus of elasticity of the concrete.

When the relative stiffness of the cell is equal to the stiffness of the concrete column the deformation of the cell will be equal to deformation of the column of concrete for the same load, P , which may be expressed in equation form

$$\Delta_c = \Delta_m \dots \dots \dots (2.4)$$

or

$$\frac{L_c \cdot P}{A_c \cdot E_c} = \frac{2 \cdot L_E \cdot P}{A_E \cdot E_S} + \frac{L_B \cdot P}{A_B \cdot E_S} + \frac{L_R \cdot P}{A_R \cdot E_S} \dots \dots \dots (2.5)$$

Substituting for  $L_c$  and dividing by P this becomes

$$\frac{2L_E + L_B + L_R}{A_c E_c} = \frac{2L_E}{A_E E_S} + \frac{L_B}{A_B E_S} + \frac{L_R}{A_R E_S} \dots \dots \dots (2.6)$$

By fixing all of the values except the length of the bar, the value of the bar length may be solved for in terms of the other parameters, the solution being given by the following equation.

$$L_B = \left[ 2 \cdot L_E \left( \frac{A_C E_C}{A_E E_S} - 1 \right) + L_R \left( \frac{A_C E_C}{A_B E_S} - 1 \right) \right] / \left( 1 - \frac{A_C E_C}{A_B E_S} \right) \dots (2.7)$$

For the Type 2 cell the length of the reduced section is zero; thus, the equation for the length of the steel bar would be as follows.

$$L_B = \left[ 2 \cdot L_E \left( \frac{A_C E_C}{A_E E_S} - 1 \right) \right] / \left( 1 - \frac{A_C E_C}{A_B E_S} \right) \dots \dots \dots (2.8)$$

Solutions of the equations with the concrete modulus as the independent variable are shown in graph form in Fig. 2.11. In the graph the total gage length,  $L_E + L_B + L_R$ , is plotted versus the concrete modulus of elasticity. As may be noted in the graph, the cell length for cell Type 1 is very sensitive to changes in concrete modulus. Since it is not practical to match the relative stiffness of the cell exactly to the stiffness of the displaced concrete, it is felt that it would be more desirable to have the cell more flexible than expected for the column of concrete. With the cells embedded in a large mass of concrete such as a drilled shaft, it is believed, the difference in stiffness would not introduce significant error.

Also considered important in the design of the cell are construction details which provide for protection both during and after placement of the shaft. The lead wire is brought through the top end cap and through a ferrule tube fitting. The lead wire may be brought to the surface either through tubing or bare. The cell shown in Fig. 2.9 was for use of copper tubing and the cell shown in Fig. 2.10 was for use without tubing. If tubing is used, the wire is threaded through the tubing and the tubing is inserted in the fitting at the top end cap. In the case where the wire is not enclosed, the ferrule fitting is clamped directly on to the wire insulation.

Waterproofing is provided by encasing the bar in a 1-5/16-inch I.D. rubber radiator hose which is clamped to the end caps by hose clamps. The cavity around the bar may be partially filled with anhydrous calcium chloride to absorb any moisture in the cell. Additional protection against the entry of water may also be provided by a pressure system which maintains a positive pressure in the cell and lead wire. The pressure system changed with each shaft installed and is presented later for each shaft.

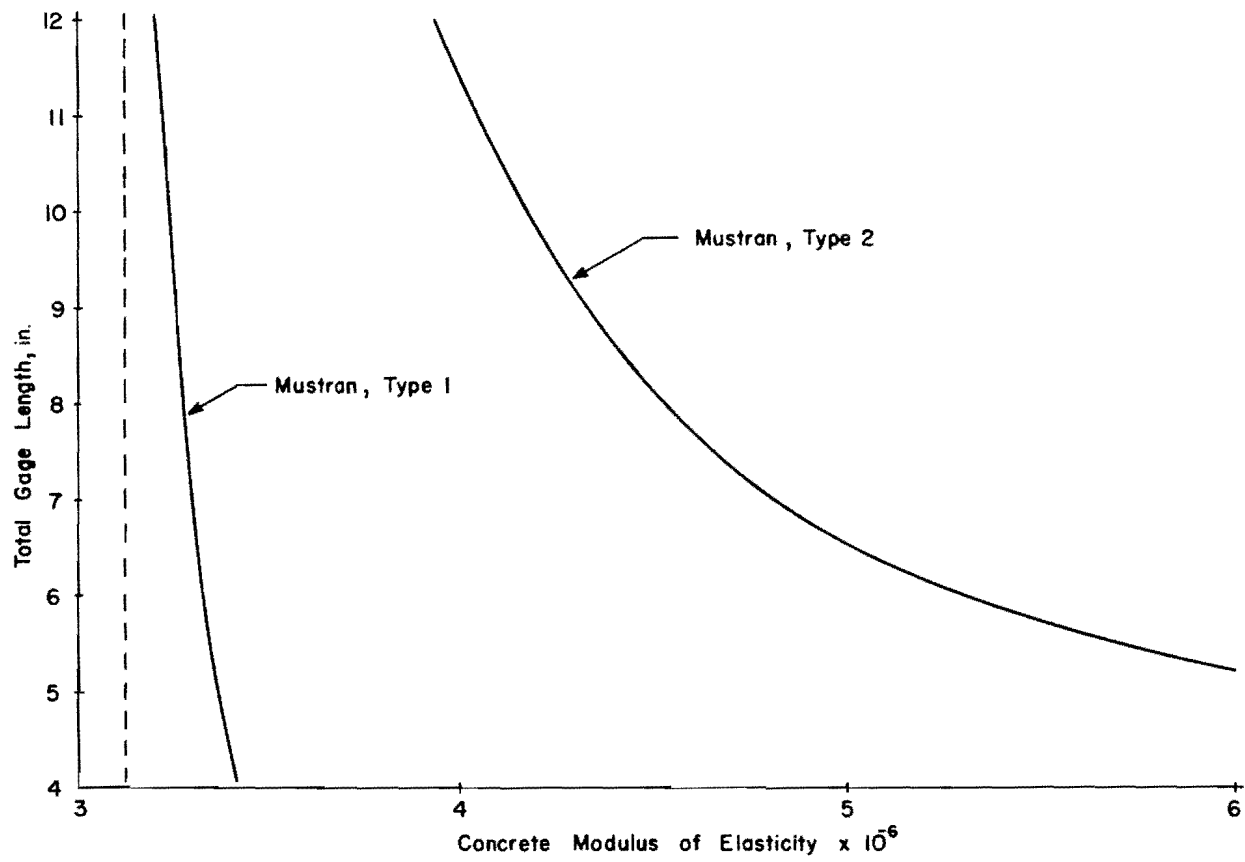


Fig. 2.11. Design Curve for Mustran Cells

The four photographs in Fig. 2.12 demonstrate the steps in the assembly of a Mustran cell.

Studies of the Type 1 cell were conducted in the laboratory to determine the relationship between concrete stress and the output from the cell. The cells were loaded by applying a load directly to the end caps and the cell output was read using a strain-indicator. A typical curve showing applied load versus strain gage reading is given in Fig. 2.13.

The cells were then cast in four inch by four inch by twelve inch concrete blocks. Cast along with the Mustran cells were embedment gages to determine the "true" concrete strain. The results of the tests conducted on the blocks are presented in Fig. 2.14. From the tests a strain multiplication factor of 5.5 was obtained for the cell. The cell was thus named Mustran which stands for Multiplying Strain Transducer. The observed value of 5.5 does not compare favorably with a value of 7.6 calculated analytically. The difference between the observed factor and the calculated factor is probably due primarily to inaccuracies in machining and to stress concentrations around the threaded ends of the gage bar.

Considering the inconsistency in the calculated multiplication factor and the laboratory observed multiplication factor, it was considered advisable to make in-shaft calibrations for the Mustran cells.



Fig. 2.12. Steps in Assembly of a Mustran Cell

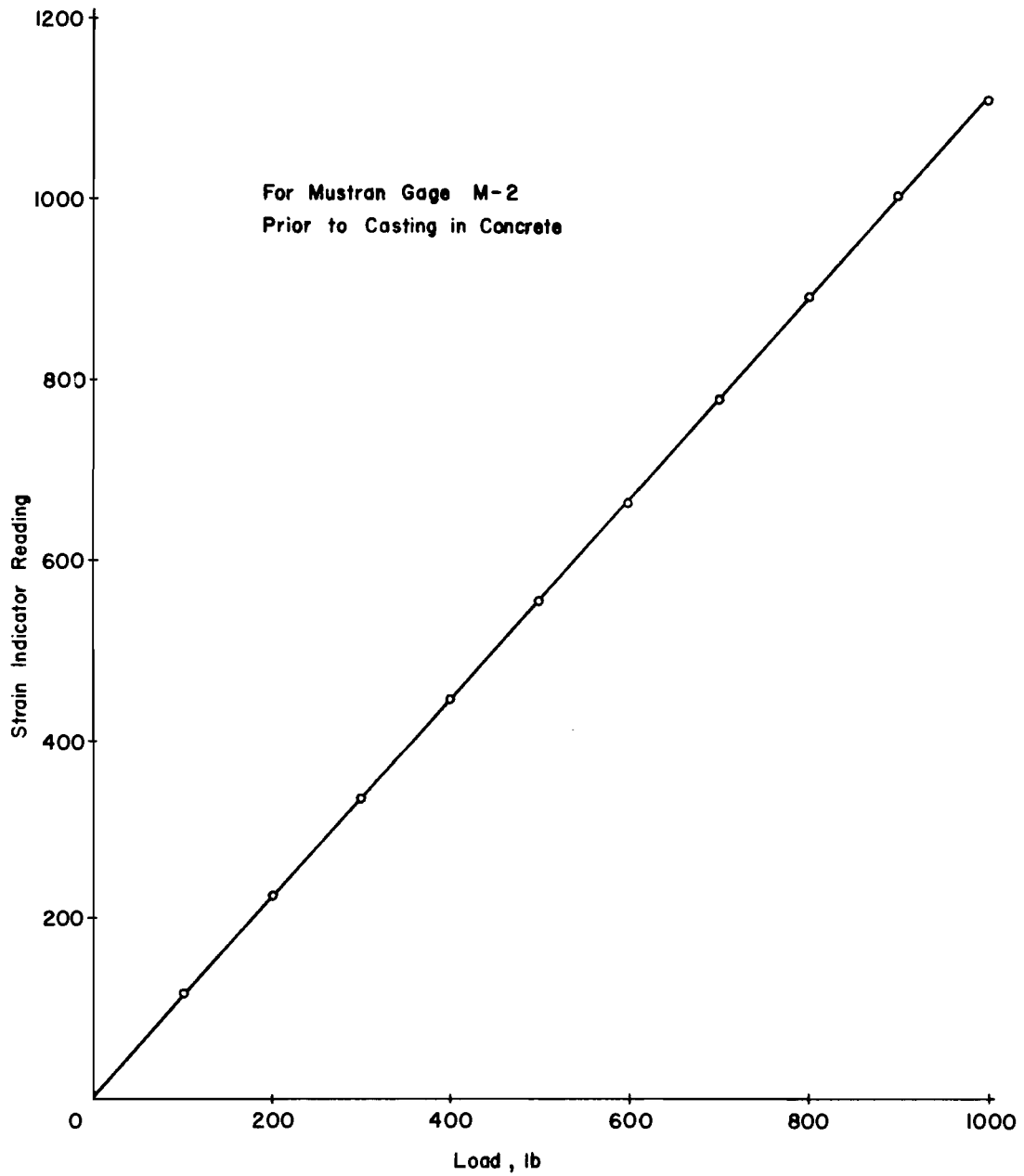


Fig. 2.13. Calibration Curve for Mustran Cell, Type 1,  
Prior to Casting in Concrete

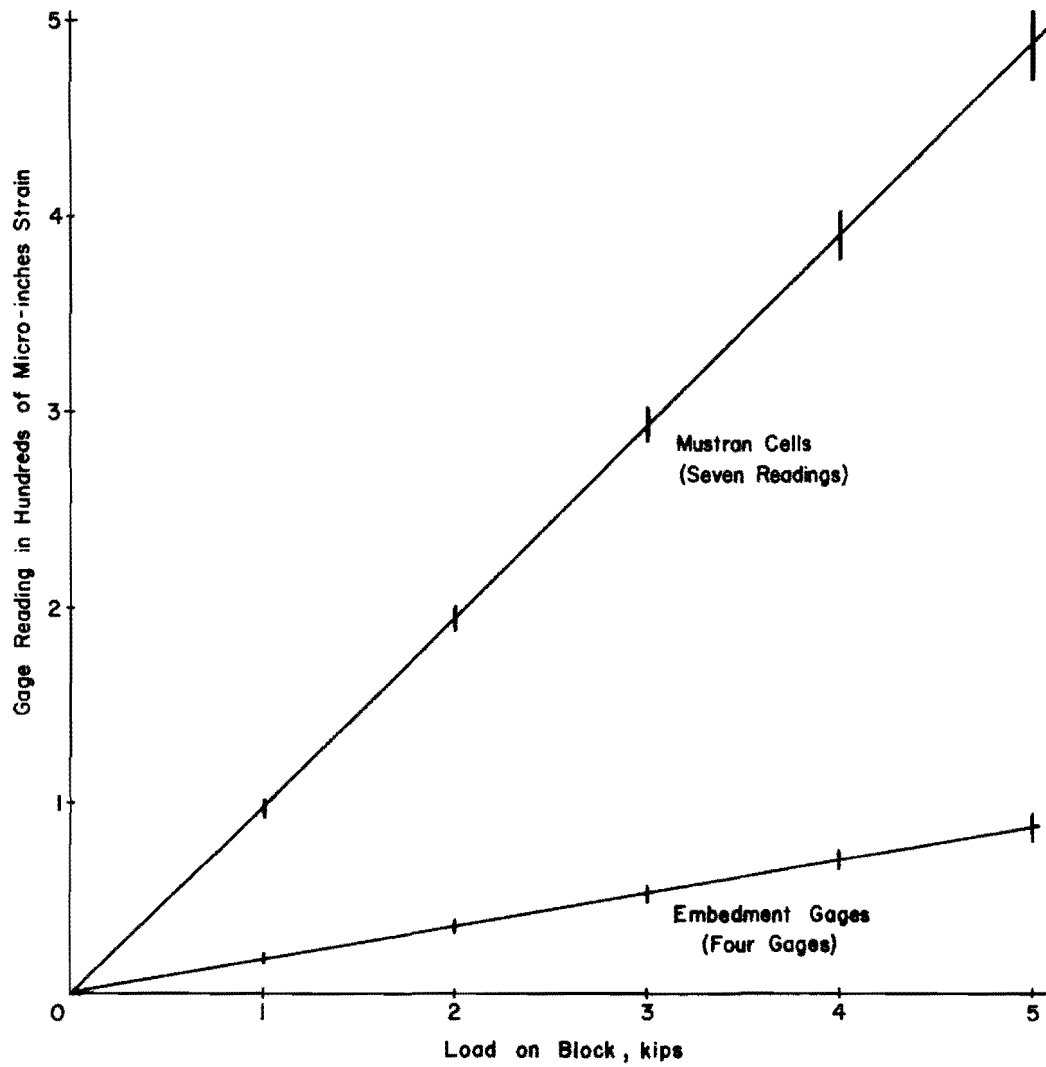


Fig. 2.14. Calibration Curve for Mustran Cell, Type 1, After Casting in Concrete Block

This page replaces an intentionally blank page in the original.

-- CTR Library Digitization Team

## CHAPTER III

### MONTOPOLIS AND SAN ANTONIO TEST SITES

#### Montopolis Test Site

At the Montopolis site, located near the community of Montopolis, a single shaft was instrumented and tested. The primary purpose of this shaft was to develop instrumentation, loading equipment, and technique as a precursor to the more complex tests to follow.

The shaft installed at this site on August 18, 1966, was 24 inches in diameter and 13 feet 4 inches long, with 12 feet 0 inches below the ground surface. The instrumentation consisted of three levels of telltales, three levels of embedment gages, three levels of thermocouples, and two levels of lateral pressure cells. The location of the instrumentation is shown in Fig. 3.1.

Embedment Gages. All embedment gages were precast in concrete blocks of three inches by seven inches by one inch. The blocks were fitted with wires to provide a means of anchoring the gages to the shaft. At each level four axial measuring gages were placed, each being used as a single active element in a Wheatstone bridge. To serve as a dummy in each circuit and to minimize temperature variations, an embedment gage was cast in a concrete block and buried a short distance from the shaft at a depth of six feet. A pair of 10-channel "switch and balance" units and a manual balance strain indicator were used in the readout of these embedment gages.

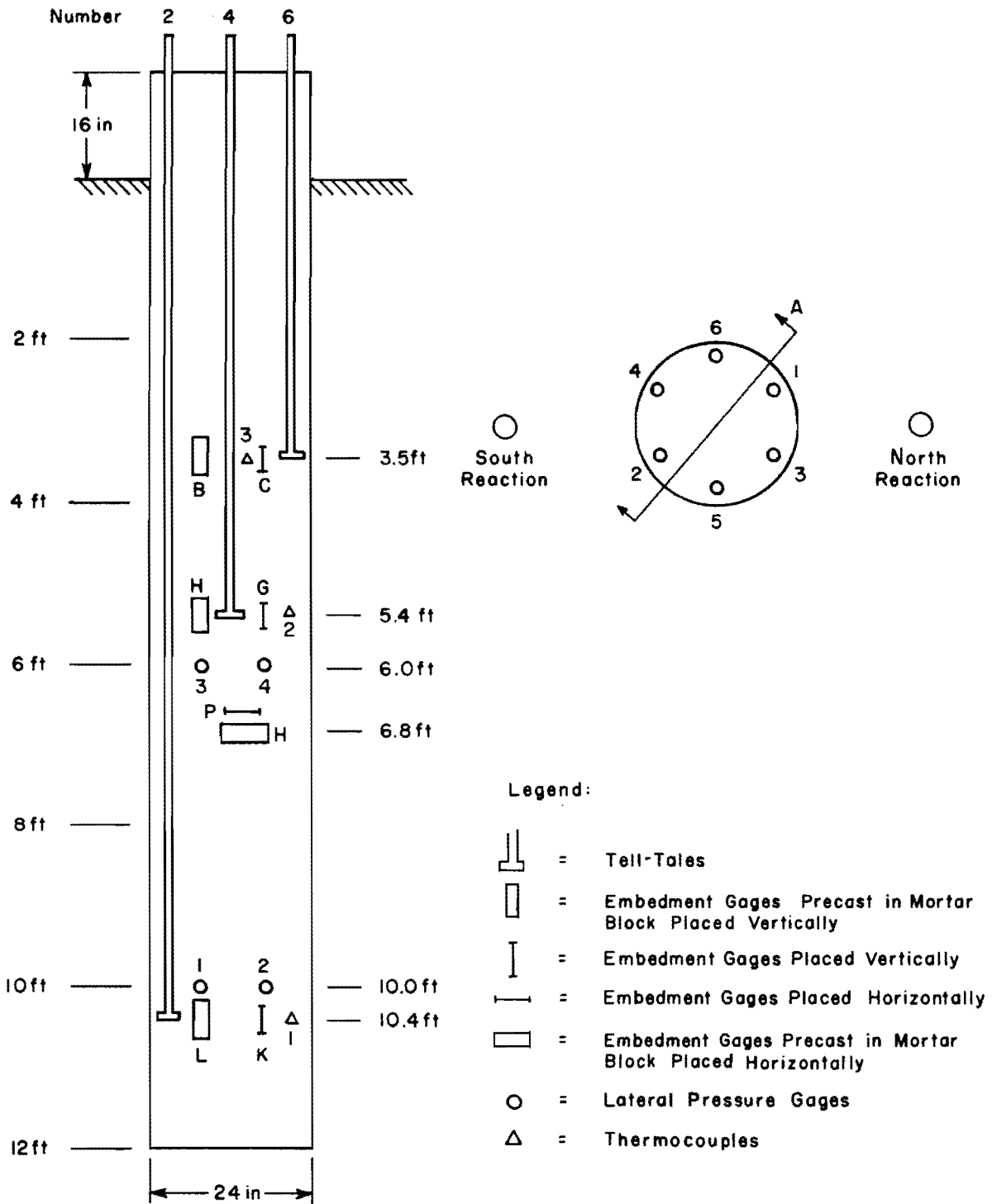


Fig. 3.1. Locations of Strain Gages, Telltales, Lateral Pressure Gages and Thermocouples for the Montopolis Site (After Reese and Hudson, Ref. 13)

Telltales. The system of telltales, as previously described, was installed. At each level two telltales were installed on opposite sides of the shaft, which in theory would compensate for any bending which may occur in the shaft.

Readout was obtained by the use of .0001-inch Ames dial indicators.

### Load Application

Application of the load was accomplished through the use of a 400-ton hand-operated hydraulic jack. The applied load was measured by use of a Bourdon pressure gage. The pressure reading was converted to load with a jack calibration factor. The loading head, settlement gages, and telltales are shown in Fig. 3.2.

### Test

A total of eight tests was carried out at this site. The testing covered the time period from October 5, 1966 to March 22, 1967. The first four tests were conducted to develop a suitable loading procedure and to check the instrumentation. For the last four tests the load was increased until failure of the shaft was accomplished. Failure for the purpose of these tests is defined as the point at which it is no longer possible to hold constant the applied load.

### Results

Within a few weeks of the installation of the shaft all of the embedment gages indicated low resistance to ground. It was suspected that water had penetrated through the splice in the lead wire. During the test, considerable drift in strain gage readings made analysis of the data difficult.



Fig. 3.2. View of Loading Head, Settlement Gages, and Telltales at the Montopolis Site (After Reese and Hudson, Ref. 13)

At the time it was felt that the drift was due either to moisture in the leads or to temperature changes at the external dummy. To reduce this drift it was suggested that the dummy be located in the shaft at the same level as the active gage, and that greater care be taken in waterproofing of splices.

The telltales gave results which indicated the general trend of load transfer. From the test it was concluded that the telltale system as installed provided a workable system.

The complete details of the Montopolis test are given by Reese and Hudson (Ref. 13).

#### San Antonio Test Site

This test site was located in San Antonio close to the intersection of SW Military Drive and U. S. Highway 90. The test shaft, installed on January 18, 1967, was 28 feet 6 inches long with 26 feet 8.5 inches below the ground surface. The instrumentation of the shaft consisted of seven levels of telltales and embedment gages, two levels of lateral pressure gages, and three levels of thermocouples. The locations in the shaft of these instruments are shown in Fig. 3.3.

Embedment Gages. Three active gages were provided for each embedment gage level with the exception of the bottom level where four were provided. As in the Montopolis test each active gage was precast in a seven inch by three inch by one inch mortar block and attached at approximately even spacing around the reinforcing cage. For each level a dummy gage to complete a half-bridge circuit was placed in a sealed container and cast in the shaft

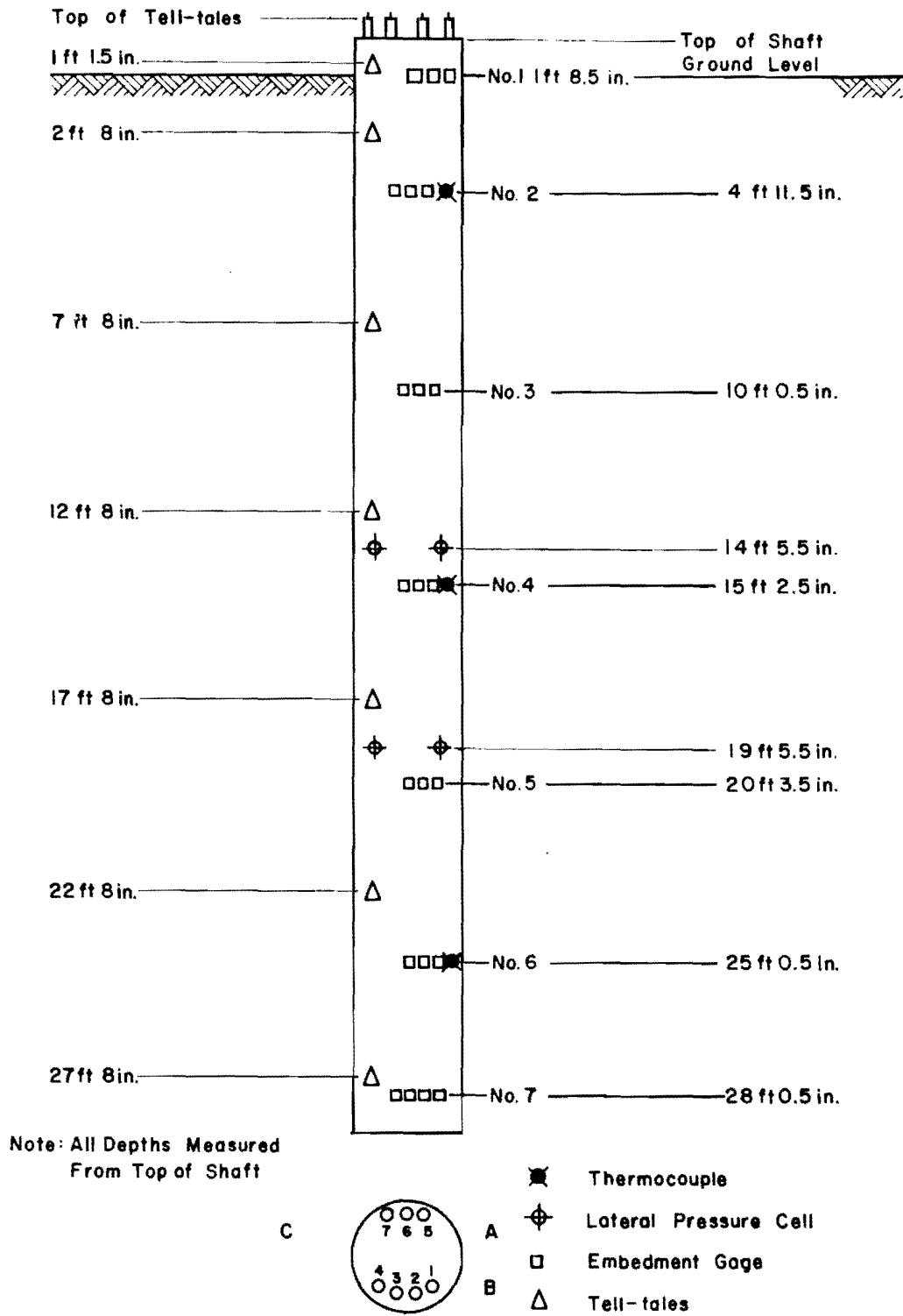


Fig. 3.3. Location of Embedment Gages, Lateral Pressure Cells, Telltales, and Thermocouples at the San Antonio Site (After Vijayvergiya, Ref. 14)

at the same level as the active gages. Great care was taken to waterproof all splices made in the lead wire.

The arrangement of the top level of embedment gages and telltales is shown in Fig. 3.4.

The readout system for the embedment gages was the same as was used in the Montopolis test.

Telltales. The same number of levels of telltales and embedment gages was used, but the depth of the levels was not the same. At each level only one telltale was installed, using the same installation procedures used at the Montopolis site.

#### Test Results

A total of five tests was conducted on the shaft between June 21, 1967 and May 14, 1968. Again, as in the Montopolis test, the embedment gages were troubled with temperature drift and low resistance to ground. Vijayvergiya (Ref. 14) concluded that the embedment gages could be used reliably only for short-term studies since with the passage of time the water migrates into the gages. Also concluded was that the dummy gage was not effective for temperature compensation and that additional work was needed to reduce the gage drift.

The telltale system worked fairly well with the exception of the telltales shorter than 10 feet, which seemed to be affected by the temperature variations. Thus, it was concluded that only for heavily loaded shafts was the telltale system satisfactory.

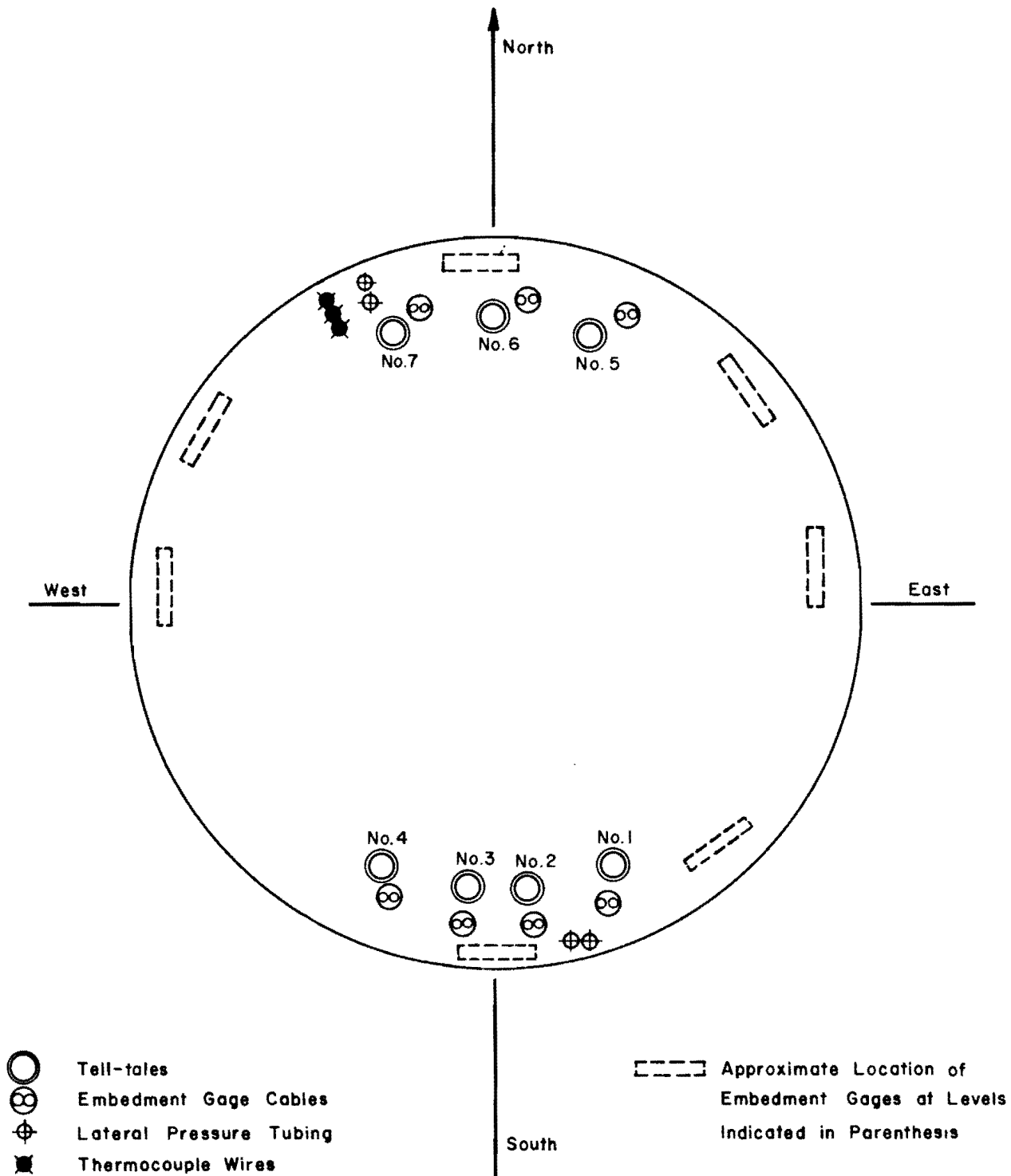


Fig. 3.4. Plan of the Shaft at the San Antonio Site Showing Details of Instrumentation (After Vijayvergiya, Ref. 14)

CHAPTER IV  
HOUSTON SH 225 TEST SITE

This test site is located in the southeastern part of Houston at the proposed interchange of Loop 610 and State Highway 225. Two shafts have already been test loaded at this site, with an additional two shafts scheduled for construction and testing during the summer of 1969.

The soil in the upper 30 feet at the site is a stiff fissured clay having a shear strength of approximately 1.0 ton per square foot. The average values of the Atterberg limits were plastic limit 23, liquid limit 63, and plastic index 40. On the unified classification system, the soil would classify as a CH. The soil was considered to be only moderately active.

The ground elevation at the site is approximately +35 feet with the water table elevation at +7 feet. In the area, the weather is very humid for most of the year. The average yearly rainfall is about 50 inches. The humid weather combined with the industrial atmosphere of the area compound the difficulties in instrumenting a drilled shaft.

Shaft 1

Shaft 1 at the Houston SH 225 site is a 30-inch diameter straight shaft 25 feet 10 inches long with 23 feet 6 inches below ground surface. Instrumentation for the shaft consists of four levels of Mustran cells, six levels

of embedment gages, six levels of telltales, one Gloetzl cell, one bottomhole cell, and three levels of thermocouples. The primary instrumentation for measurement of the axial load was to be embedment gages, telltales, and the bottomhole cell. The location of the instrumentation is given in Fig. 4.1. For the Mustran cells and Gloetzl cell, this was a test to evaluate them as methods of measuring axial loads in a drilled shaft.

Embedment Gages. In an attempt to increase stability, two complete bridge circuits were installed at each level. The dummy gages were placed in a sealed container and embedded in the shaft at the same level as the active gages. As additional protection against moisture, the lead wires from the active arm to the junction container were placed inside flexible rubber tubing, and the lead wires from the junction were run to the surface through one-half-inch outer diameter copper tubing. All splices were made inside of the sealed container. Prior to installation in the shaft the system was purged with dry nitrogen and sealed. In Fig. 4.2 a complete embedment gage assembly is shown. Note that all lead wires from the dummy junction to the gages were enclosed in flexible rubber tubing. The wire from the junction to the surface was enclosed in copper tubing after installation in the reinforcing cage of the shaft.

Telltales. The same procedure was used in installing the telltales at this site as was used at the San Antonio site, one telltale being installed at each level.

Gloetzl Cell. The Gloetzl cell was embedded in the shaft just above the ground surface. Placement was accomplished by stopping the concrete pour at the desired level and hand placing the cell in the shaft. The pressure lines were taken out through the sides of the shaft to the pump.

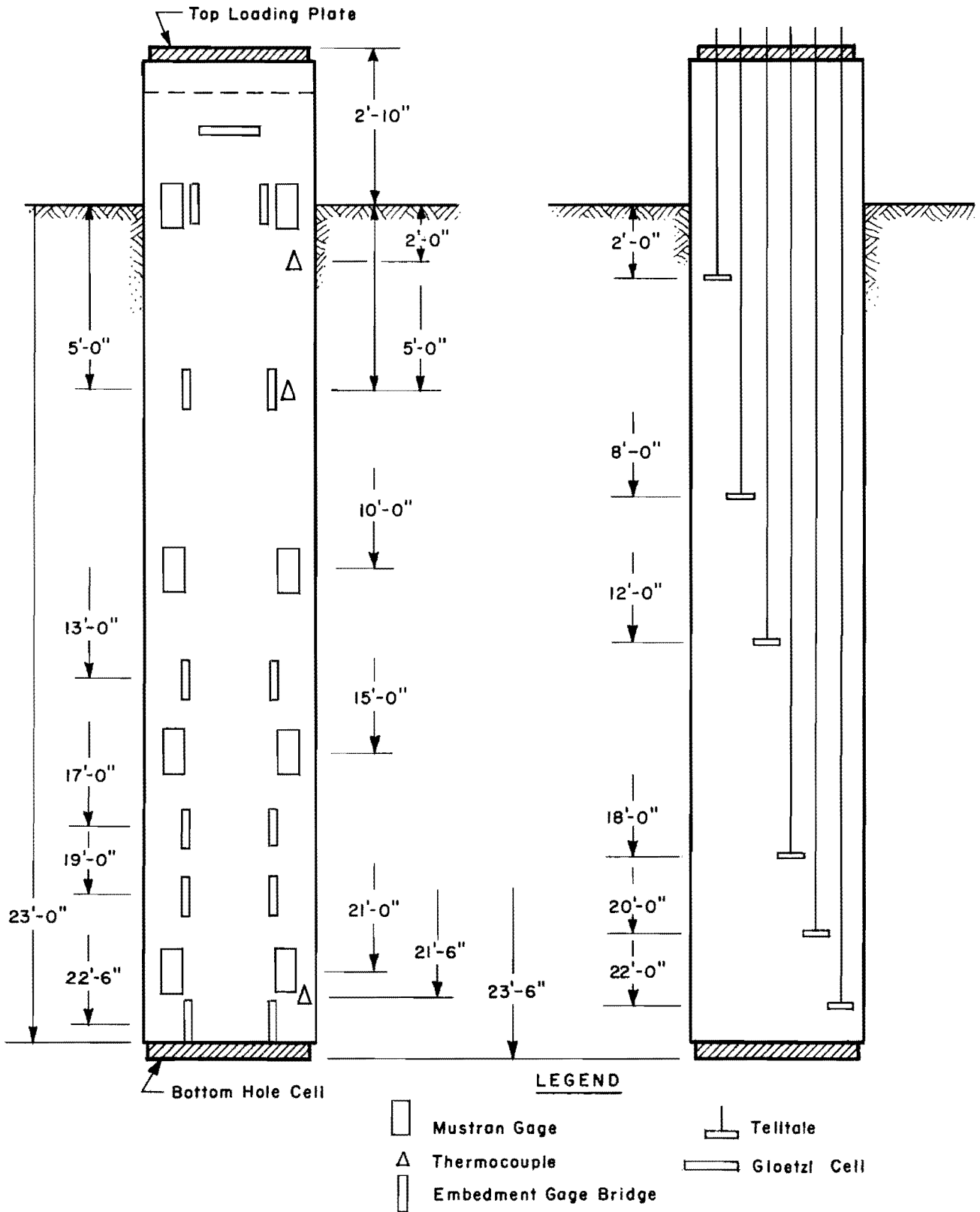


Fig. 4.1. Location of Instrumentation, Houston SH 225 Site, Shaft 1

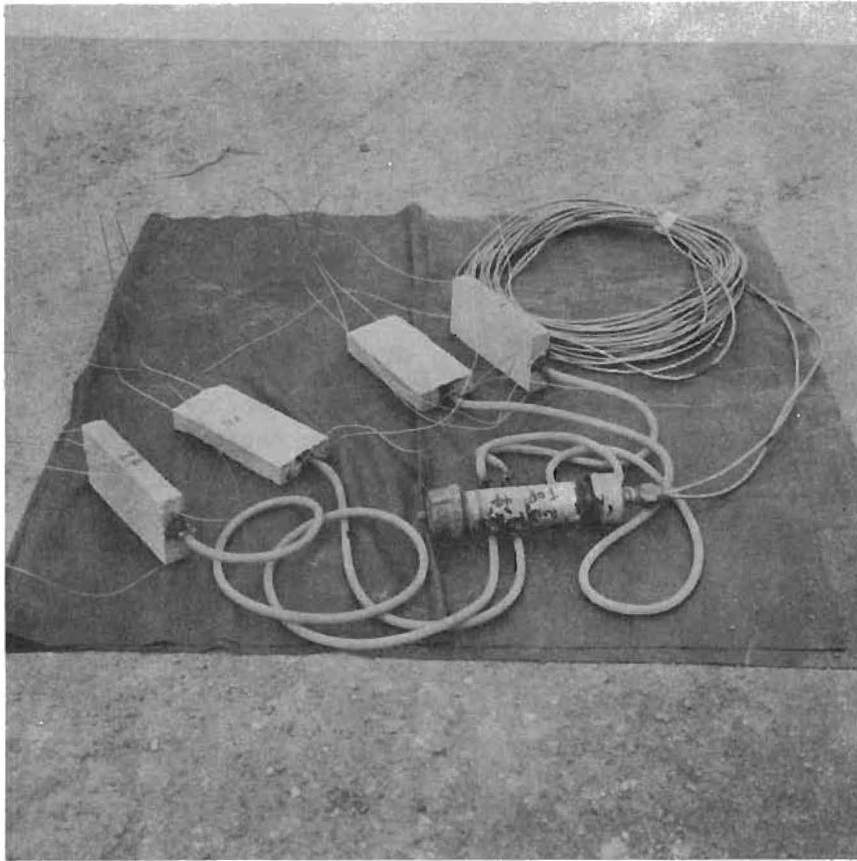


Fig. 4.2. Embedment Gage Assembly

Bottomhole Cell. The bottomhole cell was placed at the bottom of the hole, using a crane, as shown in Fig. 4.3. After placement and during the time that the cell was being connected to the pressure system, water seeping into the hole covered the cell with approximately two inches of water. With the application of pressure to the system, nitrogen could be seen bubbling through the water covering the cell. Due to the amount of nitrogen escaping, keeping pressure on the system for any length of time would have been impossible. As an alternative to the pressure system, the cell was filled with a nonconductive transformer oil. After filling, the ends of the copper tubing were capped and sealed. Once prior to the first test and once after the first test, new oil was pumped down the tubing containing the lead wire. This oil forced any water which had seeped into the cell up the return line. Pumping oil into the cell continued until all the water in the cell had been expelled. Thus, the bottomhole cell was kept operable for as long as possible.

Mustran Cells. The Mustran cells for Shaft 1 were of the Type 1 design, shown in Fig. 2.9, and were constructed to provide for a circulating nitrogen pressure system. Since Shaft 1 was the first shaft in which Mustran cells had been used, this was an evaluation test for the Mustran cells.

Each cell was precast in a four inch by four inch by twelve inch concrete block as shown in Fig. 4.4. The U-bolts and seating groove seen in Fig. 4.5 were provided to obtain positive anchorage to the cage reinforcing. The blocks containing the cells may be seen attached to the vertical reinforcing in Fig. 4.5. After attachment the lead wire was threaded through a three-eighths-inch outer diameter copper tubing which was to extend out



Fig. 4.3. Placing of Bottomhole Cell

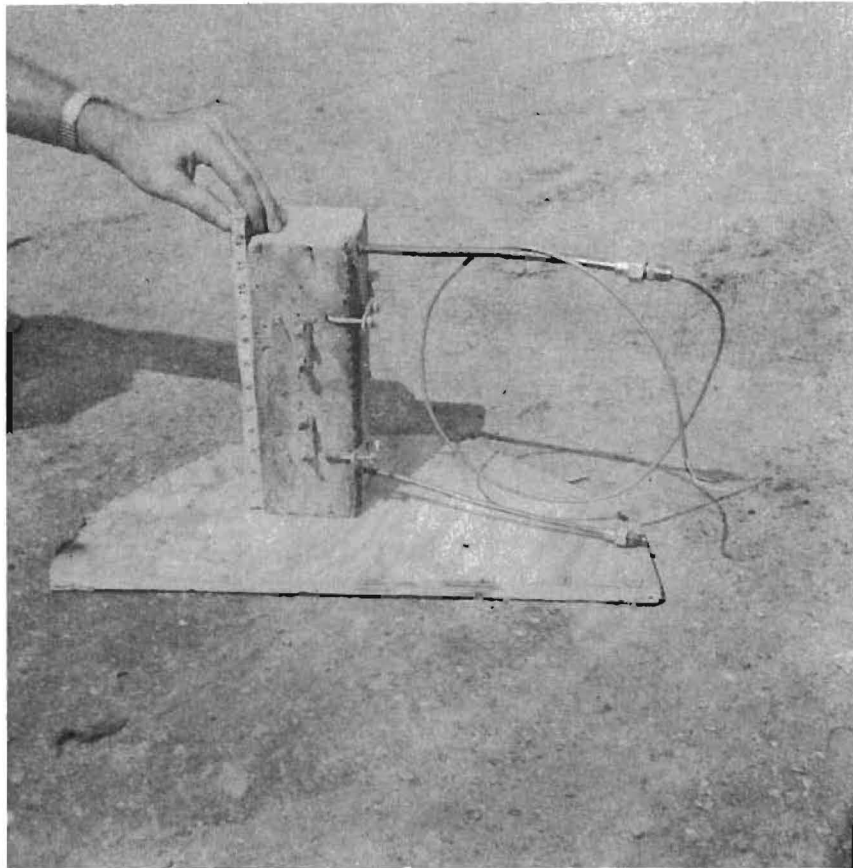


Fig. 4.4. Mustran Cell Cast in Concrete Block

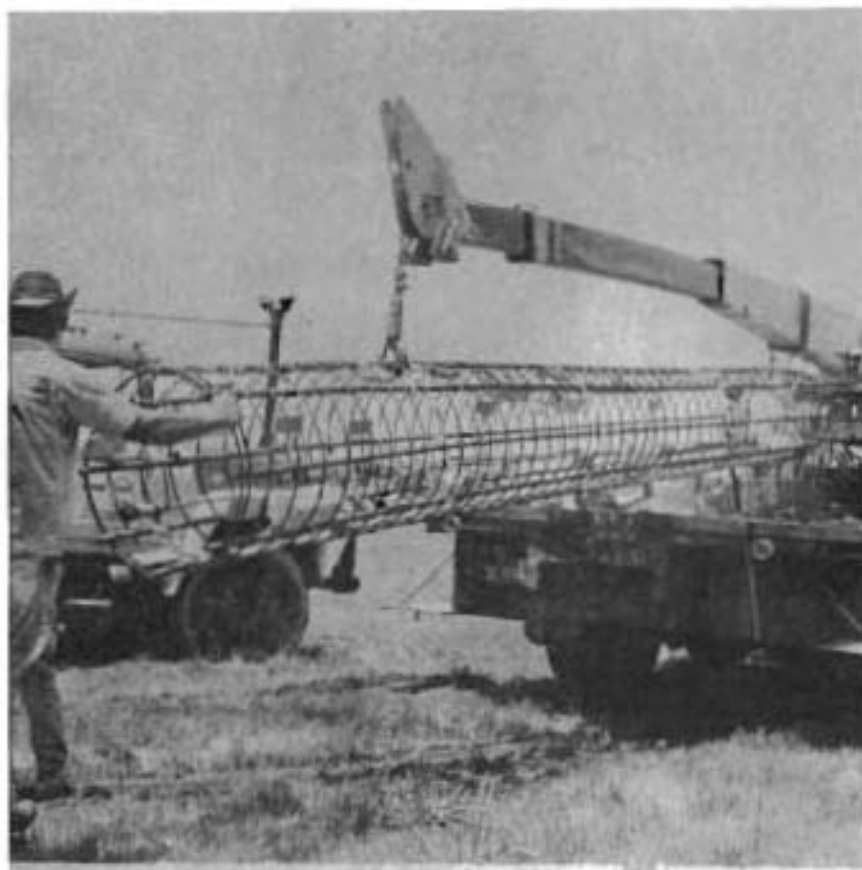


Fig. 4.5. Instrumented Reinforcing Cage

the top of the shaft. A feed-through device was made by driving pins through a teflon plug to which the leads were soldered. A one-quarter-inch outer diameter copper tubing was run from the bottom of the cell out the top of the cage to a manifold system. Pressure was applied to the manifold from a nitrogen supply through a pressure regulator. A schematic of the system is shown in Fig. 4.6.

Installed in the shaft were two cells at each of four levels for a total of eight cells. After installation two cells showed low resistance (less than  $10^6$  ohms) to ground. This was probably due to collection of moisture in the cells prior to installation of the pressure system. By circulating nitrogen through the faulty cells the resistance was brought up to an acceptable value.

During and after the placing of the concrete a pressure of approximately 10 psi was maintained on the system. This pressure was maintained at all times except while readings were being taken, until January 6, 1969, at which time the nitrogen supply was removed from the system.

#### Load Application

To apply the load, only one 500-ton hydraulic jack was required. The pressure to the hydraulic jack was supplied by an air-operated hydraulic pump. The system is shown in schematic in Fig. 4.7. The applied load was measured by use of a Bourdon pressure gage as was done at San Antonio and Montopolis. The loading head, jack system, and pumping system are shown in Fig. 4.8.

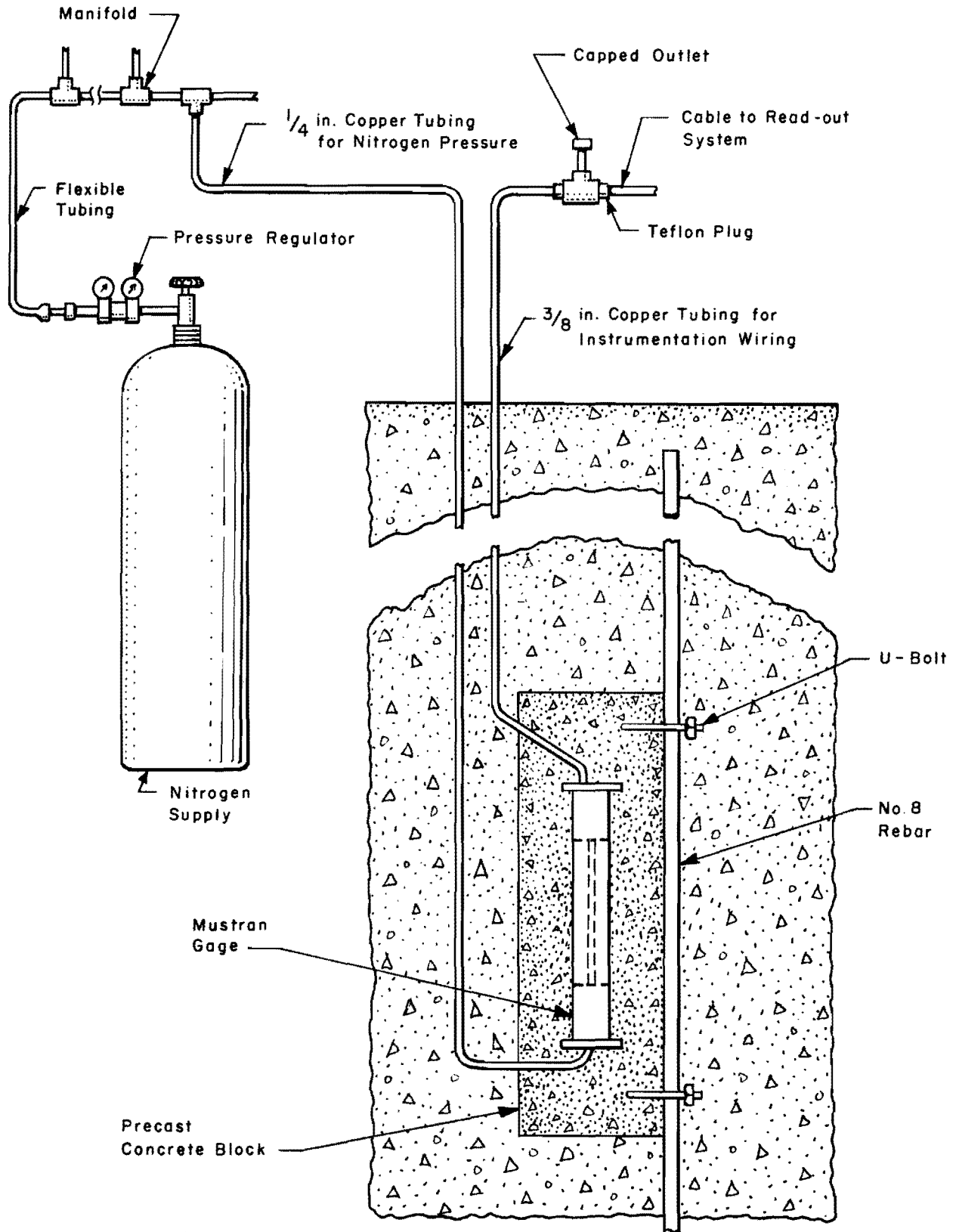


Fig. 4.6. Schematic of Mustran Instrumentation System, Houston SH 225 Site, Shaft 1

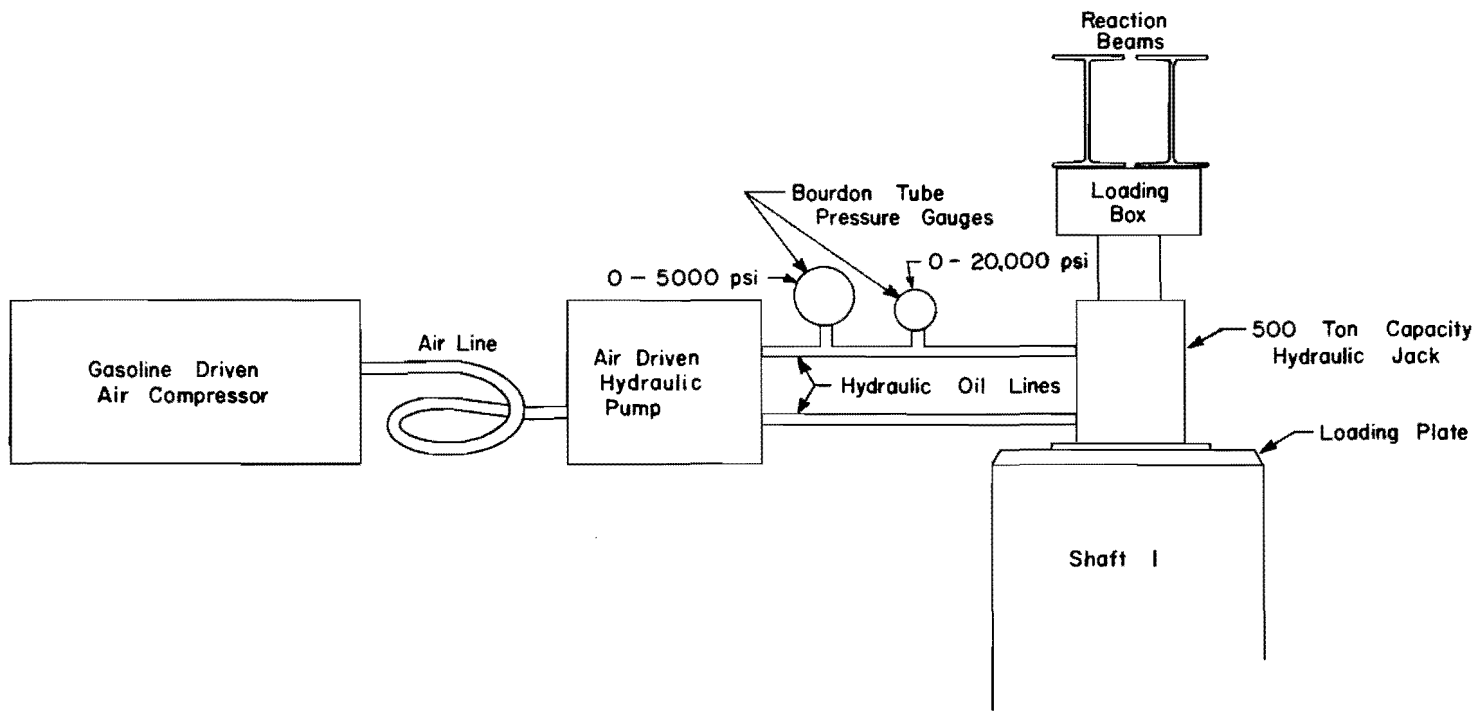


Fig. 4.7. Schematic of Loading System



Fig. 4.8a. Shaft Head and Loading Jack

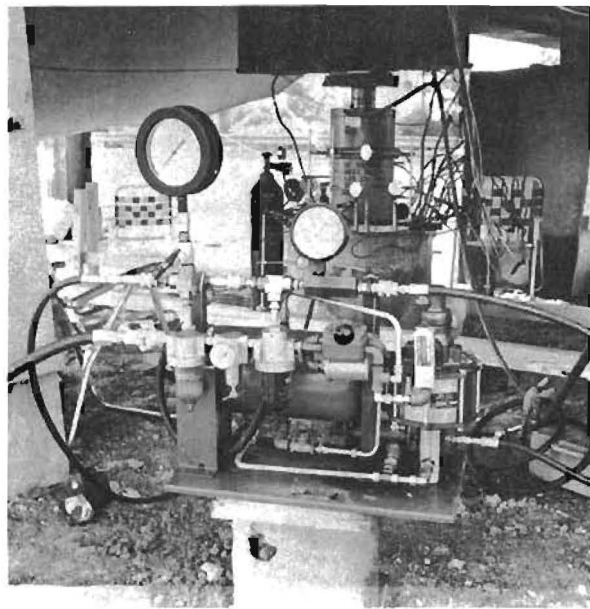


Fig. 4.8b. Hydraulic Pump for Applying Load

Readout System for Embedment Gages, Bottomhole Cell, and Mustran Cells

Primary power of 110 volts AC was provided by a single 3 KW portable generator. Measuring bridge power was regulated at 6 volts DC by a 0.01 per cent regulated electronic power supply unit.

Data from the electrical instrumentation was recorded in digital form using the Honeywell Model 620 Data Logging System, as shown in Fig. 4.9. The full-bridge circuits were connected through a balancing circuit to a 40-channel stepping switch scanner. The scanner routed the measuring bridge outputs to an automatic ranging digital voltmeter which drove a digital printer. The printout was on four-inch adding machine tape. The scanning rate for the system was approximately one reading per second.

For converting the reading of the embedment gages and Mustran cells to circuit strain the following equation is used:

$$\epsilon = \frac{E_o}{KV} \dots \dots \dots (4.1)$$

where

$E_o$  = the reading, in microvolts,

$K$  = the gage factor,

$V$  = applied voltages, in volts,

$\epsilon$  = the circuit strain or  $\frac{\epsilon_1 - \epsilon_2 - \epsilon_3 - \epsilon_4}{4}$ , and

$\epsilon_1$ ,  $\epsilon_2$ ,  $\epsilon_3$ , and  $\epsilon_4$  are the individual arm strains.

The procedure for converting the circuit strain,  $\epsilon$ , into actual material strain is dependent on the circuit construction. Since in the embedment

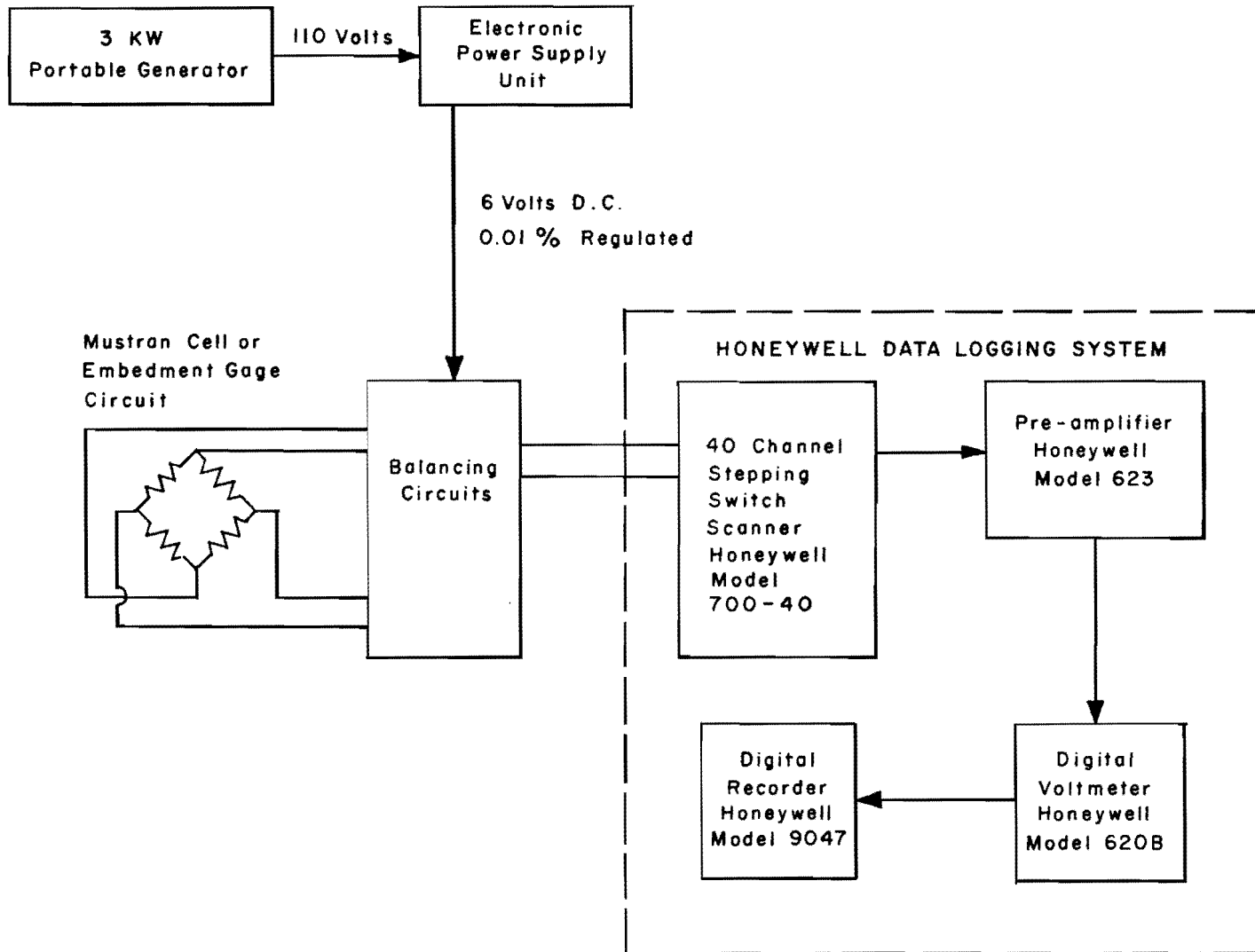


Fig. 4.9. Honeywell Data Logging System

gage circuits there are two active arms and two dummy arms,  $\epsilon_1 = \epsilon_3 = \epsilon_c$  and  $\epsilon_2 = \epsilon_4 = 0$ ; therefore,  $\epsilon = \epsilon_c/2$ , where  $\epsilon_c$  is the strain in the concrete. Thus, the equation for converting the embedment gage reading to concrete strain becomes

$$\epsilon_c = \frac{2 \cdot E_o}{KV} \dots \dots \dots (4.2)$$

For the embedment gages the gage factor is 2.12 and the applied voltage is six volts. Therefore,  $\epsilon_c = E_o/6.36$ .

For the Mustran cells a direct calculation can be made for the strain in the steel bar at the gage location, but not for the concrete strain. All of the gages are active; therefore, the circuit strain,  $\epsilon$ , is equal to  $2.66 \epsilon_s$ , where  $\epsilon_s$  is the strain in the steel. With the gage factor being 2.02 and the applied voltage being six volts, the equation becomes

$$\epsilon_s = \frac{E_o}{8.1} \dots \dots \dots (4.3)$$

With the Mustran cell this steel strain is not directly related to the concrete strain; therefore, the output must be related to concrete strain by the calibration curves of Fig. 2.14. The constant relating cell strain to concrete was 5.5, giving the relationship  $\epsilon_c = \epsilon/5.5$ . From this relationship, the following relationship between voltage output and concrete strain was obtained.

$$\epsilon_c = \frac{E_o}{16.7} \dots \dots \dots (4.4)$$

The readings for the bottomhole cell were converted directly from voltage to load by use of the laboratory calibration curve (Fig. 2.5).

### Load Tests

Thus far a total of three tests on Shaft 1 has been carried to failure. The first two of these tests were conducted on August 29, 1968, and the third was conducted on December 10, 1968. Each test was a quick test in which the load was increased in 10-ton increments and held for 2-1/2 minutes. Readings were taken at 30 seconds and again at 2 minutes after the incremental load had been applied. The load was removed in 25-ton increments with each incremental load also being held for 2-1/2 minutes. Readings were again taken at 30 seconds and 2 minutes after removal of the load increment.

### Results

Life of the Electrical Instrumentation. Within a very short time after being installed, the complete bottom level of embedment gages indicated low resistance to ground. Since both bridge circuits of this level went bad at the same time, it was assumed that water had gotten into the container where the dummies and wire splices were located. By the time Tests 1 and 2 were conducted, one additional embedment gage circuit was showing low resistance to ground. Thus, by the date of the first test, 3 embedment gage circuits out of a total of 12 were indicating trouble. An additional two circuits were bad by the time of the third test, making a total of five bad circuits.

Although the resistance to ground of the bottomhole cell was low for the first two tests, the readings were stable and the cell appeared to be

functioning properly. Shortly before Test 3 the cell shorted completely to ground and was not used again.

After the initial low resistance reading by two Mustran cells, which was corrected immediately after the shaft installation, all of the Mustran cells continued to show high resistance to ground through the first two tests. At the time of the third test, although the resistance to ground did not indicate trouble, one of the top level Mustran cells was acting erratically and was assumed to be bad. All of the other cells were operating properly.

Long-Term Stability. After installation in the shaft, the embedment gages drifted so erratically that no useful information could be obtained from the long-term monitoring of these gages.

A drift curve for one of the Mustran cells from the time of first casting in the concrete block to the date of first testing is shown in Fig. 4.10. The pattern of change in cell readings is generally the pattern of strains expected in the concrete due to curing and to moisture and temperature variations. Very large changes are noted with changes in the moisture conditions such as are seen when the sample block is removed from water. A similar large change can be noted at the time when the shaft was installed. After the curing of the shaft the readings appeared to remain stable with no erratic changes.

The bottomhole cell was monitored after placement and up to the time of the first test. The information obtained is shown in graph form in Fig. 4.11. As can be seen, the cell indicated a decrease in load as the concrete cured, and by the time of the first test was indicating almost no load on the

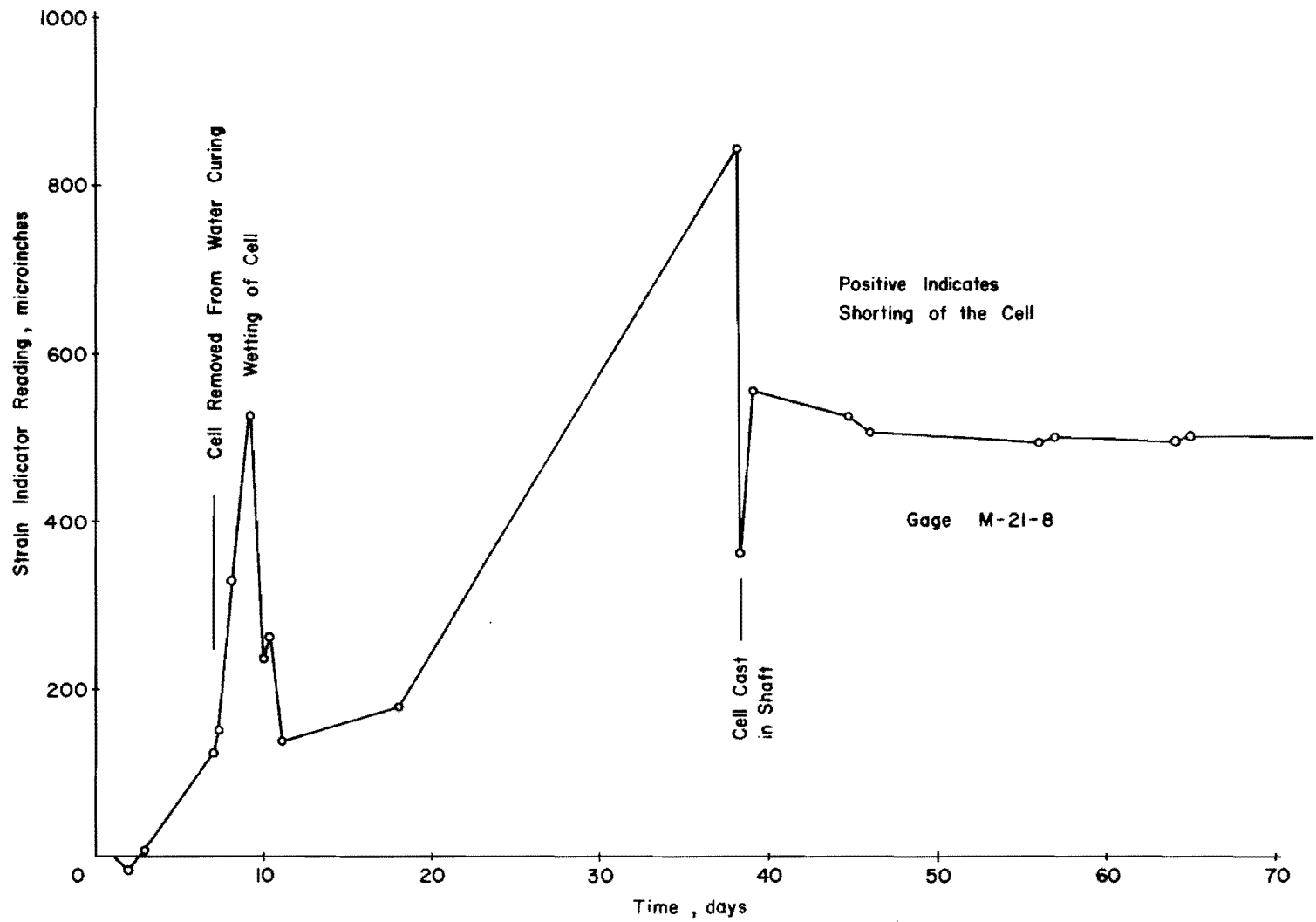


Fig. 4.10. Mustran Cell Readings After Casting in Concrete

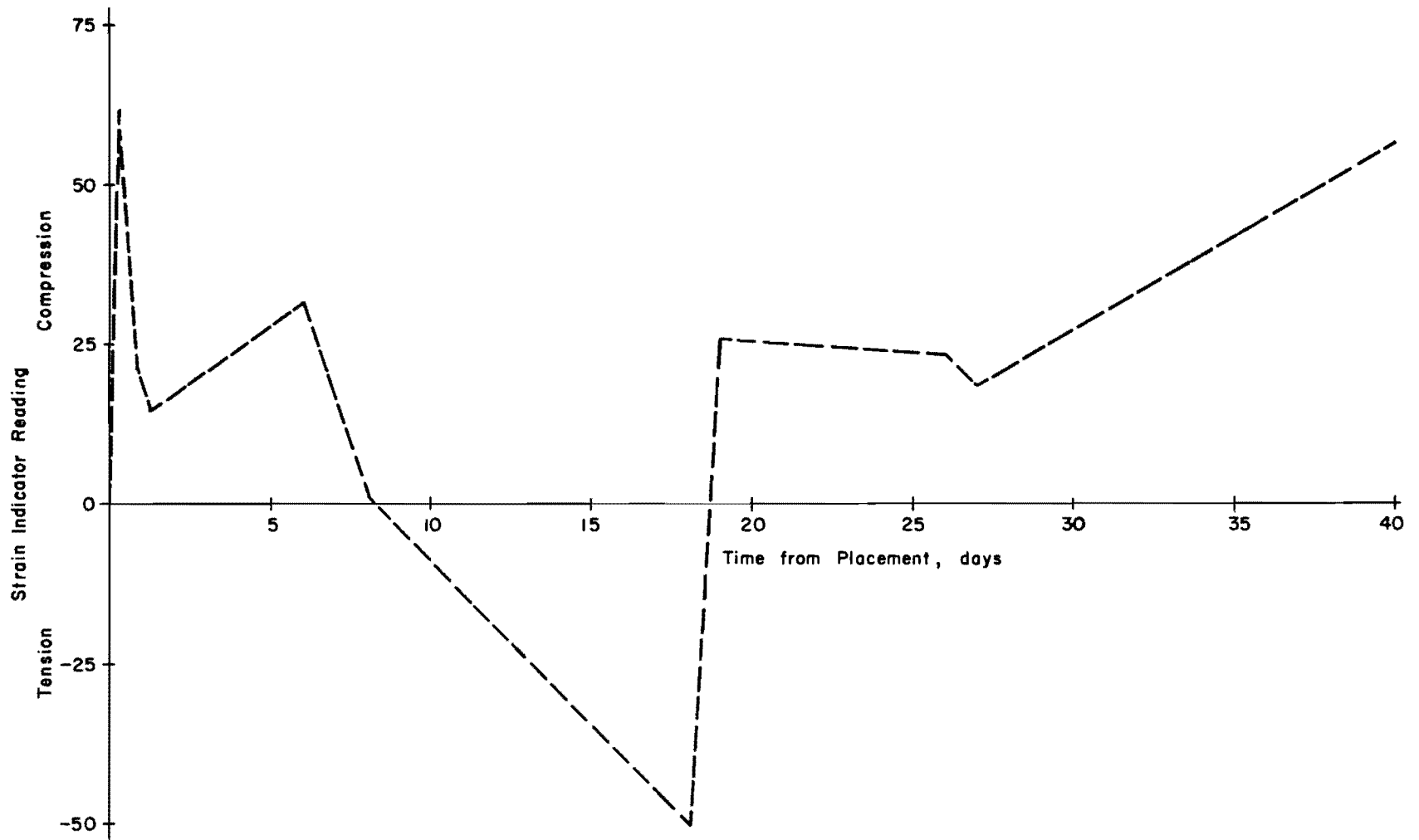


Fig. 4.11. Bottomhole Cell Readings After Placement

bottom of the shaft. One erratic reading appeared on the eighteenth day, which is believed to be a blunder. If this reading is not used, the data appears to be quite satisfactory.

Short-Term Stability. The electrical gages were monitored for a period of time immediately preceding the start of the test. The monitoring consisted of continuously powering the gages with the six-volt power supply and using the digital readout system to record the indicated reading. Readings were taken every 30 minutes from 5:40 p.m. on August 28 until 6:55 a.m. on August 29, 1968.

The drift in the bottomhole cell during this time amounted to only 0.48 ton of load change. Thus, the drift was considered to be insignificant and was ignored in the analysis of the data.

The drift of the Mustran cells varied from a maximum of 193 microvolts to as little as 8 microvolts. This maximum change represents an indicated false load of approximately 20 tons. As can be seen in Fig. 4.12, only cells M-0-2 and M-15-7 had a drift which would give an indicated false load of greater than one ton in the 13 hours. Since the test was to last for only approximately two hours, it was felt that even the maximum drift present was within acceptable limits and would not warrant making drift corrections to the data. Figure 4.13 gives four typical drift curves for the monitoring period. Cell M-0-2 indicates a drift which is probably due to moisture in the cell. Since this drift is insignificant in the analysis of the test, no attempt to reduce the drift was made. If it had been necessary, the cell could have been dried by circulating dry nitrogen through the system.

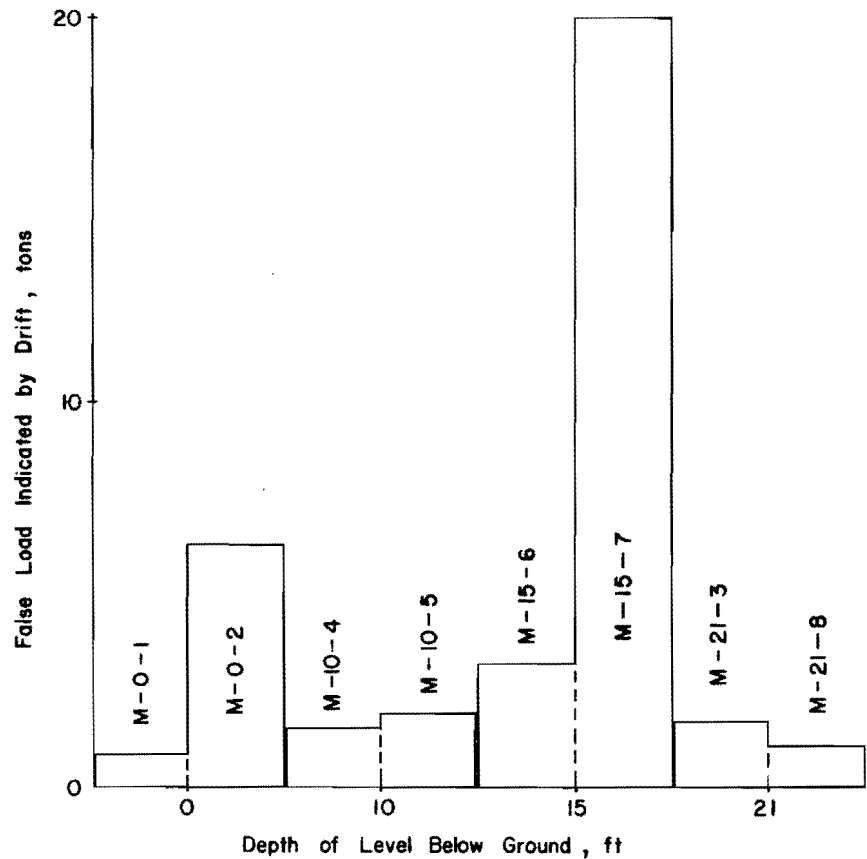


Fig. 4.12. Magnitudes of Drift for Mustran Cells, Houston SH 225 Site, Shaft 1

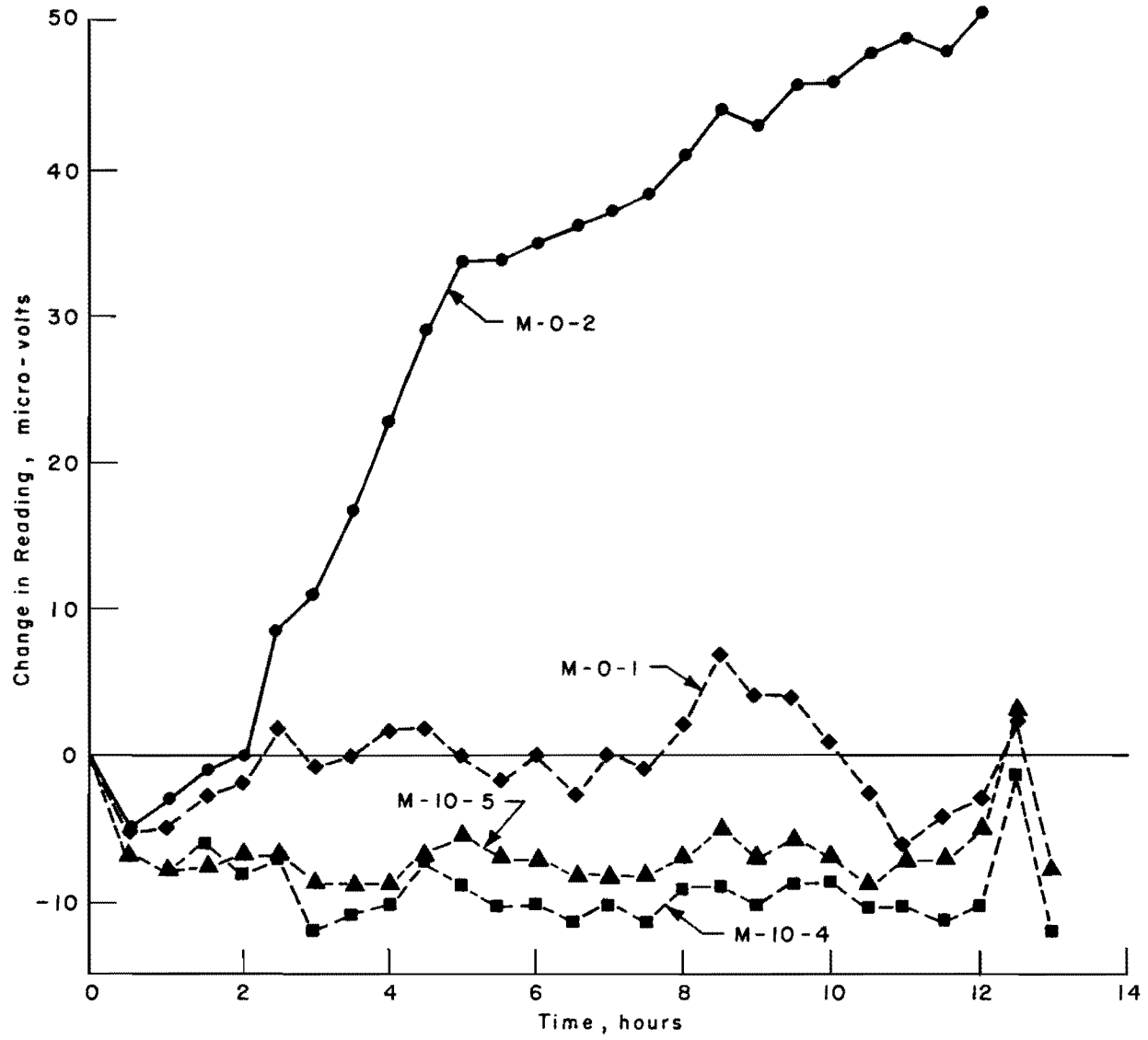


Fig. 4.13. Drift Curves for Mustran Cells, Houston SH 225 Site, Shaft 1

The drift in the embedment gages was much greater than that in the Mustran cells or the bottomhole cell. The magnitudes of the drift during the 13 hours preceding the test can be seen in Fig. 4.14. As is noted, only two of the embedment gage circuits, E-17-1 and E-17-2, had a drift of small enough magnitude to be ignored in the data reduction.

### Data Reduction

Data reduction of the electrical gages was accomplished through the use of a computer program especially written for the project. The top set of gages for both the Mustran cells and the embedment gages served as in-shaft calibration gages. The calibration curve is obtained by fitting a third order least squares curve through the readings of the top gages. The calibration curve for the Mustran cells and embedment gages, as plotted by the computer for Test 1, are shown in Figs. 4.15 and 4.16, respectively.

Each of the curves is a third order polynomial being forced through the origin, therefore having the form  $0 + A_1X + A_2X^2 + A_3X^3$ , where  $A_1$ ,  $A_2$ , and  $A_3$  are the constants obtained from the least squares curve fit. For the particular curves shown for the Mustran,  $A_1$ ,  $A_2$ , and  $A_3$  are equal to 207.7, 0.07, and -0.00003, respectively. For the embedment gages the constants are 456.9, 0.67, and -0.0007, respectively. It may be noted that the constants for the higher ordered terms are much smaller for the Mustran cell calibration curve than for the embedment gage calibration curve. The calibration polynomials are applied to the readings at each level to obtain the indicated load at each level.

The load at the tip of the shaft was calculated by multiplying the bottomhole cell reading by the calibration constant for this cell.

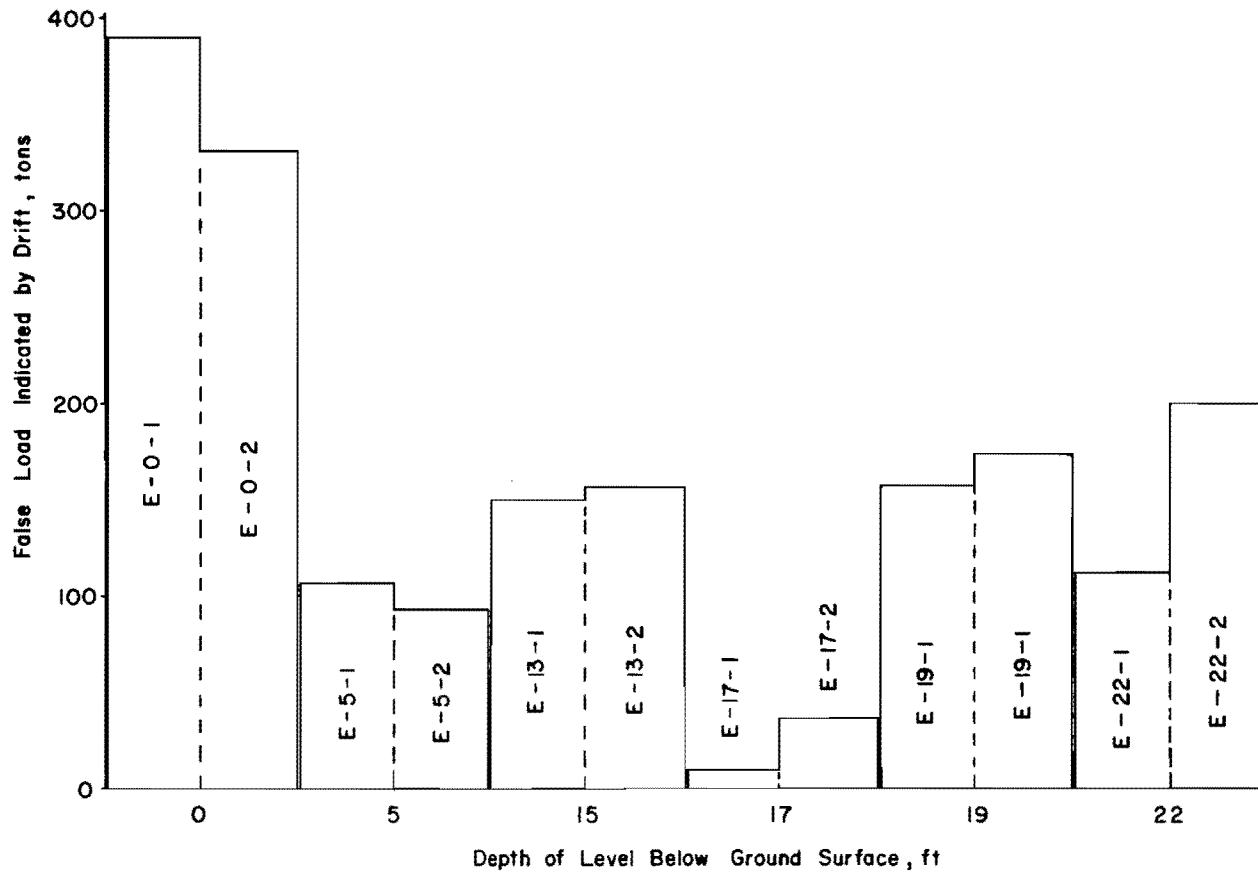


Fig. 4.14. Magnitudes of Drift for Embedment Gages, Houston SH 225 Site, Shaft 1

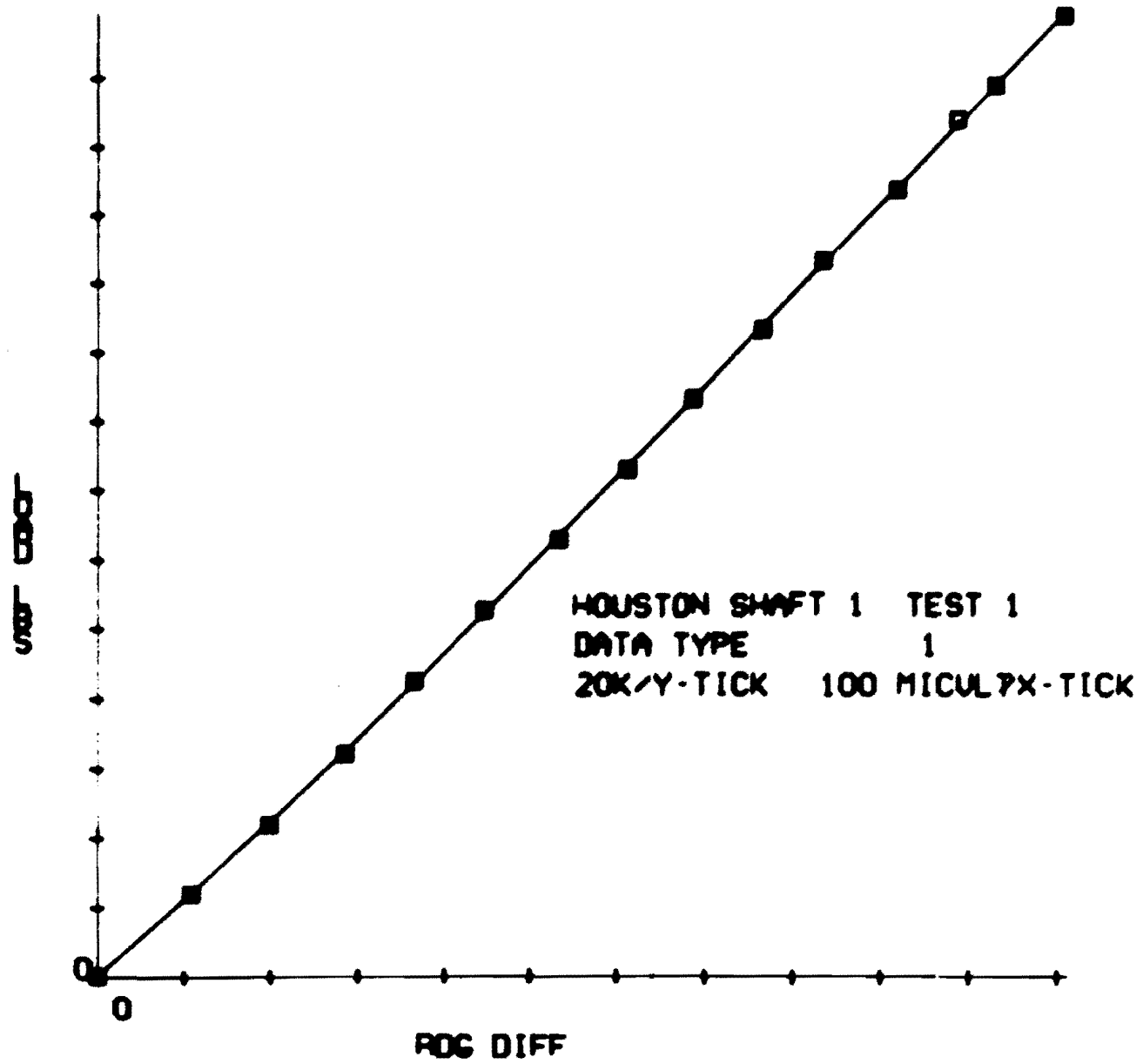


Fig. 4.15. In-Shaft Calibration of Mustran Cells, Houston SH 225 Site, Shaft 1, Test 1

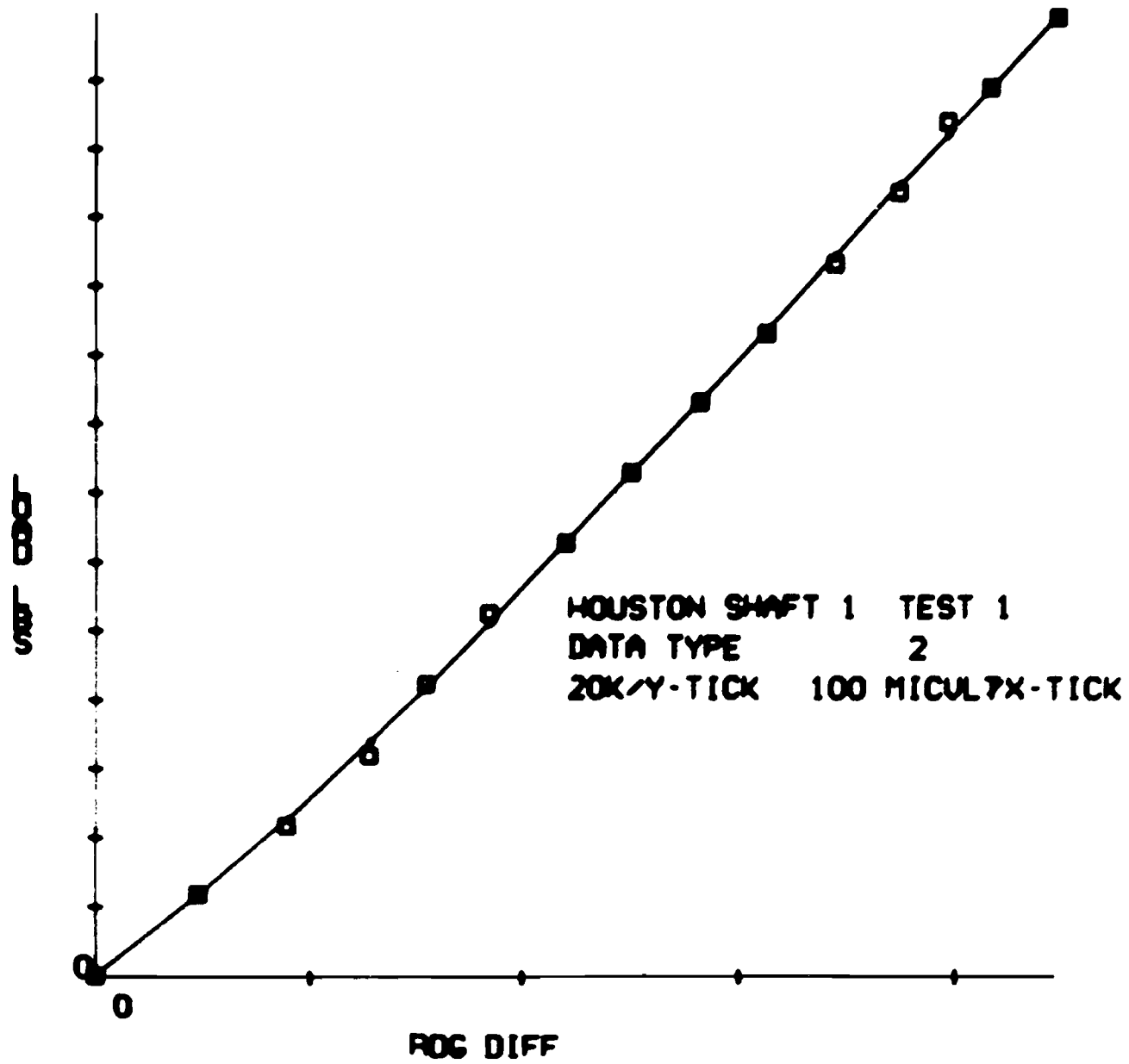


Fig. 4.16. In-Shaft Calibration of Embedment Gage, Houston SH 225 Site, Shaft 1, Test 1

After the load at each level was determined for a particular applied load, either a third or a fourth order least squares fit was fitted through the indicated loads to obtain the load-transfer curve. The curve fit used has the special features of forcing the curve through the applied load and providing no load transfer at the ground level. An example of one of the load-transfer curves obtained by a least squares curve fit through the Mustran cell and bottomhole cell data is shown in Fig. 4.17.

The load transfer at any point, being the slope of the load-transfer curve, is found by taking the derivative of the least squares polynomial. The deformation of the shaft is found by integrating the polynomial and dividing by the area and modulus of elasticity of the shaft.

#### Shaft Bending

Since each level of Mustran cells consisted of two cells, on opposite sides of the shaft, it was possible to note the amount of bending present in the shaft. This bending was quite large as can be seen in the plot of the individual cell reading for the top level (Fig. 4.18). Although the plots of the individual readings are greatly nonlinear, the average of the two readings appears to be about as linear as could be expected for indirect type cells. Bending was also noted all along the shaft. As the load increased, the bending became worse especially at the lower levels. As soil beneath the shaft failed in bearing, the lower level cells indicated a very large increase in the bending. It is felt that it is essential for the cells to be placed in the shaft in such a way as to counter the effect of the bending.

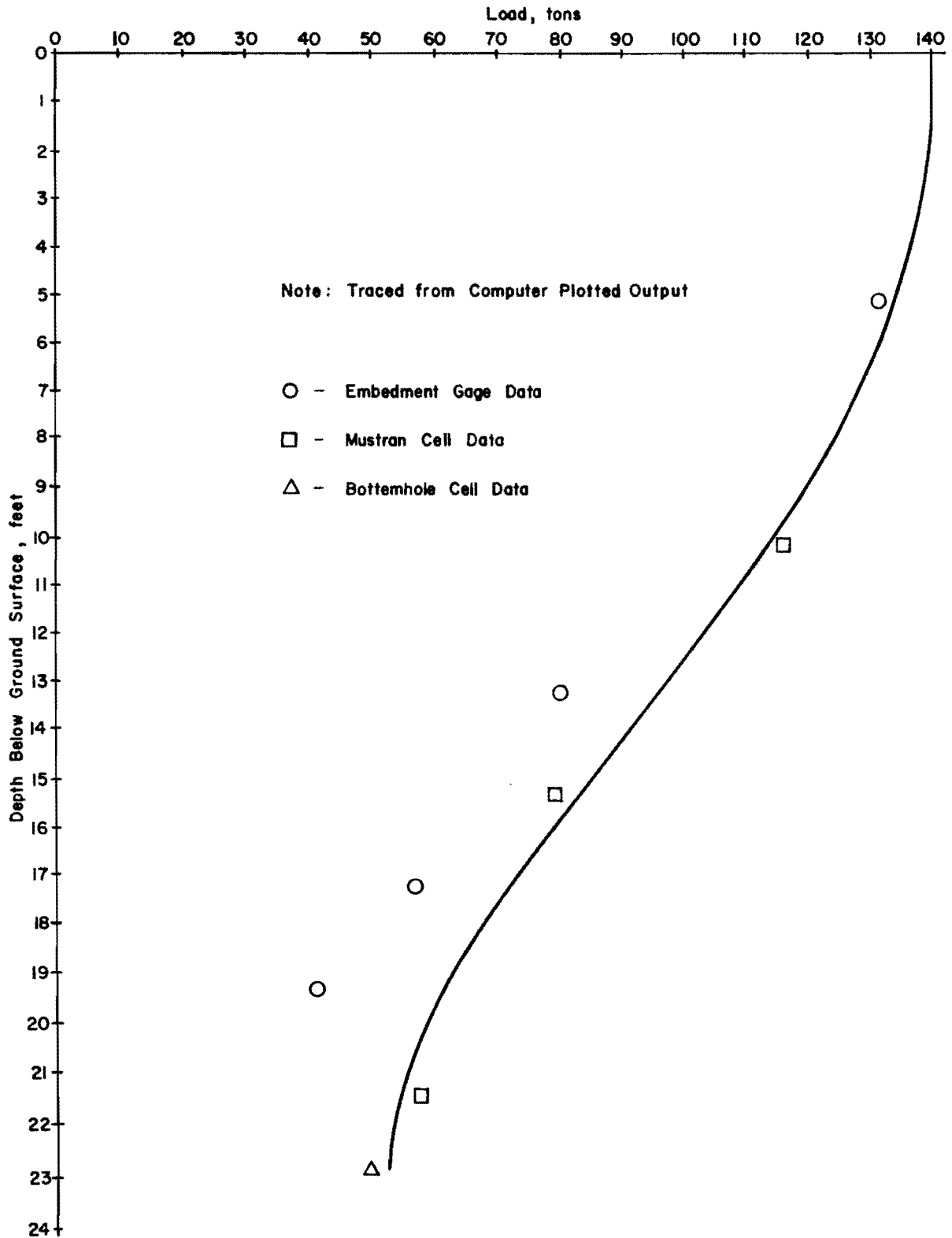


Fig. 4.17. Load-Transfer Curve for 140-Ton Applied Butt Load, Houston SH 225 Site, Shaft 1, Test 1 (Fit Through Mustran Cell and Bottomhole Cell Data Only)

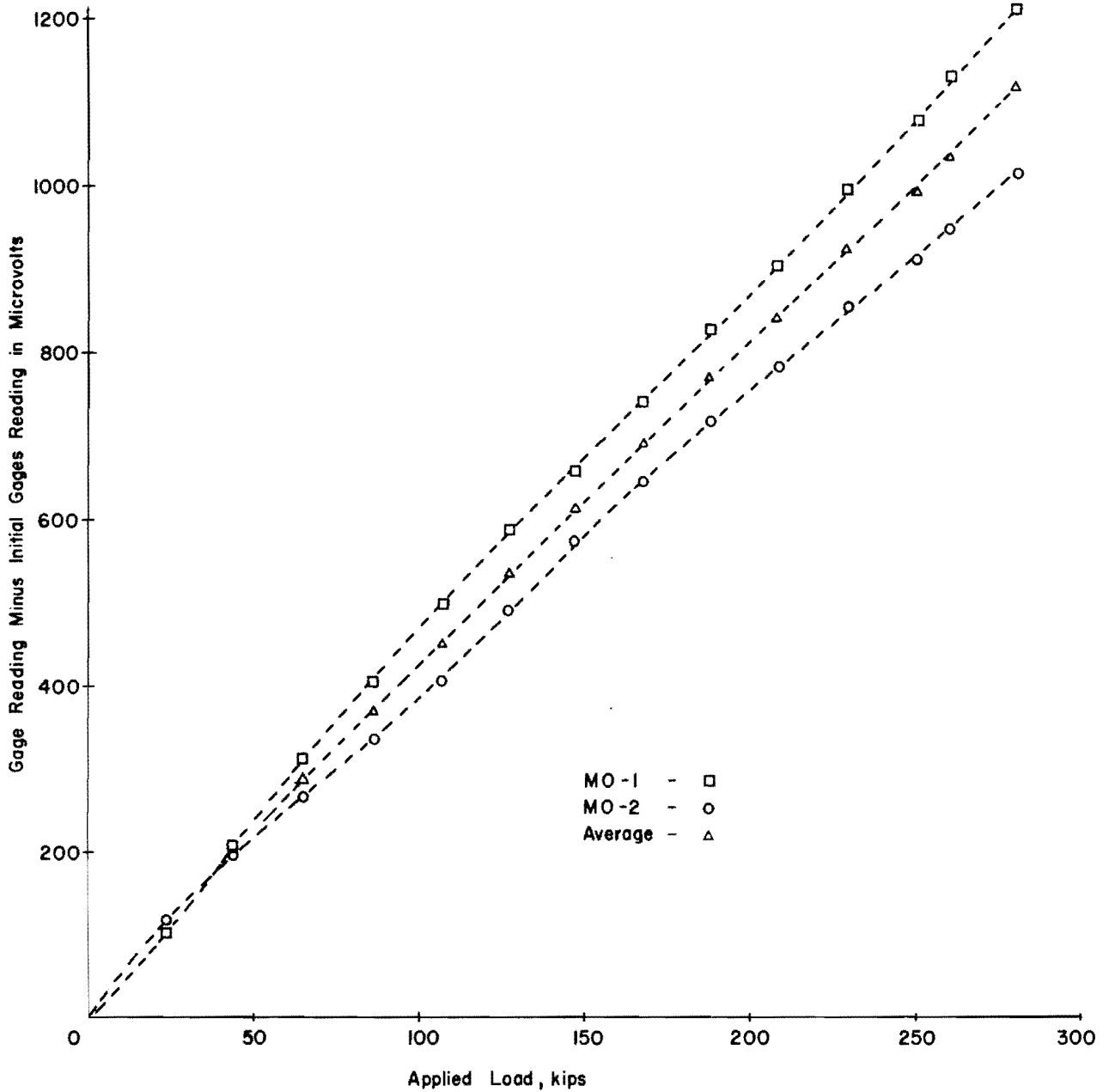


Fig. 4.18. Calibration Level for Mustran Cells

### Discussion of Test Results

Gloetzl Cell. The pressure reading for the cell changed by only 26 psi over the entire load range of the test. This would be less than two psi change per ten tons of applied load to the shaft. Based on these results the Gloetzl cell was concluded to be unsatisfactory as axial load measuring instrumentation for this project.

Telltales. The data obtained from the telltales was far from satisfactory. The relatively small concrete deformation did not provide movements adequate for accurate reading with dial gages. Only one telltale had been placed at a level and no provisions had been provided to correct for the bending in the shaft. Since the movements were so small, rather large relative error could have been caused by temperature changes and by friction between the rods and tubing.

Bottomhole Cell. As can be seen in Fig. 4.17, which is a least squares curve fit through the Mustran and bottomhole cells, the bottomhole cell gave results which compared favorably with the load indicated by the Mustran cells immediately above. A small amount of error may have been introduced at the higher applied load by the soil pressing in the rubber membrane walls of the cell and providing uplift to the top plate. This error appears to be small and does not introduce appreciable error in the data analysis. The load indicated by the bottomhole cell versus the applied butt load is shown in Fig. 4.19. In this figure, it is noted that the curve is apparently linear up to an applied load of approximately 90 tons. Above 90 tons the sides of the shaft start shedding load until the bottom of the shaft is picking up more load per load increment than the applied load increment.

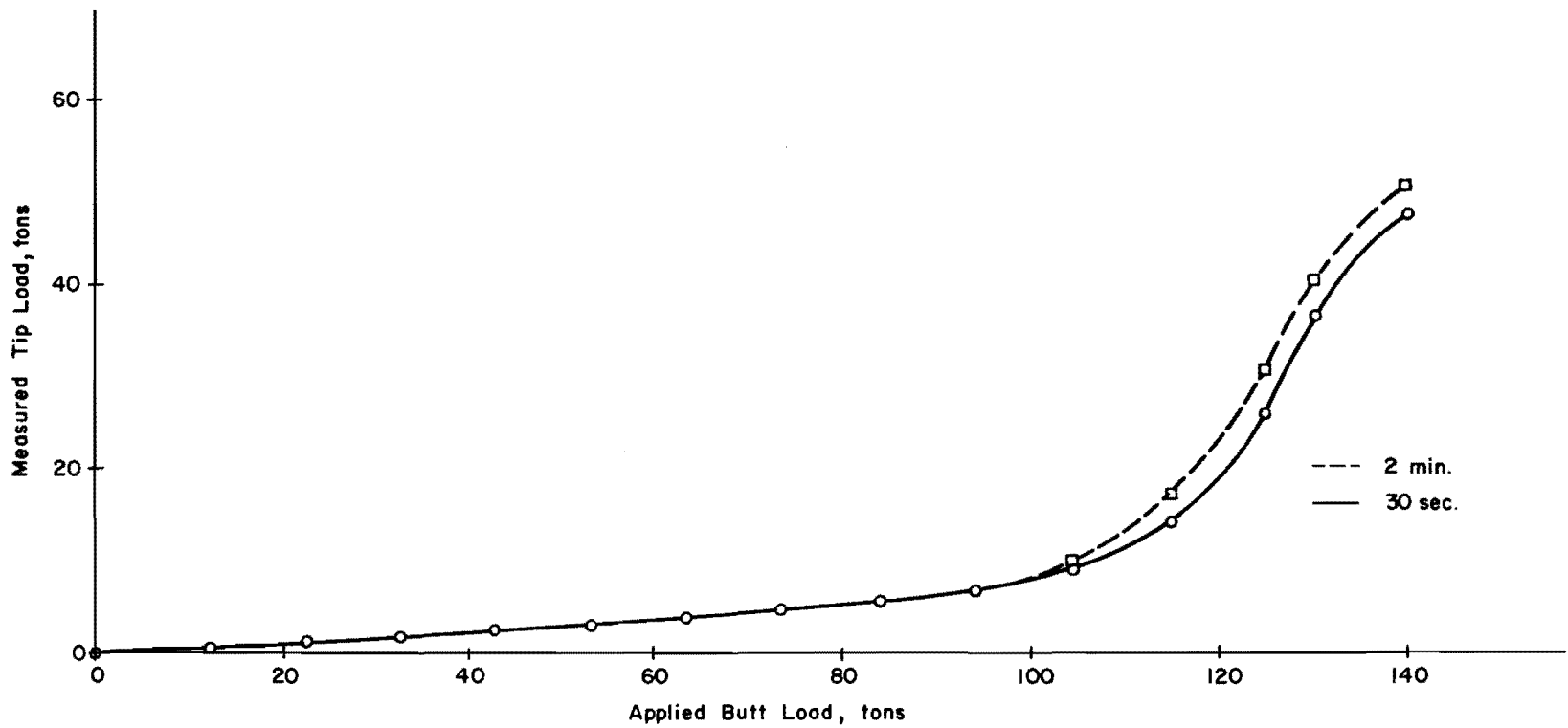


Fig. 4.19. Load Indicated at Shaft Tip by Bottomhole Cell  
Houston SH 225 Site, Shaft 1, Test 1

Mustran Cells and Embedment Gages. The results from the Mustran cells were very encouraging, in that all cells remained operative for the first two tests and only one cell indicated trouble by the time of the third test. The data appeared about as accurate as could be expected from an indirect system. The cell drift was small enough so that no drift corrections were necessary. The load-transfer curve obtained by use of only the Mustran data and the bottomhole appears very good, as can be seen in Fig. 4.17. Figure 4.20 is a typical curve obtained by a set of Mustran cells. This curve for the 21-foot level compares favorably with the curve for the bottomhole cell. The same load shedding is observed at this level as was observed at the bottom.

When compared to the Mustran cell system, the embedment gage system appears to be almost unsatisfactory as an instrumentation system. Even prior to the first test several of the circuits were showing low resistance to ground and were not usable. Large drift corrections were necessary in order to obtain accuracy which would give useful results. As can be noted in Fig. 4.17, the Mustran cell readings compare more closely with the data obtained with the bottomhole cell than does the embedment gage data.

The concrete modulus may be calculated both from the top level of embedment gages and the top level of Mustran cells. For example, given applied load of 280,000 pounds, the concrete stress in the shaft at the top level of instrumentation would be 375 psi. The average reading obtained from the top level embedment gages for this applied load was 444 microvolts. Thus, the concrete strain,  $\epsilon_c$ , may be calculated from the formula given previously as being equal to  $444 \div 6.36 = 69.7$  micro-inches. This would

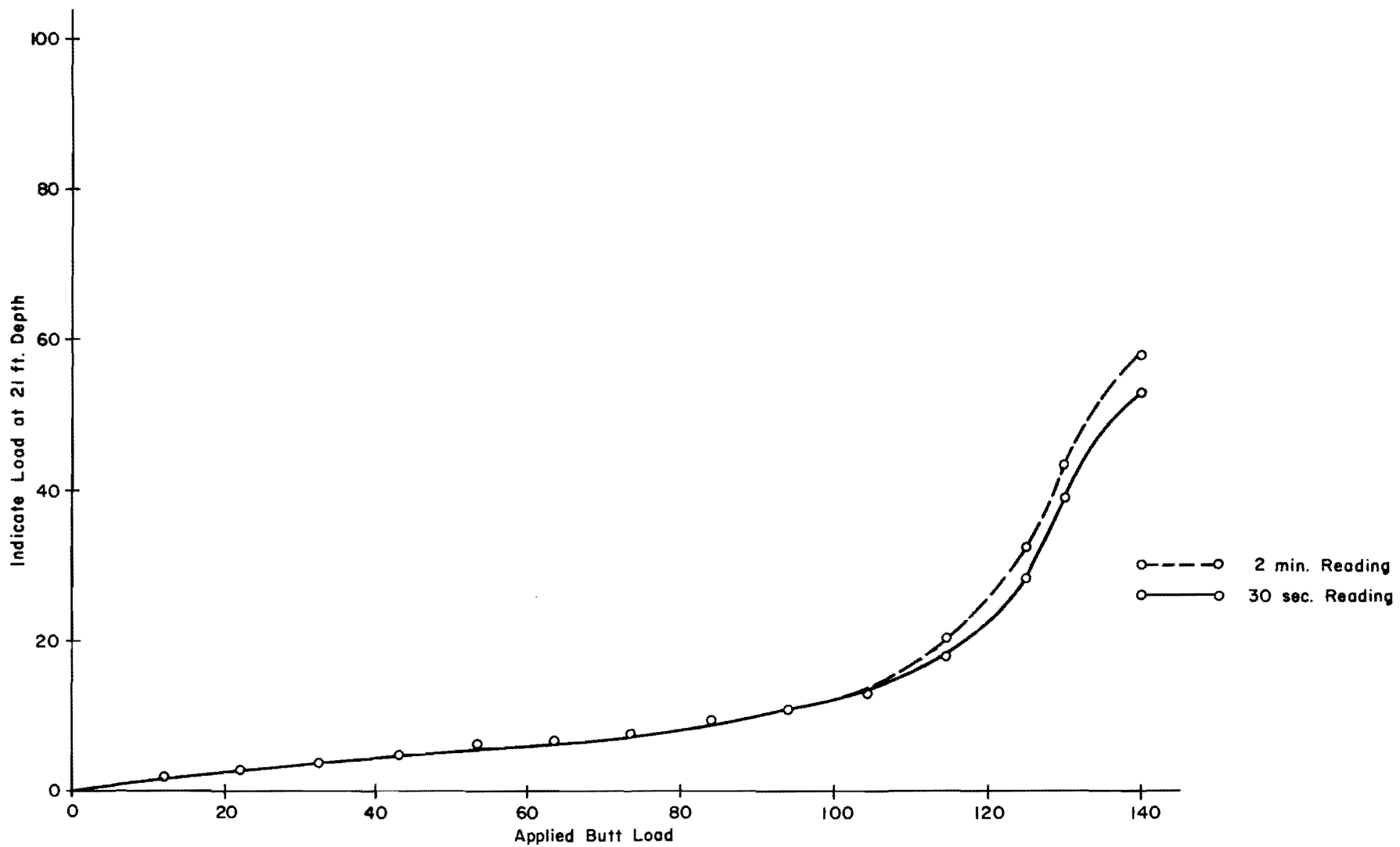


Fig. 4.20. Load Indicated at 21-Foot Depth by Mustran Cells  
Houston SH 225 Site, Shaft 1, Test 1

indicate a modulus of  $5.4 \times 10^6$  psi for the concrete. The average reading for the top two Mustran cells was 1117, giving an indicated strain of 66.8 micro-inches or a modulus of  $5.6 \times 10^6$  psi. A modulus value of  $5.7 \times 10^6$  psi was determined from modulus tests of specimens taken at the time of the shaft installation. This would indicate that the multiplication factor for the Type 1 Mustran cell as determined in the laboratory was very close to the true multiplication factor. By the use of this factor, the cell reading may be converted into true concrete strains.

#### Shaft 2

Shaft 2 was a belled shaft with the bottom of the bell 23 feet 6 inches below ground surface. The diameter of the straight portion of the shaft was 30 inches. The diameter of the base of the bell was approximately seven feet six inches, and the height from the base of the bell to the top of the bell was four feet six inches. The shaft is shown in elevation in Fig. 4.21.

The instrumentation of the shaft consisted of seven levels of Mustran cells, three levels of embedment gages, four levels of telltales and three levels of thermocouples. The primary instrumentation system was considered to be the Mustran cells.

Mustran Cells. A total of 23 Type 2 Mustran cells and one Type 1 Mustran cell was installed in the shaft. The Type 2 cells were to be the primary instrumentation for the measurement of the axial loads and the Type 1 cell was installed to determine if this type cell could be used in a heavily-loaded shaft. The cells were not precast in concrete blocks as was done for Shaft 1, but were tied directly to the reinforcing spiral as is

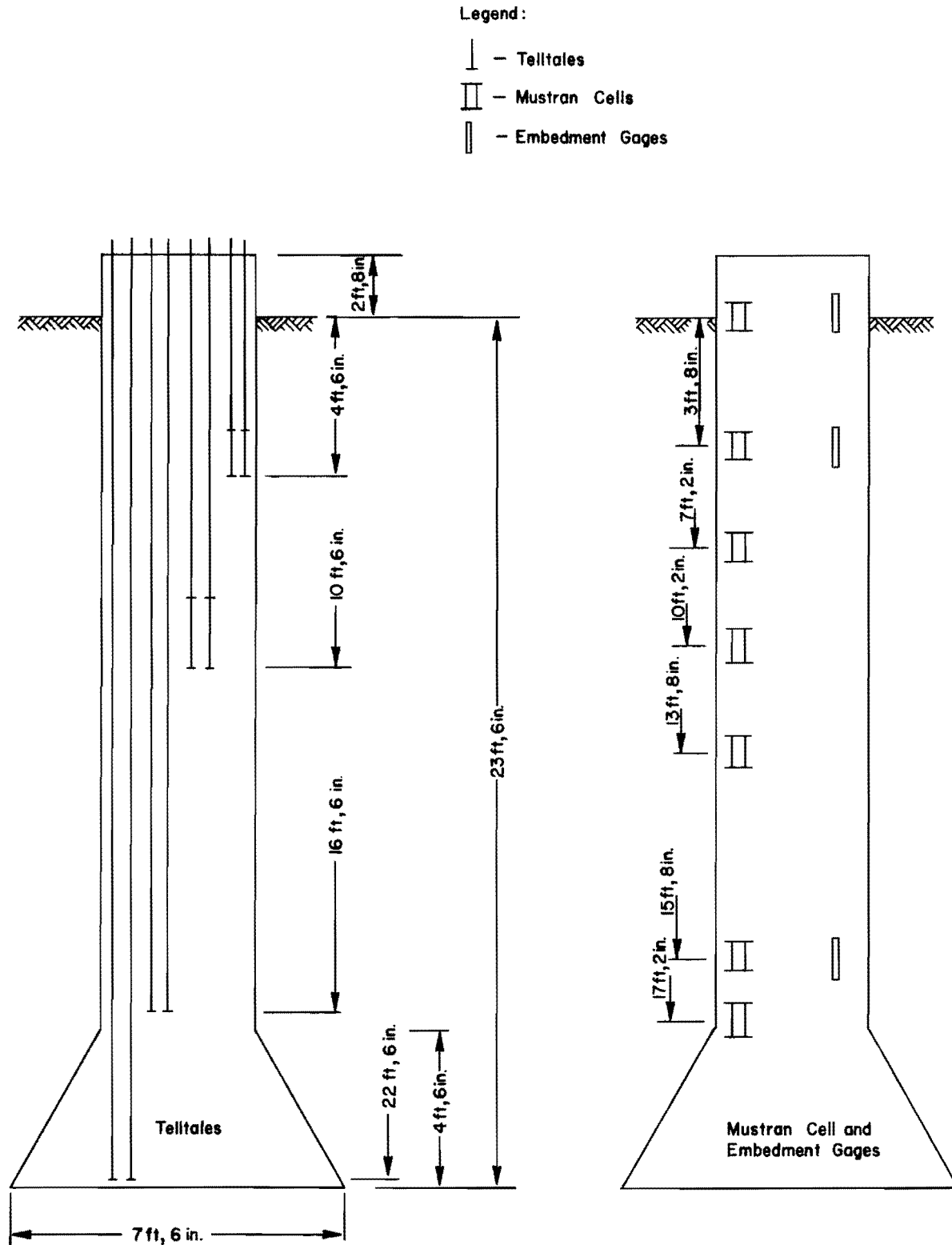


Fig. 4.21. Location of Instrumentation, Houston SH 225 Site, Shaft 2

shown in Fig. 4.22. By placing the cells directly in the shaft it was hoped that some information could be obtained concerning the strains in the concrete during curing.

All the Type 2 cells, with the exception of three cells, had the same general type of pressurization system as was used in the first shaft. The three exceptions were pressurized through the wire without being enclosed in copper tubing. Two of these three cells were not provided with returns. Plastic tubing returns were used on four of the cells in lieu of copper tubing. The description of the Type 2 cells is shown in Table 1.

Prior to installation in the shaft, each of the three special cells was pressure tested under water to 30 psi to insure that there were no leaks in either the instrumentation cable, the cell proper, or the return tubing. Pressure tests on the cells where the instrumentation cable was enclosed in copper tubing could not be conducted prior to cell installation. A check for leaks was made after cage instrumentation and system pressurization by coating all joints and cells with a water-soap solution. This testing disclosed several leaks which were corrected prior to the time the shaft was installed in the ground.

It had been planned to have the cells at each level spaced uniformly around the shaft to compensate for bending, but due to the large amount of instrumentation tubing, and wiring tied to the reinforcing cage, exact spacing was not possible. This mass of instrumentation can be seen in Fig. 4.23, which shows the instrumented reinforcing cage from the top looking toward the bottom. The fact that the cells were not spaced evenly around the shaft is believed to have been one cause of difficulty in the analysis of the data.

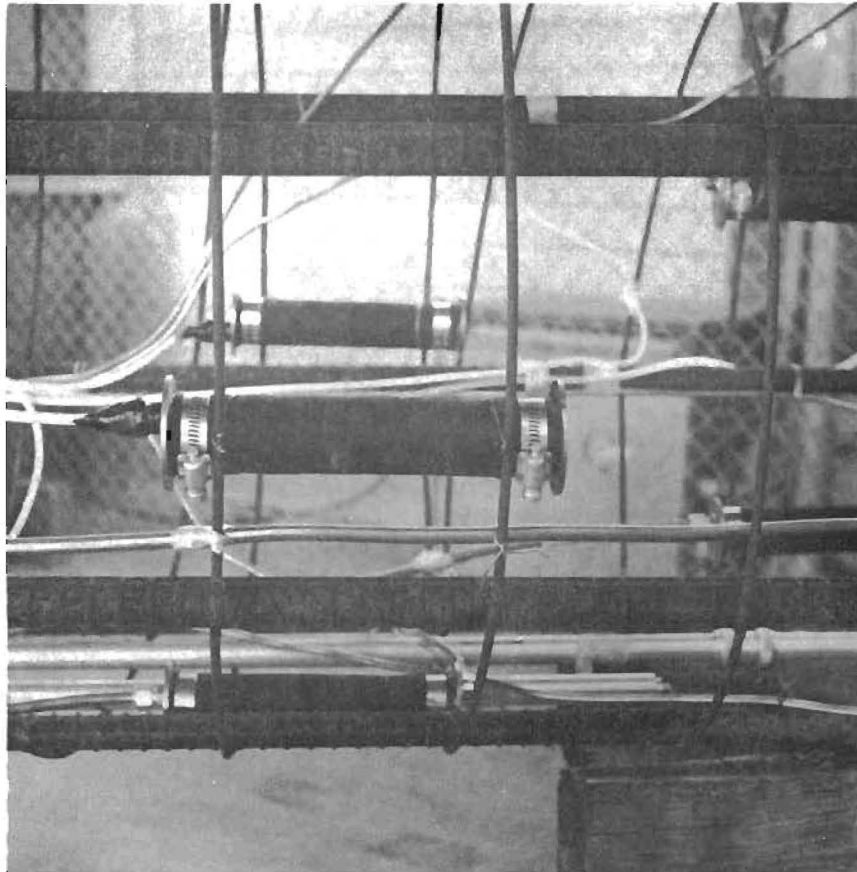


Fig. 4.22. Mustran Cell Fixed to Reinforcing Cage,  
Houston SH 225 Site, Shaft 2

TABLE 1. MUSTRAN CELLS INSTALLED IN SHAFT 2

Level No.	Depth Below Ground Surface	Number Cells	Pressure System
1	0' 0"	3	Lead wires enclosed in copper tubing. Copper tube return. No desiccant.
2	3' 8"	3	Same as Level 1.
3	7' 2"	3	Same as Level 1.
4	10' 2"	3	Same as Level 1, except plastic tubing used for returns.
5	13' 8"	3	Same as Level 1.
6	15' 8"	4	Two cells same as Level 1. Two cells pressurized through lead wire and no return. Cell filled with desiccant.
7	17' 2"	4	Three cells same as Level 1. One cell pressurized through lead wire with plastic tube return.

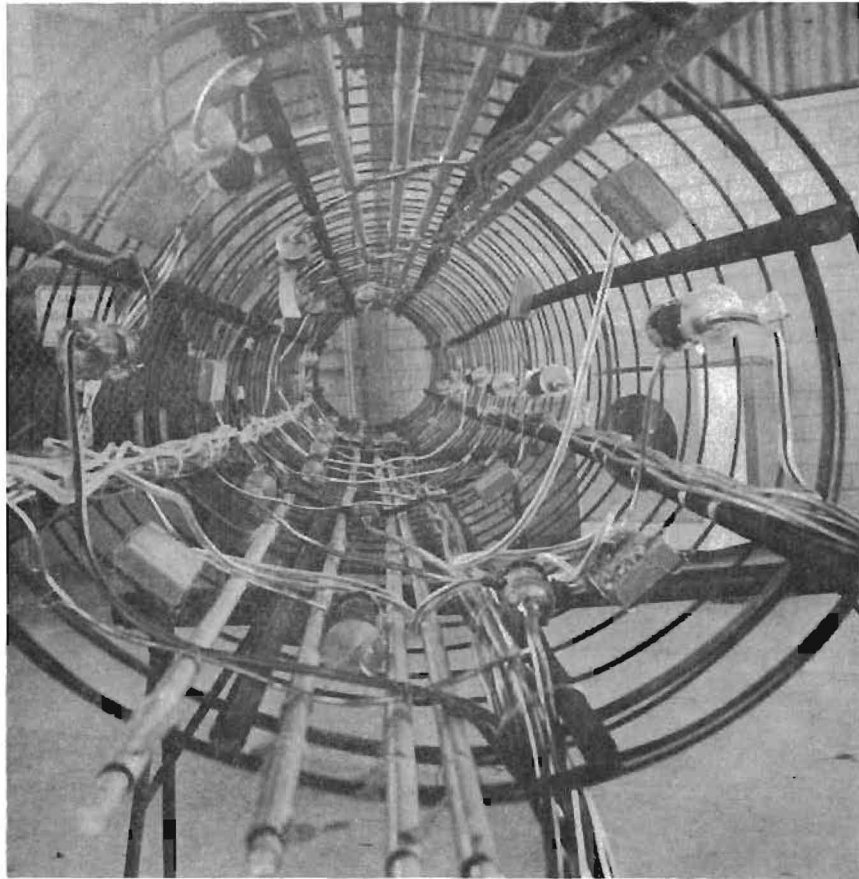


Fig. 4.23. Instrumented Reinforcing Cage,  
Houston SH 225 Site, Shaft 2

The manifold for the pressure system was greatly simplified from the first manifold by the use of rubber tubing. The manifold, shown in schematic in Fig. 4.24, was constructed by providing a 6-inch length of 4-inch-diameter heavy wall pipe with 24 hose connections. One connection was used to run a one-fourth-inch inside diameter rubber hose to a nitrogen supply. From 20 of the connections, 3/8-inch inside diameter rubber hose was connected to the copper tube carrying the wire to the cells. The remaining three connections were used for one-fourth-inch inside diameter hoses which were fitted directly over the instrumentation wire from the special cells. Thus, by pressurizing the manifold, all 23 gages were pressurized. The shaft head, along with the pressure system is shown in Fig. 4.25. The major fault of this manifold was in the difficulty of disconnecting and reconnecting in order to obtain a set of gage readings.

Embedment Gages. The primary purpose of using embedment gages was to provide a direct comparison between the embedment gages and the Mustran cells. Therefore, the levels were placed so as to correspond with levels of Mustran cells as shown in Fig. 4.21.

The installation procedure was essentially the same as was used in the first shaft of this site, that is, each level consisted of two full-bridge circuits. The dummies were again enclosed in containers which were embedded in the shaft at the same level as the active gages.

Telltals. The same system of telltales was used in Shaft 2 as was used in Shaft 1 except that two telltales were placed at each level in order to compensate for bending of the shaft. This gave a total of eight telltales for four levels.

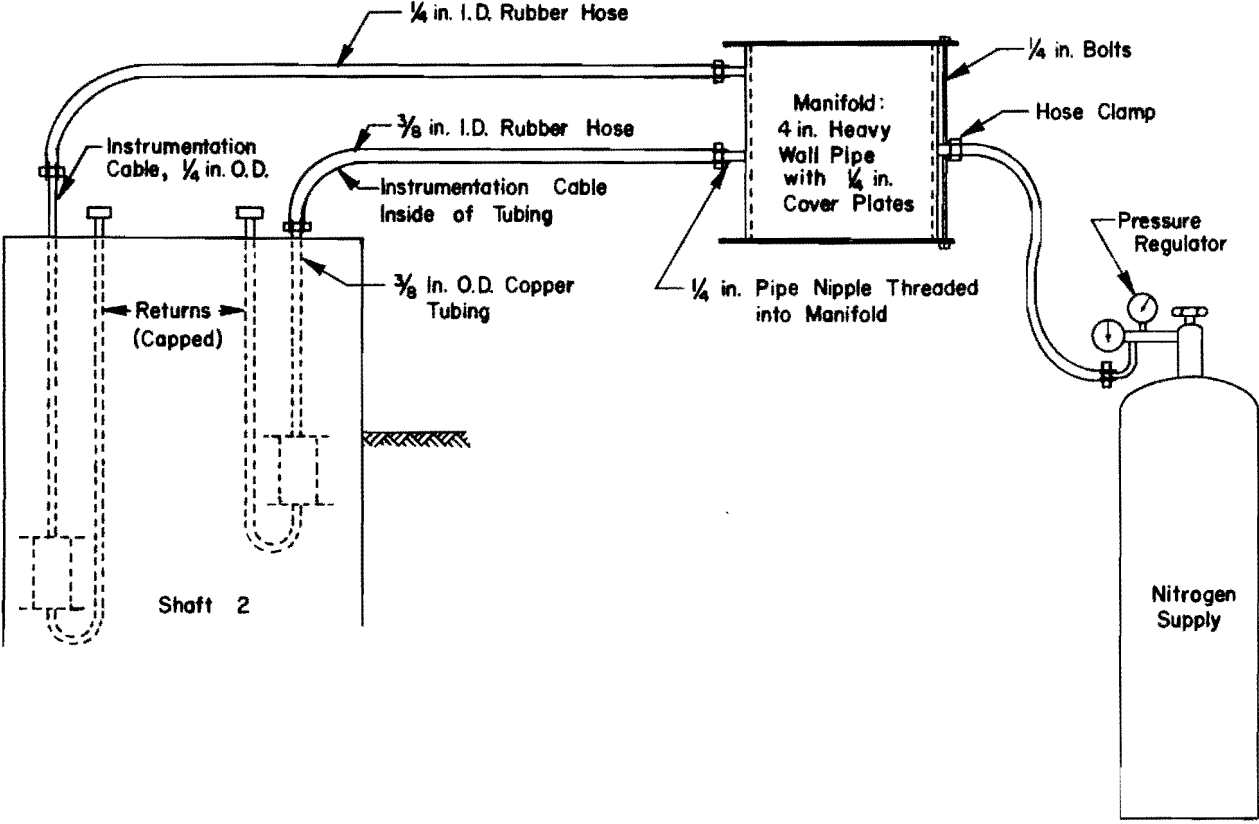


Fig. 4.24. Schematic of Mustran Instrumentation System, Houston SH 225 Site, Shaft 2



Fig. 4.25. Shaft Head and Mustran Manifold System,  
Houston SH 225 Site, Shaft 2

### Load Application

Essentially the same air-driven hydraulic load system was used as was used for Shaft 1. Since the loads were expected to exceed the capacity of one jack, two jacks were employed. To provide more accurate and reliable measurements of the applied load, a pressure transducer was added to the system. The transducer provided a 3.0 milivolt readout per volt of applied voltage for 20 ksi. Thus, for an applied voltage of 6.67 volts, the readout will be one microvolt per psi. The readout of the transducer was accomplished along with the Mustran cells and embedment gages by the Honeywell Data Logging System used in the Shaft 1 tests. The resolution of this system was 1 microvolt and the stability was approximately  $\pm 5$  microvolts. Thus, with 6.67 applied voltage the load resolution was 1 psi  $\pm 5$  psi.

### Results

Life of the Electrical Instrumentation. Before placement of the embedment gages and Mustran cells, all of the indicated leakage resistances were well above  $10^9$  ohms. Immediately after placing, one of Level 7's Mustran cells indicated a short (less than  $10^6$  ohms) to ground. This cell, although it continued to show low resistance to ground, appeared to function properly with very little drift. Since the cell did continue to function properly, it was concluded that the cell suffered mechanical damage during placement, and that no moisture had penetrated the cell.

The leakage resistance of all other gages remained high up to the time of the first test. After the first test, the bottom level of embedment gages began to indicate low resistance to ground and was considered to be lost. Since both circuits at the level indicated trouble at the same time, the probable cause was water entering the junction box.

Long-Term Drift. The drift of most of the Mustran cells of Shaft 2 was about the same as that of the cells in Shaft 1. Of special interest was the drift of the three cells with pressurized wire. The cells M-16-21 and M-16-19 were pressurized through the lead, but were not provided with a return line. Each of these two cells had been filled with desiccant just prior to the sealing of the cell. The third cell, M-18-24, was provided with a plastic tubing return, but was not filled with desiccant. It was noted that the cells filled with desiccant were exceptionally stable, whereas the cell not filled with desiccant appeared to contain more possible drift.

The embedment gages again showed very erratic readings, and no useful information could be obtained over a long period of time.

Short-Term Stability. All of the Mustran cells and all of the embedment gages with the exception of the top level of embedment gages were stable enough over the period of time covered by the first test that no drift corrections were necessary in the reduction of the data. The drift curve for the top level of embedment gages is shown in Fig. 4.26. As can be seen, the drift during the test appears to be approximately 350 microvolts. This change would be equivalent to a change caused by an applied load of approximately 120 tons. Thus it was necessary to include in the reduction of the data, provisions of the drift in this set of gages. Since this drift was present only in the top gages and was approximately the same for both circuits, it was felt that drift was due to temperature changes affecting the dummies enclosed in the junction box.

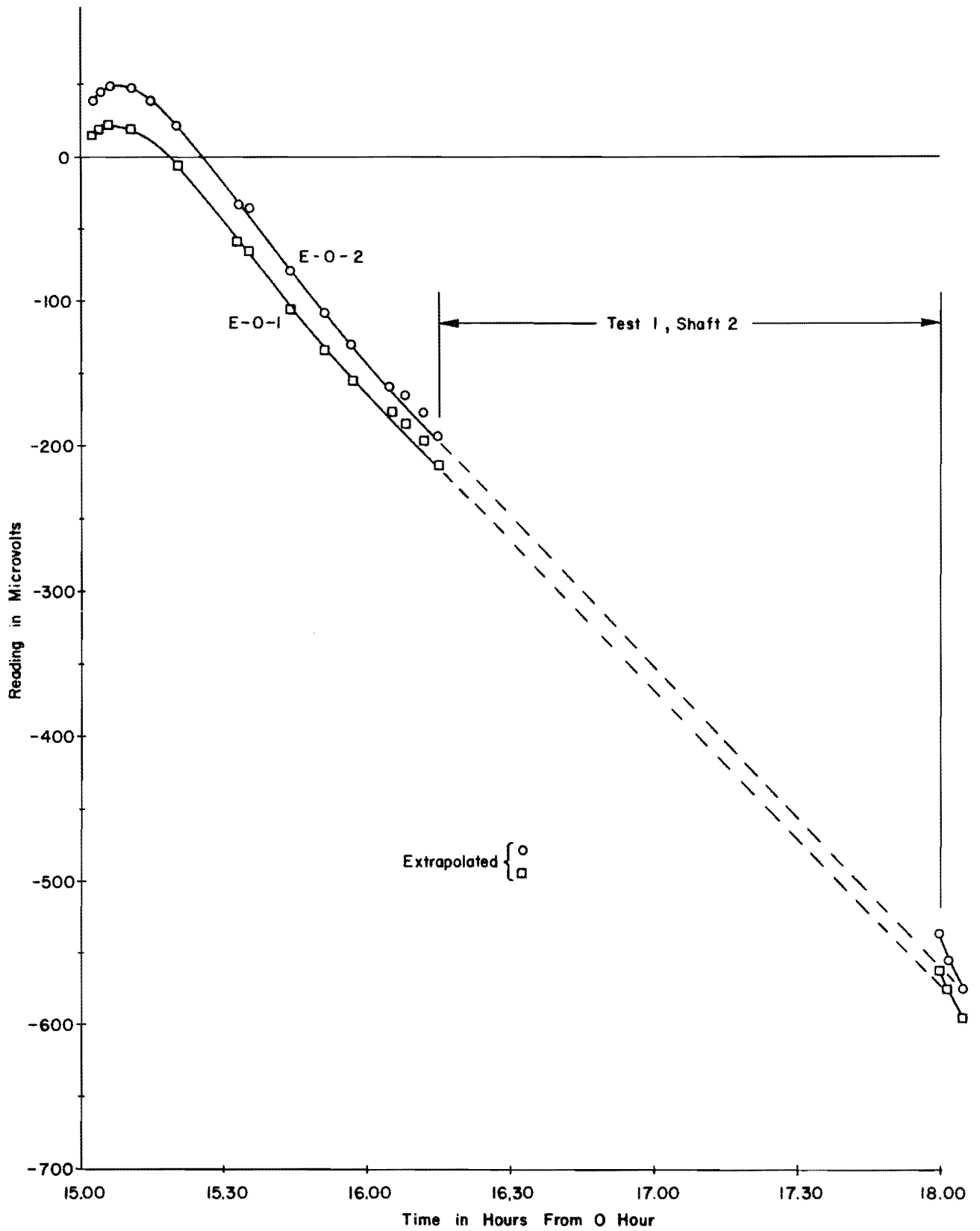


Fig. 4.26. Drift Curve for Calibration Level of Embedment Gages, Houston SH 225 Site, Shaft 2, Test 1

### Shaft Bending

The bending of Shaft 2 was even more pronounced than the bending of Shaft 1. The bending which appeared to increase greatly as the base of the shaft began to take up load is quite evident in the data from the Mustran cells and from the telltales, as shown in Fig. 4.27 and Fig. 4.28. As can be seen, the error could be quite great if compensation is not made for this bending. Consider, for example, the Mustran gages at Level 6 (15 feet 8 inches below the ground surface). If the average reading is taken as the correct reading, the cell M-16-18 is in error by 50 per cent for an applied load of 300 tons and by 36 per cent for an applied load of 500 tons. The bending indicated by the telltales was similar, and had not two telltales per level been used, completely false results would have been obtained.

Each embedment gage circuit, as in Shaft 1, contained two active arms on opposite sides of the shaft and therefore automatically compensated for the bending.

### Discussion of Test Results

Since no laboratory study had been made for the Mustran cell, Type 2, to determine the multiplication factor for this cell, no direct comparisons between the top levels of Mustran cells and embedment gages is possible. By using the top embedment gages to calculate the concrete strain, the cell multiplication for cell Type 2 was determined to be approximately 2.9. The concrete modulus of elasticity for the shaft was calculated from the embedment gages as being about  $5.4 \times 10^6$  psi.

Using the data from the top level of Mustran cells and embedment gages, the constants for the calibration polynomials were determined. The load

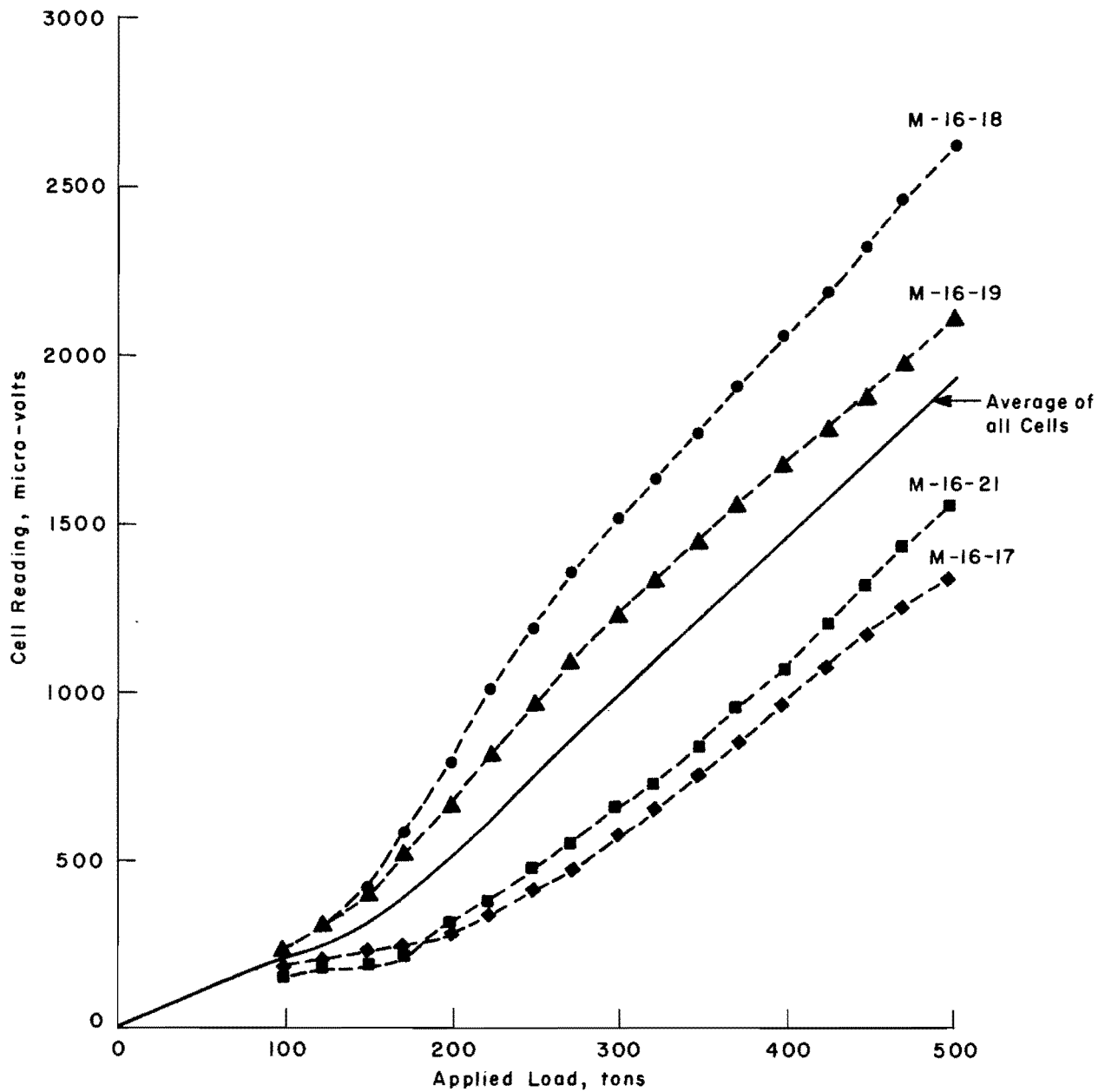


Fig. 4.27. Readings for Mustran Cells at 16-Foot Depth, Houston SH 225 Site, Shaft 2, Test 1

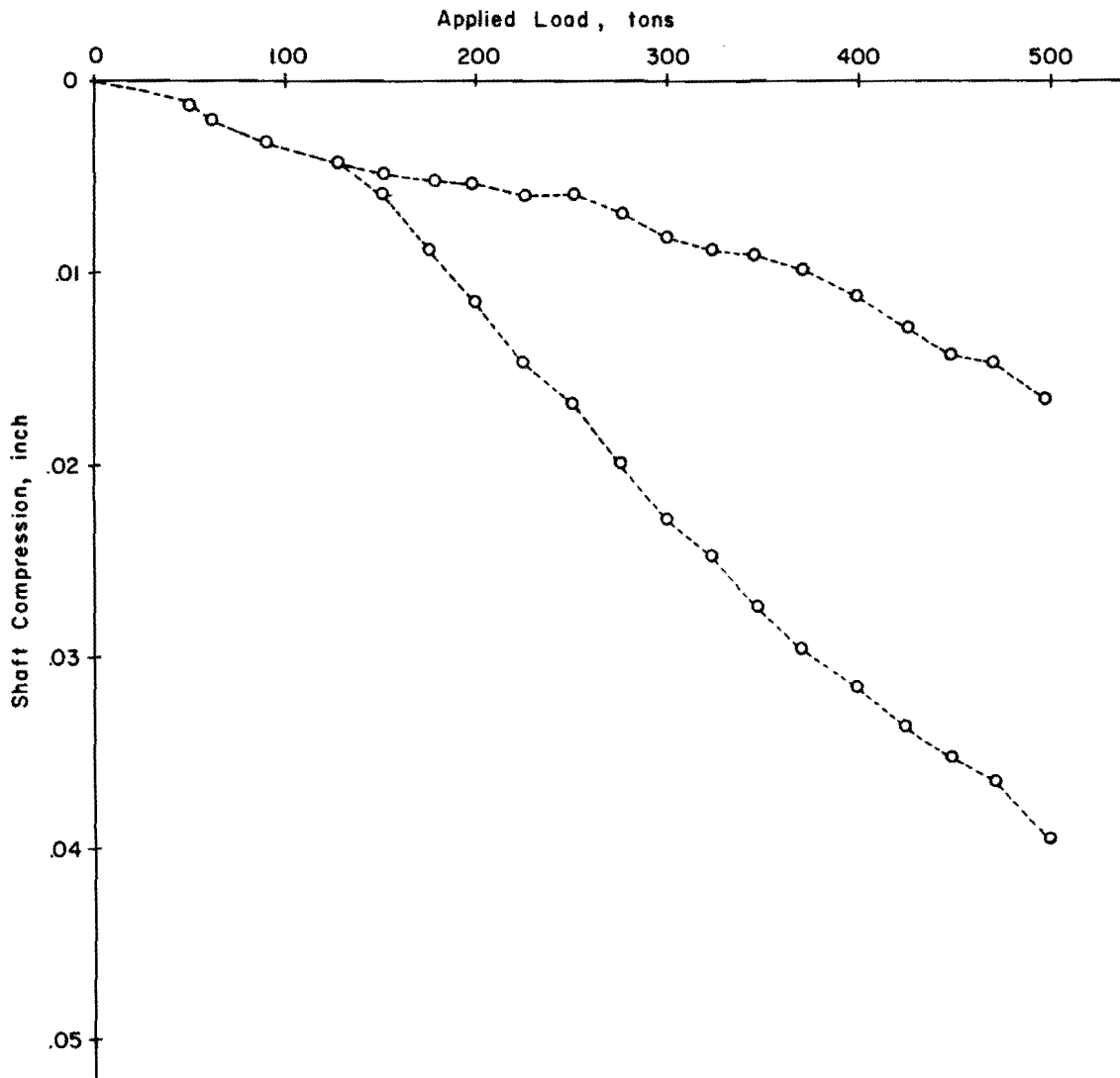


Fig. 4.28. Compression in Shaft as Indicated by Second Level of Telltales, Houston SH 225 Site, Shaft 2, Test 1

transfer curve for each load was then found by applying the polynomials to the reading. A typical load-transfer curve obtained in this manner is shown in Fig. 4.29. There appears to be considerably more scatter in the data from this shaft than from Shaft 1. This scatter is believed to stem from the fact that the gages of every level were not spaced exactly evenly around the shaft and from variation in the modulus of the concrete at different depths.

One method used to reduce the data scatter was to determine a calibration constant for each level. This is possible for this shaft since, past the applied load of 170 tons, all of the incremental applied load is transferred to the base. Thus it may be noted in Fig. 4.27 that the calibration constant for Level 6 of the Mustran cells can be calculated from the straight line portion of the curve from an applied load of 170 tons to an applied load of 500 tons as being approximately 4.66 microvolts output per ton of load in the shaft. A typical load-transfer curve obtained from the individually calibrated levels of gages is shown in Fig. 4.30. The scatter in the data appears much less and the resulting load-transfer curve is believed to represent much more accurately the load in the shaft.

In making a comparison of the embedment gages and Mustran cell data obtained at depths 3 feet 8 inches and 15 feet 8 inches below ground, if the Mustran cell data is taken as accurate, then for an applied load of 400 tons (the typical curve shown in Fig. 4.30), the embedment gages at the 3 foot 8 inch depth are in error by 2.9 per cent and the gages at the 15 foot 8 inch depth are in error by 7.5 per cent.

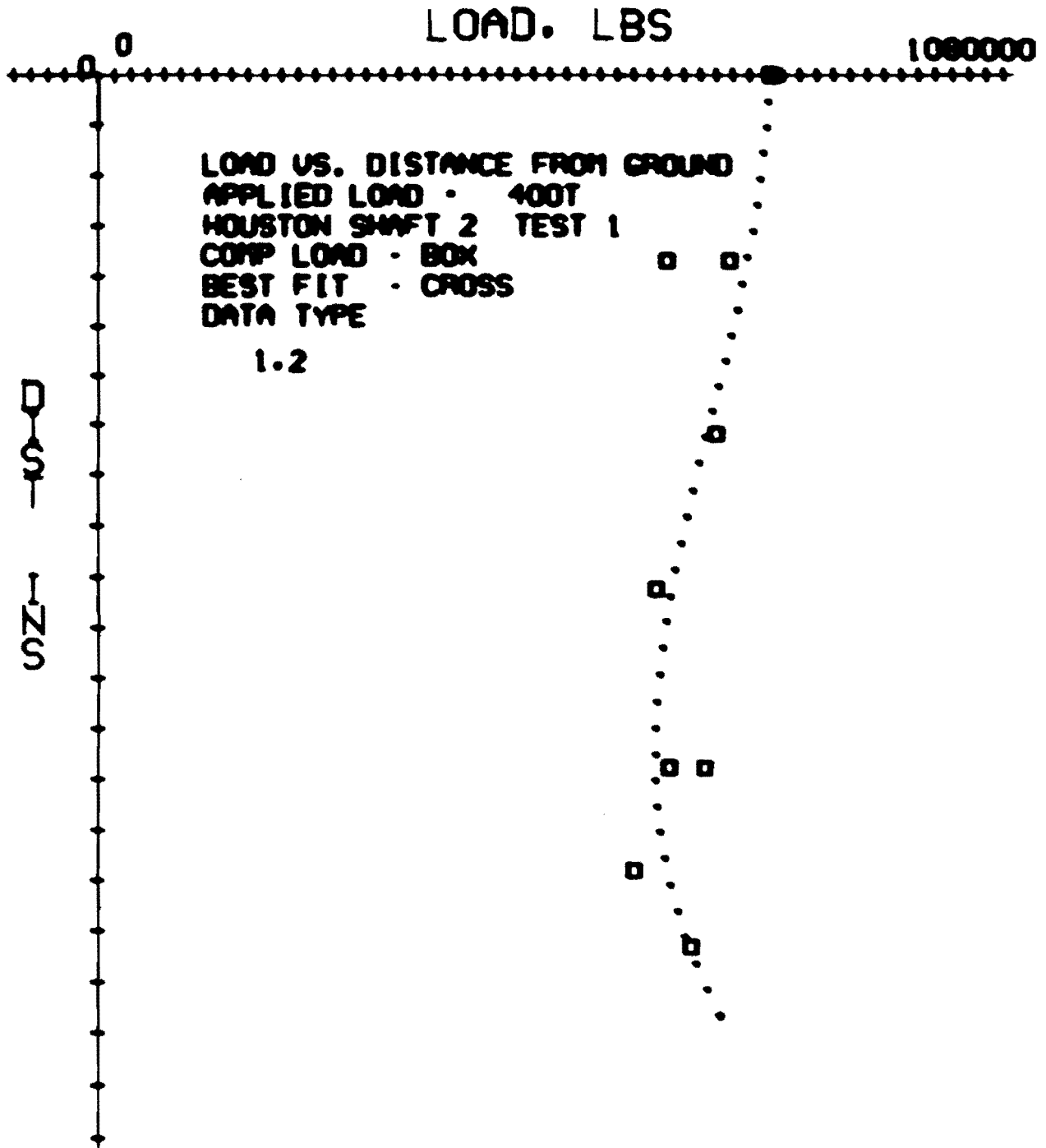


Fig. 4.29. Typical Load-Transfer Curve,  
Houston SH 225 Site, Shaft 2, Test 1

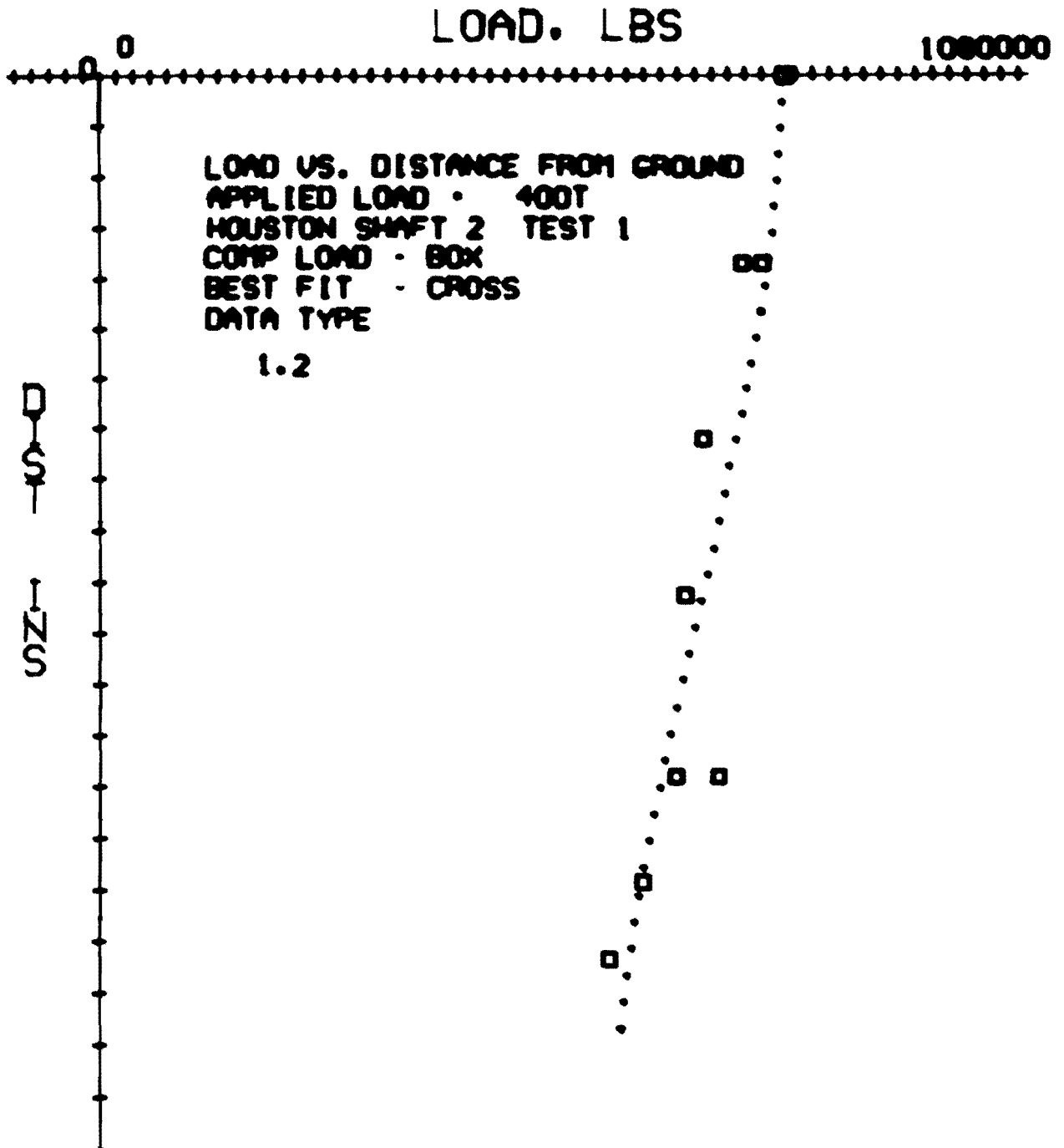


Fig. 4.30. Load-Transfer Curve Using Individual Calibration Constants, Houston SH 225 Site, Shaft 2, Test 1

In order to compare the data obtained from the telltales with the data from the Mustran cells, the movements along the shaft were calculated from the Mustran load-transfer curves. These movements, and the movements measured by the use of telltales, are plotted on Fig. 4.31 for applied loads of 200 tons, 300 tons, and 400 tons. The movements measured by the telltales appear to agree very closely with the calculated deflections, but small errors in measurements can make relatively large errors in the measured compression of the shaft. Consider the shaft compression from the top of the shaft to the second level of telltales. The compression indicated by the telltales would be 0.0185 inch, and the calculated compression would be 0.0250 inch. Assuming the calculated value to be correct, then the telltale reading would be in error by 26 per cent. The direction of this error is in the same direction as would be caused by friction between the telltale and the casing.

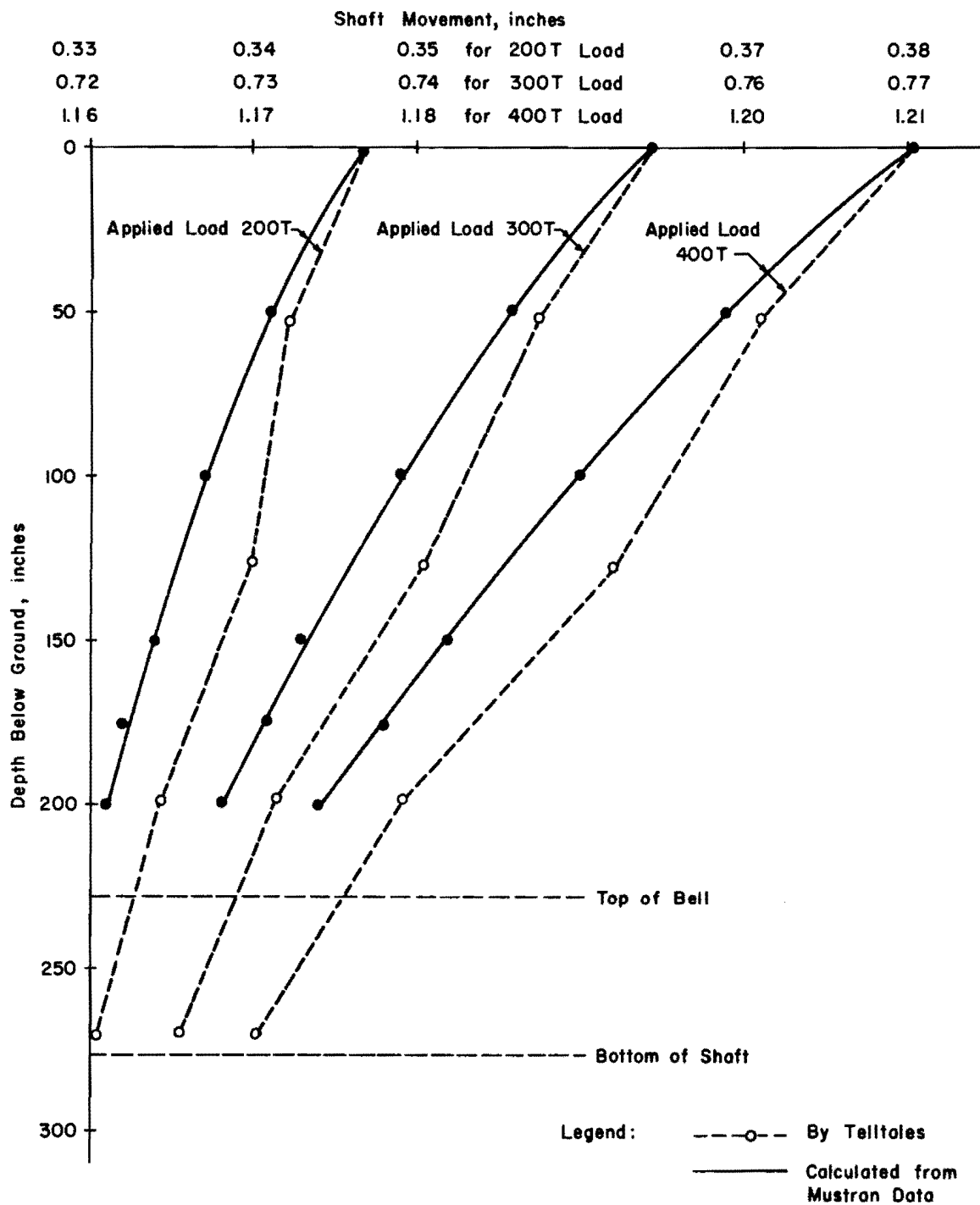


Fig. 4.31. Shaft Movement, Houston SH 225 Site, Shaft 1, Test 1

This page replaces an intentionally blank page in the original.

-- CTR Library Digitization Team

## CHAPTER V

### CONCLUSIONS AND RECOMMENDATIONS

The conclusions and recommendations presented are based on the four drilled shafts described previously. Additional information concerning the Mustran cells will be available at the completion of the tests of the two drilled shafts being presently installed at the Houston SH 225 site.

#### Conclusions

Telltales. Telltales provide a reliable and economical means for instrumenting a drilled shaft to obtain approximations of the load transferred. The results cannot be expected to be of the accuracy required in basic research to determine the relationship between shaft behavior and soil parameters. The largest source of error is in friction between the rod and the casing.

Embedment Gages. Embedment gages are limited in their use in drilled shafts by the lack of reliability and stability. The cause of the unreliability appears to be due to moisture penetrating the splices in the lead wire. Penetration of the plastic jacket of the gage may also be occurring. The lack of stability is due to both the moisture penetration and to the difference in the effect of temperature changes on the active and dummy gages. The results obtained when the gages are functioning properly are satisfactory for most short term tests. Even in short term tests, care must

be taken to determine the amount of drift which exists in the system. The accuracy which is obtained from properly functioning gages is about as good as can be expected from an indirect instrumentation system.

Gloetzl Cell. The one Gloetzl cell installed gave no usable results. This, coupled with the fact that the readout system was not compatible with the type tests being conducted, was the cause for the abandonment of the Gloetzl cell as a system for measuring axial loads in drilled shafts.

Bottomhole Cell. The bottomhole cell proved to be an excellent method for measuring the tip load of a drilled shaft. With the exception of the waterproofing technique, the design used was satisfactory. It is believed that with improvements in waterproofing techniques, the cell would be a very effective instrumentation system. One waterproofing technique is suggested in the recommendations.

Although the bottomhole cell is very effective, the cost per level of instrumentation is very high and the installation difficult.

Mustran Cells. The Mustran cell offers a reliable and stable system that is sufficiently accurate for most drilled shaft tests. The accuracy of the system is limited by the dependence on the properties of the concrete and shaft. The cell is relatively expensive and time consuming to build, but once constructed is easy to install in the shaft.

The system of pressurization through the lead wire proved highly effective against moisture. The design of the sealing system as shown for the Type 2 cell in Fig. 2.10 was adequate and alleviated the requirement for the use of copper tubing. Desiccant in the cell provided for a very stable cell and would be considered a must for a long-term test.

By pressure testing the cells prior to installation, reliability is greatly increased. The installation procedure used in either the first or the second shaft at Houston proved satisfactory.

The manifold systems used for both Houston shafts were difficult to handle and required excessive time for connecting and disconnecting. Suggestions for improvement of the manifold are presented in the recommendations.

### Recommendations

The instrumentation system used in any drilled shaft test must be compatible with the requirements of the test program. Only when all of the factors involved are considered can the proper instrumentation system be selected. In the case with the test being conducted by The University of Texas, the Mustran cell was adopted for use in the remaining two shafts to be tested. In other tests where only an estimate of the load transferred is required, telltales may be the best system; or in very short term tests, embedment gages may prove adequate. If a very high degree of accuracy is desirable, then the test may warrant combination of Mustran and bottomhole cells. Certainly two systems, not discussed previously, which should be considered are the vibrating-wire strain gages and the weldable strain gages.

The following recommendations are offered for the system discussed.

#### Telltales.

1. Telltales may be used where economics is a major factor and a high degree of accuracy is not required.
2. Care must be taken to keep the rod straight in order to keep the friction between the rod and casing to a minimum.

3. Two telltales should be installed at each level.

#### Embedment Gages.

1. Full-bridge circuits should be used with the dummy gage embedded in the concrete as close as possible to the active gage.
2. All splices should be made in a sealed container.
3. Extra levels of gages are recommended as insurance against gage loss.

#### Bottomhole Cell.

1. The bottomhole cell is recommended where a high degree of accuracy is required.
2. It is suggested that the wiring system be changed such that each of the three individual load cells may be read separately.
3. The waterproofing could be more easily accomplished by waterproofing of the individual load cells.
4. A rigid siding should be provided to prevent soil from pushing between the two plates.

#### Mustran Cells.

1. The Mustran cell is recommended as an adequate system for use in most drilled shaft tests.
2. For stability the cell should be filled with desiccant.
3. The sealing system, as shown in Fig. 2.10, is adequate and no copper tubing is required.
4. Each cell should be pressure tested prior to installation.
5. Precasting the cells in concrete is optional.

6. The manifold system should be redesigned to provide more convenient means of disconnecting and connecting the pressure system. One suggested system is shown in Fig. 5.1. It may be desirable to run studies to determine if the pressure system is required. For a test involving a number of cells, the pressure system is recommended as insurance against possible leaks.

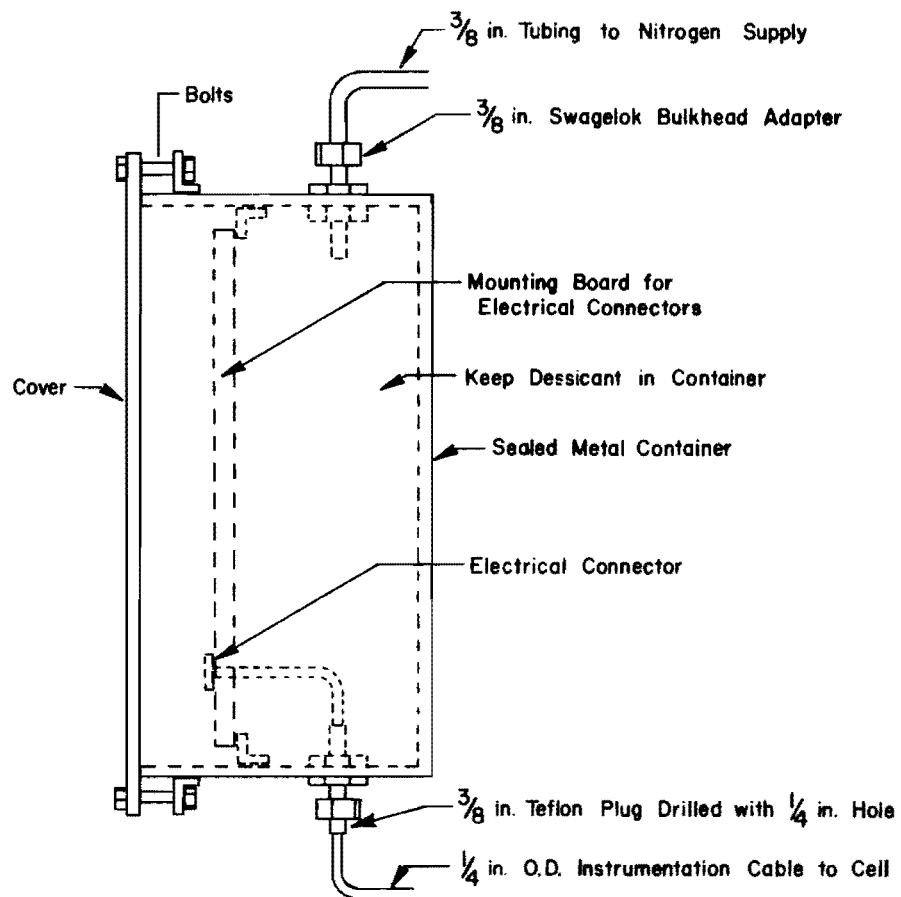


Fig. 5.1. Suggested Design of Manifold System for Mustran Cells

## REFERENCES

1. Coyle, H. M., and Reese, L. C., "Load Transfer for Axially Loaded Piles in Clay," Journal of the Soil Mechanics and Foundations Division, American Society of Civil Engineers, March, 1966, pp. 2-26.
2. Skempton, A. W., "Cast In-Situ Bored Piles in London Clay," Geotechnique, Vol. IX, December, 1959, pp. 153-173.
3. Whitaker, T., Cooke, R. W., and Clarke, G. W., "100 Ton Load Cell for Pile Loading Tests," Engineering, Vol. 194, November 23, 1962.
4. Whitaker, T., and Cooke, R. W., "An Investigation of the Shaft and Base Resistance of Large Bored Piles in London Clay," Symposium on Large Bored Piles, Institution of Civil Engineers, London, February, 1966.
5. DuBose, L. A., A Comprehensive Study of Factors Influencing the Load Carrying Capacity of Drilled and Cast-in-Place Concrete Piles, Parts I and II, Texas Highway Department Project No. RP-4, Texas Transportation Institute, College Station, Texas, October, 1956.
6. Investigation for Building Foundation in Expansive Clays, Vols. I and II, U. S. Army Engineer District, Fort Worth Corps of Engineers, Fort Worth, Texas, April, 1968.
7. Mohan, D., Jain, G. S., and Kumar, V., "Load-Bearing Capacity of Piles," Geotechnique, March, 1963, pp. 73-86.
8. Snow, R., "Telldatales," Foundation Facts, Fall, 1965, pp. 12-13.
9. Osgerby, C., and Taylor, P. T., "Vibrating-Wire Load Cell for Long-Term Pile Tests," Experimental Mechanics, September, 1968, pp. 429-430.
10. Brown, J. B., "Measurement of Lateral Earth Pressure Against a Drilled Shaft," M.S. Thesis, The University of Texas at Austin, Austin, Texas, June, 1967.
11. Campbell, David B., "The Determination of Soil Properties In Situ," M.S. Thesis, The University of Texas at Austin, Austin, Texas, January, 1970.
12. Ehlers, C. J., "The Nuclear Method of Soil-Moisture Determination at Depth," M.S. Thesis, The University of Texas at Austin, Austin, Texas, October, 1968.

13. Reese, L. C., and Hudson, W. R., "Field Testing of Drilled Shafts to Develop Design Methods," Research Report Number 89-1, conducted for the Texas Highway Department, Center for Highway Research, The University of Texas at Austin, Austin, Texas, April, 1968.
14. Vijayvergiya, V. N., "Load Distribution for a Drilled Shaft in Clay Shale," Ph.D. Dissertation, The University of Texas at Austin, Austin, Texas, November, 1968.